INVESTIGATION OF VARIATIONS AND IMPACTS OF TROPICAL CYCLONE PRECIPITATION IN TEXAS (1950-2009)

A Dissertation

by

LAIYIN ZHU

Submitted to the Office of Graduate Studies of
Texas A&M University
in partial fulfillment of the requirements for the degree of

DOCTOR OF PHILOSOPHY

Chair of Committee,	Steven M. Quiring
Committee Members,	Oliver W. Frauenfeld
	Inci Güneralp
	Walter G. Peacock
Head of Department,	Vatche P. Tchakerian

August 2013

Major Subject: Geography

Copyright 2013 Laiyin Zhu

ABSTRACT

This dissertation examines the causes of variations in tropical cyclone precipitation (TCP) and the relationship between TCP and river discharge in Texas. The dissertation has three major objectives: 1) investigate the spatial and temporal variations of TCP in Texas from 1950 to 2009, 2) construct seasonal statistical forecast models for TCP and identify the primary factors controlling TCP in Texas, and 3) examine how TCP contributes to the extreme precipitation and river discharge in watersheds surrounding the city of Houston.

An automated extraction method is developed to identify TCP from 60 years of precipitation data from Cooperative Observing Network gauges. Texas receives an average of 123.5 mm of TCP/year, which is ~13% of the state's mean annual precipitation. September is the month with the most TCP, and it receives an average of 18.5 mm. Long-term trends (>50 years) in TCP are evident at some locations, but there are no statistically significant long-term trends in aggregated annual TCP metrics. Despite the lack of long-term trends, TCP metrics show some spectral power at periodicities of ~2-3 years, ~5-8 years, and >10 years. Areas within 400 km of the coast have higher risk of extreme daily TCP (>100 mm), but inland Texas can also occasionally experience extreme TCP. In some areas in southeastern Texas the probability of receiving >100 mm of daily TCP in any given year is ~0.30 (i.e., daily TCP exceeds 100 mm, on average, 1 out every 3 years).

The best seasonal forecast models of TCP can explain >20% variance based on three or fewer predictors. ENSO is the most important control of TCP in Texas. La Niña,

the major driver in all TCP models, reduces the vertical wind shear in the Caribbean and tropical Atlantic and therefore generates more precipitating storms in Texas. Maximum Potential Velocity (MPV) in the Gulf of Mexico and vorticity in the Atlantic Hurricane Development Region (MDR) are also important predictors of TCP and they can increase the R^2 by ~0.2. The negative relationship between MPV and vorticity with the TCP are due to the fact that TCs with weaker wind speed and slower translation speed tend to contribute much more to both extreme and total TCP. Sea level pressure in the Gulf of Mexico, SST in the Caribbean and North Atlantic Oscillation are also identified as useful predictors in some of the models.

TCP is associated with many of the annual maximum discharge events in watersheds near Houston. Urbanization can significantly increase river discharge generated by TCP. Both the annual maximum discharge and 90 percentile discharge have increased significantly in many watersheds in Houston. Although no long-term trend can be observed in the TCP and TCP-related extreme discharge, there may be an increased risk of floods from TCP because of the statistically significant increases in annual maximum discharge that have been observed. There are also increased uncertainties in flood risk because extreme precipitation, including TCP, is projected to become more variable in the future.

ACKNOWLEDGEMENTS

I would like to particular thank Dr. Steven Quiring for all his guidance and support as my advisor. He is the person who led me to the right way of doing scientific research, inspired me with brand new ideas, and encouraged me to pursue my scientific dreams. I also would like to appreciate Dr. Oliver Frauenfeld, Dr. Inci Güneralp, and Dr. Walter Peacock for their help and suggestions during the years I was at TAMU. I am grateful for all of the good times with my friends from the Department of Geography and other departments at TAMU. You are really one of the most cherished parts in these 5 years of my life. Many thanks for the financial support from the Geography program of TAMU, the U.S. Department of Energy, and the Southern Company.

Finally, I would like to express my deep thanks to my parents. I am able to feel your loves and connections anytime even it is thousands of miles away from home. Those Saturday night talks were really helpful: like lights in the dark night, they offered me hopes and courage when I was desperate.

NOMENCLATURE

AO	Arctic Oscillation (unitless), global predictor
ATL	Atlantic Ocean (100ºW to 2.5ºW, 0ºN to 30ºN), regional domain
ATP	Air Temperature at the surface, local predictor (ºC)
CAR	Caribbean sea (87ºW to 61ºW, 9.5ºN to 21.5ºN), regional domain
CST	Central Standard Time
CV	Cross Validation
ECA	Eastern Caribbean Sea, based on dividing the Caribbean Sea into two sub-regions at 74ºW, regional domain
EGM	Eastern Gulf of Mexico, based on dividing the Gulf of Mexico into two sub-regions at 87.5ºW, regional domain
EMD	Eastern hurricane Main Develop Region, based on dividing the MDR into these two sub-regions at 52ºW, regional domain
ENSO	El Niño-Southern Oscillation
GMX	Gulf of Mexico (95ºW to 80ºW, 20ºN to 30ºN) regional domain
HURDAT	Atlantic basin hurricane database
IDW	Inverse Distance Weighting
ITCZ	Inter-tropical convergence zone
J2M	June of previous year to May
LULCC	Land Use Land Cover Change
M2M	March to May
MAE	Mean Absolute Error

MAY	May
MDR	Atlantic Main Development Region (MDR) (85ºW to 20ºW, 10ºN to 20ºN) regional domain
MPV	Maximum potential wind velocity (m/s), regional predictor
MRBT	Moving ROCI Buffer Technique
NAO	North Atlantic Oscillation (unitless), global predictor
NCAR	The National Center for Atmospheric Research
NCEP	National Centers for Environmental Prediction
NIÑO34	Niño 3.4 (170ºW to 120ºW, 5ºS to 5ºN), global domain
NIÑO3	Niño 3 (150ºW to 90ºW, 5ºS to 5ºN), global domain
NIÑO4	Niño 4 (160ºE to 150ºW, 5ºS to 5ºN), global domain
OSAT	Objective Synoptic Analysis Technique
PDO	Pacific Decadal Oscillation (unitless), global predictor
PREW	Precipitable Water, local predictor (kg/m^2)
QBO	Quasi-Biennial Oscillation (unitless), global predictor
RHUM	Relative Humidity, local predictor (%)
ROCI	Radius of Outer Closed Isobar
RSST	Relative SST, difference between the target region SST and tropical SST, regional and global predictor
SAPI	Sahel Precipitation Index (unitless), global predictor
SHUM	Specific Humidity, local predictor (kg/kg)
SLP	Sea Level Pressure, local and regional predictor (millibars)

SOI	Southern Oscillation Index (unitless), global predictor
SOM	Soil Moisture, local predictor (mm)
SST	Sea Surface Temperature, regional and global predictor (ºC)
TC	Tropical Cyclone
TCP	Tropical Cyclone Precipitation
TMPA	Multisatellite Precipitation Analysis
TRMM	Tropical Rainfall Measuring Mission
TX	Texas (94.5ºW to 107ºW, 25.5ºN to 36.5ºN), local domain
UWIND	Zonal Wind, local predictor (m/s)
USGS	U.S. Geological Survey
UTC	Coordinated Universal Time
WCA	Western Caribbean Sea, based on dividing the Caribbean Sea into two sub-regions at 74ºW, regional domain
WGM	Western Gulf of Mexico, based on dividing the GMX into two sub-regions at 87.5ºW, regional domain
WRF	Weather Research and Forecasting Model
VOR	850 mbar Vertical Vorticity (× 10−5 s−1), regional predictor
VSHR	850–200 mbar Vertical Shear (kt), regional predictor
VWIND	Meridional Wind, local predictor (m/s)
WMD	Western Hurricane Main Develop Region, based on dividing the MDR into these two sub-regions at 52ºW, regional domain

TABLE OF CONTENTS

Page

ABSTRACT ii

ACKNOWLEDGEMENTS iv

NOMENCLATURE v

TABLE OF CONTENTS viii

LIST OF FIGURES x

LIST OF TABLES xv

1. INTRODUCTION 1

1.1 Research Background 1
1.2 Research Objectives 3
1.3 Intellectual Merit and Broader Impacts 4

2. STATE OF THE KNOWLEDGE 5

2.1 TCP Characteristics 5
2.2 TC and TCP Modeling 6
2.3 Extreme Precipitation, Extreme Discharges, and TCP 7

3. STUDY AREA, DATA AND METHODOLOGY 9

3.1 Study Area 9
3.2 Data 11
3.2.1 TC track Data & Precipitation Data 11
3.2.2 Climatic/Oceanic Forcing Data 12
3.2.3 USGS Historical Discharges and Land Use/Cover Change Data 18
3.3 Methods and Models 20
3.3.1 TCP Extraction, Interpolation and Statistical Analysis for Objective 1 20
3.3.2 Multiple Regression Model for Objective 2 27
3.3.3 Statistical Tests for Objective 3. 30

4. TEMPORAL AND SPATIAL VARIATIONS IN TCP IN TEXAS 33

4.1 Spatial Variation of TCP 33
4.1.1 Daily TC Characteristics and TCP 33
4.1.2 Monthly TCP 39

4.1.3 Annual TCP 40
4.2 Temporal Variation 44
4.3 TCP Extremes 53
4.3.1 Probability of Extreme TCP Events 53
4.3.2 Historical Maximum Events 55
4.4 Conclusions 57

5. STATISTICAL FORECASTING MODELS FOR SEASONAL TCP IN TEXAS 60

5.1 Model Comparison 60
5.2 Parameter Analysis and Possible Physical Mechanisms 66
5.2.1 ENSO 71
5.2.2 MPV and Vorticity 73
5.2.3 Other Predictors 81
5.3 Summary and Conclusions 83

6. EXTREMES IN TROPICAL CYCLONE PRECIPITATION AND DISCHARGE IN WATERSHEDS NEAR HOUSTON 85

6.1 Land Use/Cover Change for the Selected Watersheds 85
6.2 Annual Maximum Discharge, TCP AND Related Discharge 88
6.3 Annual Daily Precipitation and TCP Days Exceeding the 90th Percentile 93
6.4 Annual Discharge Ratios and TCP-related Discharge Ratios Exceeding the 90th Percentile 98
6.5 Composites of Extreme Precipitation and Discharge Related to Land Use 101
6.6 Conclusion and Discussion 107

7. SUMMARY AND CONCLUSIONS 111

7.1 Summary 111
7.2 Conclusions 112
7.3 Future Research 114

REFERENCES 116

LIST OF FIGURES

Page

Figure 3.1. a. Distribution of COOP stations used in the study (only the stations with complete 60 year records (red cross) are used in the time series analysis, stations with 50+ year records (blue dots) are used in the spatial analysis), b. An example of how a Tropical Cyclone Precipitation (TCP) day is defined and the boundary used to extract rain gauges. This example is from Hurricane Ike (September 12-14, 2008). 9

Figure 3.2. The San Jacinto River Basin and the selected watersheds.....10

Figure 3.3. Spatial domain for independent variables used for TCP modeling: North Atlantic (NATL), Main Develop Region (MDR), Caribbean (CAR) and Gulf of Mexico (GMX).....15

Figure 3.4. Probability of annual TCP (ATCP), TCP percentage(ATCPP) and TCP events (ATCPE) compared with probability of their associated normal distribution (ATCP, ATCPP and ATCPE are normalized to fit in the same scale).....29

Figure 4.1. a. Distribution of daily TC direction of movement, b. Histogram of TC translation speed for all TCs that influenced Texas between 1950 and 2009. 35

Figure 4.2. Box-Whisker plot of total TCP volume for 4 groups of TC events divided by average TC translation speed. Boxes represent 25th and 75th percentile inter-quartile ranges. Median extents are shown by the red line in each box. Whiskers (black horizontal lines) represent approximately +/–2.7σ and 99.3% coverage if the data are normally distributed. Extents larger (smaller) than the whiskers are shown as individual red crosses. 36

Figure 4.3. Distribution of daily precipitation (mm) (interpolated and gage-based) by quadrant with respect to the direction of movement and center of the TC 38

Figure 4.4. Spatial distribution of mean monthly TC precipitation (mm) (1950-2009): a. June, b. July, c. August, d. September, e. October. 41

Figure 4.5. Spatial distribution of a. Mean annual TC precipitation (mm), b. Contribution of TC precipitation to annual precipitation (%). 43

Figure 4.6. Number of stations with statistically significant (95% confidence, Mann-Kendall) decreasing and increasing trends in annual TCP. 45

Figure 4.7. Number of stations with statistically significant (95% confidence, Mann-Kendall) decreasing and increasing trends in mean daily TCP (a) and maximum daily TCP (b). 47

Figure 4.8. Original time series (black line), linear trend (red line), and 9-year moving average (blue line) for the following TCP metrics: a. Annual TCP, b. Annual TCP volume, c. Annual TCP days, d. Mean daily TCP area, e. Mean daily TCP, f. Annual maximum daily TCP..... 49

Figure 4.9. Power spectra for annual TCP metrics (black line) compared with the 85% and 95% confidence limit of the "red" noise references: a. annual TCP, b. annual TCP volume, c. annual TCP day numbers, d. annual average daily TCP area, e. annual average daily TCP, f. annual maximum daily TCP..... 52

Figure 4.10. Spatial distribution of annual frequency of a. Daily TCP >50 mm, b. Daily TCP >100 mm (calculated from stations with 50+ years of data)..... 54

Figure 4.11. a. Spatial distribution of maximum daily TC precipitation (mm), b. Ten extreme TCs that influenced the greatest area in Texas for the maximum daily TCP, c. Month of occurrence of the maximum daily TCP value at each grid point. 56

Figure 5.1. Observed and modeled TCP: (a.) annual TCP (models with n1), (b.) TCP percentage (models with n2), (c.) TCP events (models with n3). The black line is for observation, the red line is for the comprehensive model ('c' series), and the green and blue represent two simple models ('s' and 'ss' series).. 61

Figure 5.2. Pearson's correlations between SSTs in Niño 4 and 3 regions and annual TCP event (ATCPE): a. May Niño 3 and 4 SST and ATCPE, b. March to May Niño 3 and 4 SST and ATCPE, c. December to May Niño 3 and 4 SST and ATCPE. The black dots represent correlations with a 90% significance..... 67

Figure 5.3. Pearson's correlations between regional predictors and the annual TCP (ATCP): a. May vorticity and ATCP, b. December to May Maximum Potential Velocity (MPV) and ATCP, c. May sea level pressure and ATCP, the black dots are points with correlation significant at 90% confidence level. 68

Figure 5.4. Pearson's correlations between regional predictors and TCP percentage (ATCPP): a. May vorticity and ATCPP, b. December to May Maximum Potential Velocity (MPV) and ATCPP, c. December to May SST and

ATCPP, the black dots are points with correlation significant at 90% confidence level. 69

Figure 5.5. Pearson's correlations between regional predictors and the TCP events (ATCPE): a. December to May Maximum Potential Velocity (MPV) and ATCPE, b. May sea level pressure and ATCPE, the black dots are points with correlation significant at 90% confidence level.. 70

Figure 5.6. Box-Whisker plot of daily TCP volume for 4 groups of TC events divided by daily TCP characteristics (maximum wind speed and translation speed). Boxes represent 25th and 75th percentile inter-quartile ranges. Median extents are shown by the red line in each box. Whiskers (black horizontal lines) represent approximately +/–2.7σ and 99.3% coverage if the data are normally distributed. Extents larger (smaller) than the Whisker are shown as individual red crosses: a. TC maximum speed and TCP volume for TCP days with rainfall area covering < 13% of Texas (232 days). b. TC maximum speed and TCP volume for TCP days with rainfall area covering 13%-64% of Texas (233 days). c. TC translation speed and TCP volume for TCP days with rainfall area covering < 13% of Texas (232 days). d. TC translation speed and TCP volume. 78

Figure 5.7. Histograms of daily TC maximum wind speed and translation speed and their quartile divisions..... 80

Figure 6.1. Land Use and Land Cover for Houston area between 1980 and 2006. 86

Figure 6.2. (8074500: Whiteoak Bayou, 8076500: Halls Bayou, 8073500: Buffalo Bayou, 8075000: Brays Bayou, 8070500: Caney Ck, 8068000: W Fk San Jacinto Rv, 8068500: Spring Ck, 8069000: Cypress Ck). 87

Figure 6.3. Annual maximum TCP (mm), annual maximum daily discharge ratio (cms/sqkm) and maximum daily discharge ratio associated with the annual maximum TCP for each selected watersheds (8074500: Whiteoak Bayou, 8076500: Halls Bayou, 8073500: Buffalo Bayou, 8075000: Brays Bayou, 8070500: Caney Ck, 8068000: W Fk San Jacinto Rv, 8068500: Spring Ck, 8069000: Cypress Ck). 89

Figure 6.4. Significant linear trends and change points in time series of mean and variance of the Annual Maximum Discharge Ratio for selected watersheds. MKT represents the Mann-Kendall linear trend test, a + (-) indicates the trend is increasing (decreasing); Sta (No Sta) means trend is stationary (not) tested by the Kwiatkowski–Phillips–Schmidt–Shin approach; CPT is for the change point passed by the Pettitt test, the year

of change is also presented with a + (-) meaning increased (decreased) mean/variance after the change point. 91

Figure 6.5. Time series of the 90th percentile daily precipitation and TCP days with precipitation larger than the 90th percentile daily precipitation. Change points (Pettitt) are detected for the time series of the 90th percentile daily precipitation. Mean values before and after the change point are displayed if the change point is statistically significant at the 5% level (dash lines), otherwise the whole sample mean is displayed (dash lines). Linear trends are also shown for time series (solid straight lines) (8074500: Whiteoak Bayou, 8076500: Halls Bayou, 8073500: Buffalo Bayou, 8075000: Brays Bayou, 8070500: Caney Ck, 8068000: W Fk San Jacinto Rv, 8068500: Spring Ck, 8069000: Cypress Ck). 95

Figure 6.6. Significant linear trends and change points in time series of mean and variance of the 90 percentile precipitation (a&b) and 90 percentile discharge (c&d) for selected watersheds. MKT represents the Mann-Kendall linear trend test, a + (-) indicates the trend is increasing (decreasing); Sta (No Sta) means trend is stationary (not) tested by the Kwiatkowski–Phillips–Schmidt–Shin approach; CPT is for the change point passed by the Pettitt test, the year of change is also presented with a + (-). 96

Figure 6.7. Time series of the 90th percentile daily discharge and days with TCP related discharge (-1 to +2 days to the TCP day) larger than the 90th percentile daily discharge. Change points (Pettitt) are detected for the time series of the 90th percentile daily discharge. The whole sample means are displayed (dash lines). Linear trends are also shown for time series (solid straight lines) (8074500: Whiteoak Bayou, 8076500: Halls Bayou, 8073500: Buffalo Bayou, 8075000: Brays Bayou, 8070500: Caney Ck, 8068000: W Fk San Jacinto Rv, 8068500: Spring Ck, 8069000: Cypress Ck). 99

Figure 6.8. Variations of the annual maximum daily precipitation, maximum TCP, maximum discharge, and maximum TCP discharge for different watersheds between 1980 and 2006 (8074500: Whiteoak Bayou, 8076500: Halls Bayou, 8073500: Buffalo Bayou, 8075000: Brays Bayou, 8070500: Caney Ck, 8068000: W Fk San Jacinto Rv, 8068500: Spring Ck, 8069000: Cypress Ck). 103

Figure 6.9. Variations of the annual 90 percentile precipitation (lines) and TCP days passing the annual 90 percentile precipitation (bars) for different watersheds between 1980 and 2006 (8074500: Whiteoak Bayou, 8076500: Halls Bayou, 8073500: Buffalo Bayou, 8075000: Brays

Bayou, 8070500: Caney Ck, 8068000: W Fk San Jacinto Rv, 8068500: Spring Ck, 8069000: Cypress Ck). 104

Figure 6.10. Variations of the annual 90 percentile discharge ratio (lines) and TCP related discharges passing the annual 90 percentile discharge ratio (bars) for different watersheds between 1980 and 2006 (8074500: Whiteoak Bayou, 8076500: Halls Bayou, 8073500: Buffalo Bayou, 8075000: Brays Bayou, 8070500: Caney Ck, 8068000: W Fk San Jacinto Rv, 8068500: Spring Ck, 8069000: Cypress Ck). 106

LIST OF TABLES

Page

Table 3.1. Description of spatial averaging areas 13

Table 3.2. Description of potential predictors used in the statistical modeling. 14

Table 3.3. Summary of the stream flow data and watershed characteristics associated with the selected USGS stations..... 19

Table 3.4. Rules and Land Use/Cover Classification..... 21

Table 4.1. Monthly TC precipitation (mm) based on the entire rainfall region. 42

Table 4.2. Summary of annual and daily TC precipitation metrics 51

Table 5.1. Model parameters and coefficients 63

Table 5.2. Observations and statistical measures of model fit and leave-one-out cross validation (CV) for a. annual TCP, b. TCP percentage, and c. TCP events. 64

1. INTRODUCTION*

1.1 Research Background

Tropical Cyclones (TC) have a major impact on people and the environment because they cause wind damage, storm surge and inland flooding with loss of life and major economic damage [*Pielke and Landsea*, 1998; *Landsea et al.*, 1999; *Pielke and Landsea*, 1999; *Villarini and Smith*, 2010a; *Emanuel*, 2011]. *Pielke et al.* [2008] demonstrated that storms from the 1996-2005 caused the second most damage when compared to the past 11 decades. In addition, hurricanes cost the U.S. $150 billion during 2004 and 2005 seasons combined.

The risk of TC-related disasters has the potential to increase in the future because TC systems are closely connected with global and regional oceanic and atmospheric conditions. Observational and modeling studies have demonstrated that higher sea surface temperatures (SSTs) are typically associated with more intense TCs [*Emanuel*, 2005]. Increases of Atlantic TC frequency in the 20th century are closely associated with both the absolute sea surface temperature in the North Atlantic [*Goldenberg et al.*, 2001; *Holland and Webster*, 2007] and the relative Atlantic SST (RSST) [*Vecchi et al.*, 2008] compared with the whole tropic ocean.*

---

* Part of this section is reprinted with permission from "Variations in Tropical Cyclone Precipitation in Texas (1950 to 2009)" by Zhu and Quiring, 2012. *Journal of Geophysical Research-Atmospheres*, in press, Copyright [2012] by John Wiley & Sons, Inc.

On the other hand, there are also arguments that the recent increases in TC activity are due to natural variability [*Landsea et al.*, 2006] or improvement in observing practices [*Henderson-Sellers et al.*, 1998; *Chang and Guo*, 2007; *Lau et al.*, 2008]. Some model simulations predict a global and regional decrease in the overall frequency of TCs in the 21st century warming conditions [*Knutson and Tuleya*, 2004; *Bender et al.*, 2010; *Knutson et al.*, 2010]. Examinations of possible variations of TC activity in a warming climate in the 21st century generally agree that the intensity of TCs in the Atlantic will increase, while the frequency will decrease or remain unchanged [*Emanuel et al.*, 2008; *Bender et al.*, 2010; *Knutson et al.*, 2010; *Villarini and Vecchi*, 2012].

In addition to strong winds and storm surge, TCs frequently produce extreme precipitation. TC precipitation (TCP) accounts for a considerable portion of both total annual precipitation and extreme precipitation along the Atlantic and Gulf of Mexico coasts in United States [*Knight and Davis*, 2007; 2009; *Kunkel et al.*, 2010]. TCP related inland flooding can also result in significant economic damage and loss of life [*Rappaport*, 2000; *Pielke et al.*, 2002]. Compared with abundant discussions for TC frequency and intensity, fewer studies have focused on generating long-term TCP climatology at the regional scale, especially with high density observations and accurate TCP extraction method. At the smaller scale, TCP may also be enhanced by the urban heat island [*Burian and Shepherd*, 2005] and aerosols [*Li et al.*, 2008]. Intensified precipitation, accompanyed by the impervious surfaces caused by the rapid process of urbanization [*Olivera and DeFee*, 2007; *Brody et al.*, 2008], can significantly increase flood risk in urban watersheds. This study will investigate the historical TCP

climatology in Texas, explain which factors control its interannual variations, and finally show the hydrological impacts of TCP in Houston and the accompanying changes in local environment.

1.2 Research Objectives

This study will answer three questions:

1. How has TCP varied temporally and spatially in Texas?
2. Which global, regional and local factors control the interannual variations in TCP in Texas?
3. How does TCP contribute to annual extreme precipitation and discharge events in Houston watersheds undergoing rapid urbanization?

To answer the first question, 60 years of TCP climatology will be collected from rain gauges in Texas using a new extraction metholology and the spatial and temporal variations in TCP will analyzed. To answer the second question, multiple linear regression models of TCP will be constructed from multiple climatic/oceanic forcings. The models will be examined and evaluated both in terms of their predictive skill and with regards to identifying plausible physical mechanisms. To answer question three, histrorical discharge data will be gathered for watersheds near Houston from USGS and compared with annual extreme precipitation (especially the TCP) and histrorical Land Use Land Cover Change (LULCC).

1.3 Intellectual Merit and Broader Impacts

This is the first analysis of TC precipitation and associated inland flooding that is based on a long-term (60 year) record. A new method for estimating TC precipitation from rain gauges has been developed and automated into set of FORTRAN codes. This method can be applied to the extraction of TCP from rain gauges in other states prone to TCs. A detailed climatology will be contructed specifically for TCP in Texas, providing a reference to the climate modeling community and state decision makers. This will also be the first study using statistical models to make seasonal forecast of TCP in a region of U.S. It will serve as a useful baseline for future simulations of TCP using high resolution regional climate models. Finally, the hydrological analysis will be the first long-term study that identifies the contribution of TCP to extreme precipitation and discharge in watersheds undergoing rapid changes in land use in the Houston area.

With a broader prospective, this research will help people living in Texas better understand TCP and the related flood risk. Besides its disastrous influences, TCP can also provide an important source of fresh water in Texas, which is especially precious during droughts.

2. STATE OF THE KNOWLEDGE*

2.1 TCP Characteristics

Recent studies indicate that extreme precipitation in the U.S. increased during the twentieth century [*Groisman et al.*, 2005] and this trend is expected to continue in the 21st century [*Min et al.*, 2011]. *Knight and Davis* [2007] demonstrated that the contribution of extreme TCP to overall precipitation increased in the southeastern U.S. between 1980 and 2004 is mainly due to an increase in the number of tropical storms. At a larger scale, there is an increasing trend in the contribution from TCs in the North Atlantic to both annual total rainfall and extreme rainfall events (i.e., top 5% of rainfall events) [*Lau et al.*, 2008]. *Kunkel et al.* [2010] reported that TC-related extreme precipitation events in the eastern U.S. doubled during 1994-2008 as compared to the long-term (1895-2008) average. *Knight and Davis* [2009] also showed that the TCP contribution to extreme precipitation increased during 1972 to 2007 due to increases in both storm frequency and intensity. *Nogueira et al.* [2010] found increasing trends in both annual TCP volume and affected area in the eastern U.S. since 1995, which are attributed to increases in TC frequency. Generally, these large-scale studies show increases in TCP in recent years, both in terms of extreme precipitation and the contribution to annual precipitation. Increases in TC frequency are responsible for much of this trend.*

---

* Part of this section is reprinted with permission from "Variations in Tropical Cyclone Precipitation in Texas (1950 to 2009)" by Zhu and Quiring, 2012. *Journal of Geophysical Research-Atmospheres*, in press, Copyright [2012] by John Wiley & Sons, Inc.

Previous studies of TCP have primarily examined TCP over the ocean [*Lau et al.*, 2008], or at continental [*Larson et al.*, 2005] or regional scales [*Shepherd et al.*, 2007; *Knight and Davis*, 2009; *Nogueira and Keim*, 2010]. There have also been a number of case studies focused on precipitation from a single TC or a small number of TCs [*Rodgers and Pierce*, 1995; *Medlin et al.*, 2007; *Matyas*, 2010]. However, very few studies have developed a long-term record of the spatial and temporal variations in TCP at the state level. Although several studies have investigated short-term forecasting of TCP [*Sippel and Zhang*, 2010] and patterns of extreme TCP cases [*Arndt et al.*, 2009; *Bosart et al.*, 2011], no one has examined the long-term TCP variations specifically in Texas.

2.2 TC and TCP Modeling

While complexities exist in both predicting long term trend of TC activities, statistical models have skills in forecasting seasonal TC frequency. *Gray* first used multiple linear regression models to make skillful seasonal forecast of TC frequency in the Atlantic [*Gray*, 1984a; b]. He showed that ENSO, Pacific Decadal Oscillation (PDO), Quasi-Biennial Oscillation (QBO) and West African rainfall are important variables for explaining seasonal variations in TC counts in the Atlantic [*Gray*, 1984b; *Gray et al.*, 1993; 1994; *Klotzbach and Gray*, 2003]. Poisson series models are also applied to forecast seasonal TC counts [*Elsner and Schmertmann*, 1993; *Elsner and Jagger*, 2004; 2006; *Villarini et al.*, 2011b] because their strengths in fitting statistical distribution of extreme values like TC activities. They indicated that North Atlantic

Oscillation (NAO), Southern Oscillation and the Tropical mean SST can also be used to model the U.S landfall hurricanes counts.

Although heavy precipitation is an important feature of landfall TCs [*Konrad*, 2001; *Nielsen-Gammon et al.*, 2005; *Konrad and Perry*, 2010; *Barlow*, 2011] and plays a considerable role in both hydrological extremes and total budget, few studies have constructed statistical models to forecast seasonal TCP amount for the U.S. This is mainly because the difficulties in accurately forecasting/modeling TCP events and the lack of an accurate long-term record of TCP. The characteristics and dynamics of a single TC are highly complex and TCP varies a lot from TC to TC [*Rodgers et al.*, 1994; *Rogers et al.*, 2003; *Villarini et al.*, 2011a].

2.3 Extreme Precipitation, Extreme Discharges, and TCP

Several studies have shown increases in precipitation and streamflow for the continental U.S. from the historical observations [*McCabe and Wolock*, 2002a; *McCabe and Wolock*, 2002b; *Groisman et al.*, 2004]. Some have also shown an increasing trend in heavy (90^{th}–95^{th} percentile) or very heavy (99^{th}–99.7^{th} percentile) precipitation in the U.S. [*Groisman et al.*, 2005; *Kunkel et al.*, 2007]. *Kunkel et al.* [2012] analyzed all meteorological causes of extreme precipitation events in the U.S. They demonstrated that TCs accounted for ~13% of all daily extreme events in the U.S. since 1908. *Kunkel et al.* [2010] and *Knight and Davis* [2009] both revealed recent upward trends in TC-related extreme precipitation for the continental U.S. Spatial differences may exist if we look at the TCP at the regional scale.

Besides climate change, human activities can also alter the characteristics of localized precipitation and discharge [*Karl and Trenberth*, 2003]. *Burian and Shepherd* [2005] discovered that the urban area and the urban downwind region recieved 59% and 30% more rainfall from noon to midnight than the upwind region in Houston. *Orville et al.* [2001] and *Li et al.* [2008] argued that the enhanced precipitation are possibly associated with the transportation of anthropogentic aerosols from the indusries in Houston. The increased urban land cover was also linked to increased precipitation in the Houston area and this was demonstrated with a coupled land surface and atmospheric model simulation by *Shepherd et al.* [2010]. Theoretically, the increased urban area leads to increases in surface temperature [*Kalnay and Cai*, 2003] and this enhances atmospheric convergence, instability and convective rainfall initiation [*Collier*, 2006]. Urbanization also increases impervious surfaces which reduces the time of concentration for runoff and increases peak discharge [*Smith et al.*, 2002; *Ogden et al.*, 2011].

Olivera and Defee [2007] examined discharge in Whiteoak Bayou watershed in Houston area and concluded that runoff depths and peak flows have increased by 146% and 159% as a result of the increases in impervious surfaces, and urbanization accounts for 77% and 32% of the increase. While there are many studies that have examined the impacts of climate change, urbanization, aerosols on extreme precipitation and discharge, few have focused on the influence of TCP on discharge. This study also considered how rapid urbanization contributes to changes in discharge.

3. STUDY AREA, DATA AND METHODOLOGY*

3.1 Study Area

Texas borders the Gulf of Mexico and has a long coastline, so it is frequently influenced by damaging TCs [*Keim and Muller*, 2007; *Islam et al.*, 2009]. The most recent major hurrcane, Hurricane Ike, caused severe damages and many deaths in Texas in 2008. There were 74 deaths directly or indirectly related to the Hurricane Ike according to *Zane et al.* [2011]. Much of the inland flooding that occurs in Texas can be attributed to TCs [*Burnett*, 2008]. Texas is the study area for this dissertation because if its geographical location in the coast of the Gulf of Mexico and the area it covers. Objectives 1 and 2 (Figure 3.1a) will focus on the entire state and Objective 3 will examine TC-induced flooding in the San Jacinto river basin. The San Jacinto River is located in southeastern Texas (Figure 3.2) and includes watersheds that cover portions of the Houston Metro Area. These watersheds are dominated by developed land use and rapid urbanization. This study will select the most representative watersheds with the most complete records. *

* Part of this section is reprinted with permission from "Variations in Tropical Cyclone Precipitation in Texas (1950 to 2009)" by Zhu and Quiring, 2012. *Journal of Geophysical Research-Atmospheres*, in press, Copyright [2012] by John Wiley & Sons, Inc.

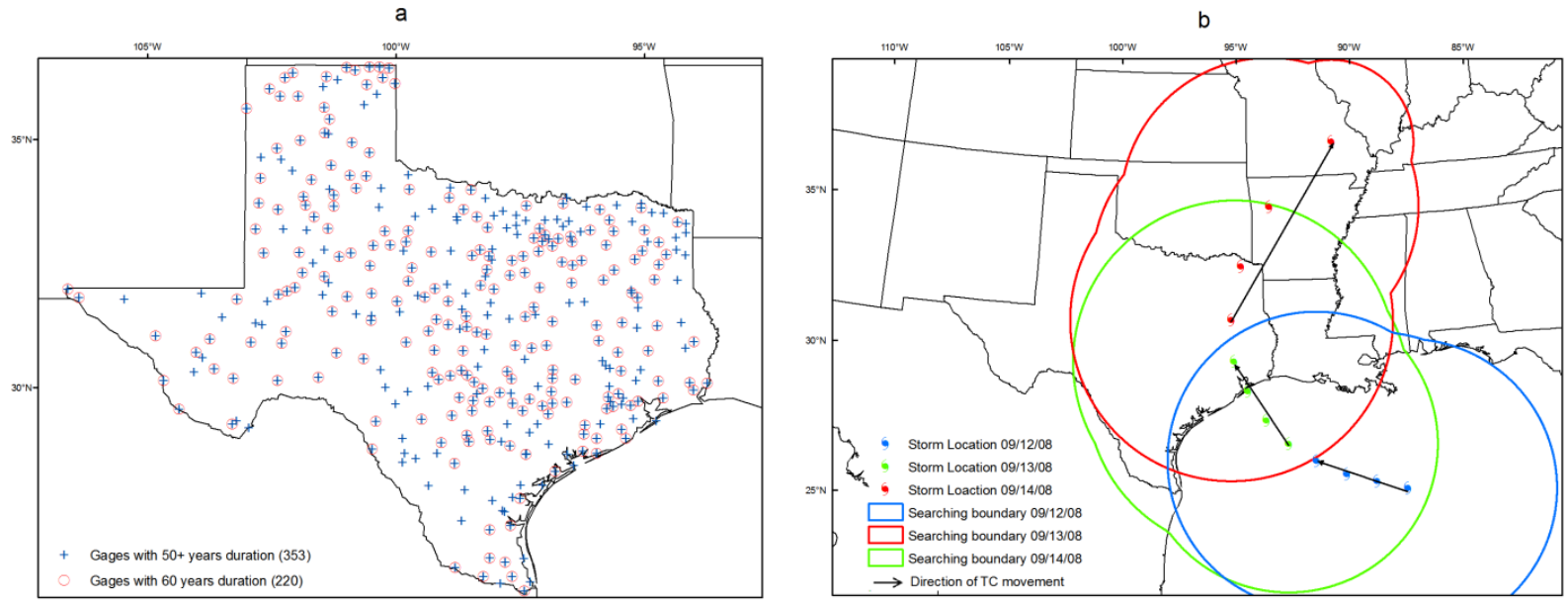

Figure 3.1. a. Distribution of COOP stations used in the study (only the stations with complete 60 year records (red cross) are used in the time series analysis, stations with 50+ year records (blue dots) are used in the spatial analysis), b. An example of how a Tropical Cyclone Precipitation (TCP) day is defined and the boundary used to extract rain gauges. This example is from Hurricane Ike (September 12-14, 2008).

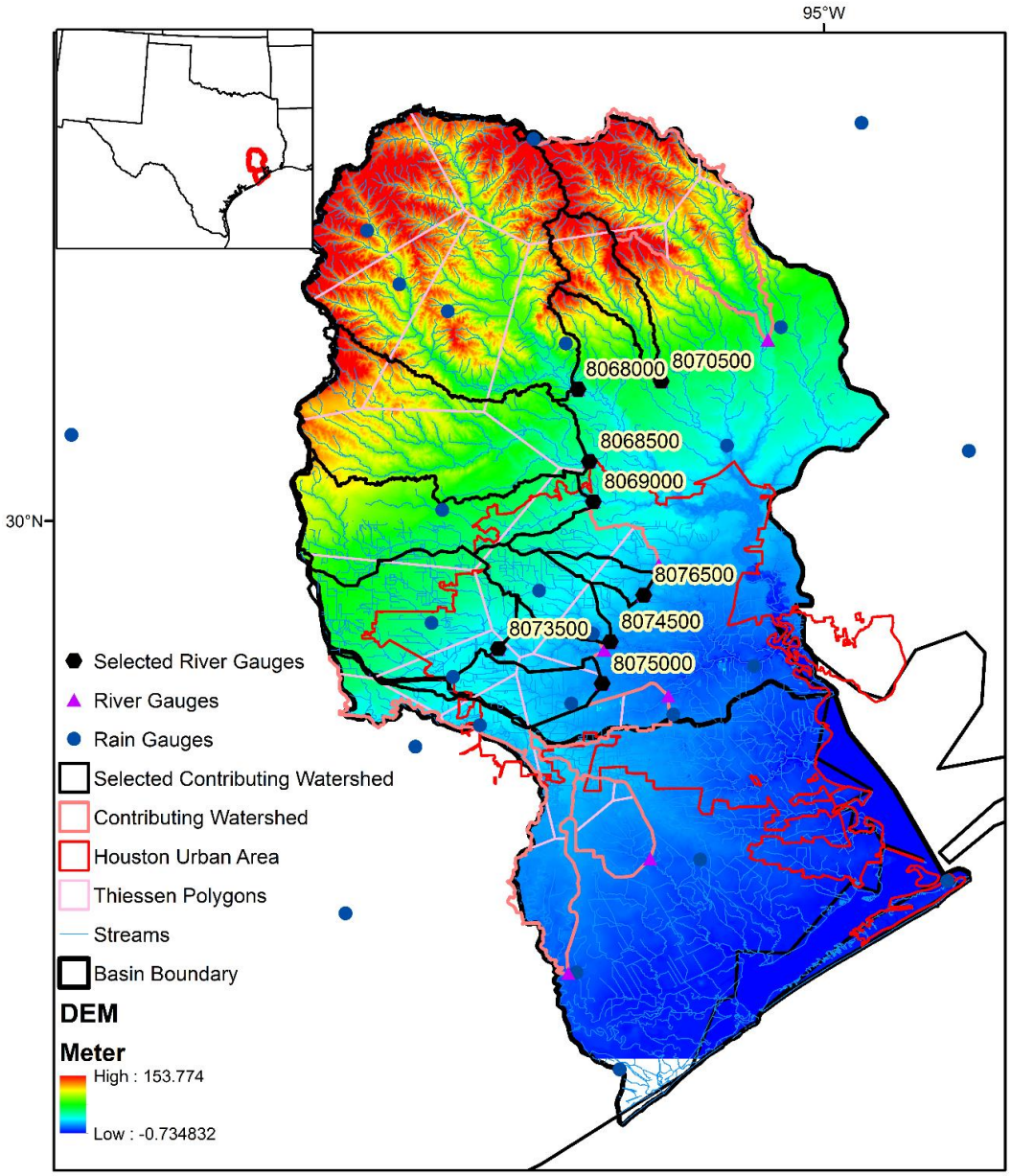

Figure 3.2. The San Jacinto River Basin and the selected watersheds.

3.2 DATA

3.2.1 TC track Data & Precipitation Data

Information about the position, size and maximum wind speed of TCs was extracted from the National Hurricane Center's Atlantic basin hurricane database (HURDAT). HURDAT has 6-hour observations of TC positions dated from 1895 to present. All tropical disturbances, depressions, storms, and category 1–5 hurricanes were included if they made landfall in Texas or passed within 500 km of Texas. Many long-term TCP studies have relied on rain gauge data [*Konrad et al.*, 2002; *Kunkel et al.*, 2010; *Nogueira and Keim*, 2010; *Barlow*, 2011]. Gauge data provide the opportunity to characterize long-term variations in TCP. The accuracy of gauge-based data are highly dependent on the density and uniformity of the gauge network. There are 1358 stations from the Cooperative Observing Network within Texas, but only 353 have relatively complete records (51 to 60 years) and only 220 are serially complete (Figure 3.1a). In this study the 353 gauges with relatively complete records were used to evaluate the spatial variations in TCP and the 220 serially complete gauges for the temporal analysis. The larger number of gauges used for the spatial analysis (353) provides a more complete spatial coverage than the 220 gauges. The temporal analysis only uses serially complete gauges to avoid biases due to differences in record length. Both the TC track and precipitation data were used for the first objective

3.2.2 Climatic/Oceanic Forcing Data

The second objective is to use the climatic/oceanic forcing variables as potential predictors to construct statistical models for seasonal TCP metrics in Texas. The NCEP/NCAR reanalysis provides global atmospheric/oceanic variables at a resolution of 2 degree on a daily basis from 1948-present. Different potential independent variables were calculated from the reanalysis data. Several climatic indices were also derived from the NCEP Climate Prediction Center (http://www.cpc.ncep.noaa.gov/data/indices/). The different spatial domains that were used to average the predictors are defined in Table 3.1. Four time periods (1, 3, 6, 12 months before the hurricane season) were used for the temporal averaging, they are abbreviated as MAY (May), M2M (March to May), D2M (December of previous year to May), and J2M (June of previous year to May). The independent variables (Table 3.2) can be classified into global, regional or local predictors according to the spatial domain that was used to calculate the variable. A number of different regions in the oceans were defined including the North Atlantic (NATL), Main Develop Region (MDR), Caribbean (CAR) and Gulf of Mexico (GMX) (Figure 3.3). All possible spatial and temporal combinations of variables that may influence the frequency and characteristics of TCs (e.g., size, intensity and translation speed) that influence Texas were considered. A total of 400 potential predictors were considered.

Table 3.1. Description of spatial averaging areas.

Abbreviation	Description, unit and domain
ATL	Atlantic Ocean (100ºW to 2.5ºW, 0ºN to 30ºN), regional domain
NIÑO34	Niño 3.4 (170ºW to 120ºW, 5ºS to 5ºN), global domain
NIÑO3	Niño 3 (150ºW to 90ºW, 5ºS to 5ºN) , global domain
NIÑO4	Niño 4 (160ºE to 150ºW, 5ºS to 5ºN) , global domain
MDR	Atlantic Main Development Region (MDR) (85ºW to 20ºW, 10ºN to 20ºN) , regional domain
WMD and EMD	Western MDR and Eastern MDR, based on dividing the MDR into these two sub-regions at 52ºW, regional domain
GMX	Gulf of Mexico (95ºW to 80ºW, 20ºN to 30ºN) , regional domain
WGM and EGM	Western GMX and Eastern GMX, based on dividing the GMX into two sub-regions at 87.5ºW, regional domain
CAR	Caribbean sea (87ºW to 61ºW, 9.5ºN to 21.5ºN) , regional domain
WCA and ECA	Western CAR and Eastern CAR, based on dividing the CAR into two sub-regions at 74ºW, regional domain
TX	Texas (94.5ºW to 107ºW, 25.5ºN to 36.5ºN), local domain

Table 3.2. Description of potential predictors used in the statistical modeling.

Abbreviation	Description and unit	Property	Usage in Model
ATP	Air temperature at the surface, local predictor (℃)	Basic	c
SHUM	Specific humidity, local predictor (kg/kg)	Basic	c
RHUM	Relative humidity, local predictor (%)	Basic	c
SOM	Soil moisture, local predictor (mm)	Basic	c
SLP	Sea level pressure, local and regional predictor (millibars)	Basic	c, s
U & V WIND	Zonal wind and meridional wind, local predictor (m/s)	Basic	c
PREW	Precipitable water, local predictor (kg/m^2)	Basic	c
SST	Sea surface temperature, regional and global predictor (℃)	Basic	c, s, ss
RSST	Relative SST, difference between the target region SST and tropical SST, regional and global predictor	Basic	c, s, ss
VSHR	850–200 mbar vertical shear (kt), regional predictor	Basic	c, s
VOR	850 mbar vertical vorticity ($\times 10^{-5}$ s^{-1}), regional predictor	Thermo-dynamic	c
MPV	Maximum potential wind velocity (m/s), regional predictor	Thermo-dynamic	c
SAPI	Sahel Rainfall Index (unitless), global predictor	Basic	c, s, ss
SOI	Southern Oscillation Index (unitless), global predictor	Basic	c, s, ss
NAO	North Atlantic Oscillation (unitless), global predictor	Basic	c, s, ss
QBO	Quasi-Biennial Oscillation (unitless), global predictor	Basic	c, s, ss
PDO	Pacific Decadal Oscillation (unitless), global predictor	Basic	c, s, ss
AO	Arctic Oscillation (unitless), global predictor	Basic	c, s, ss

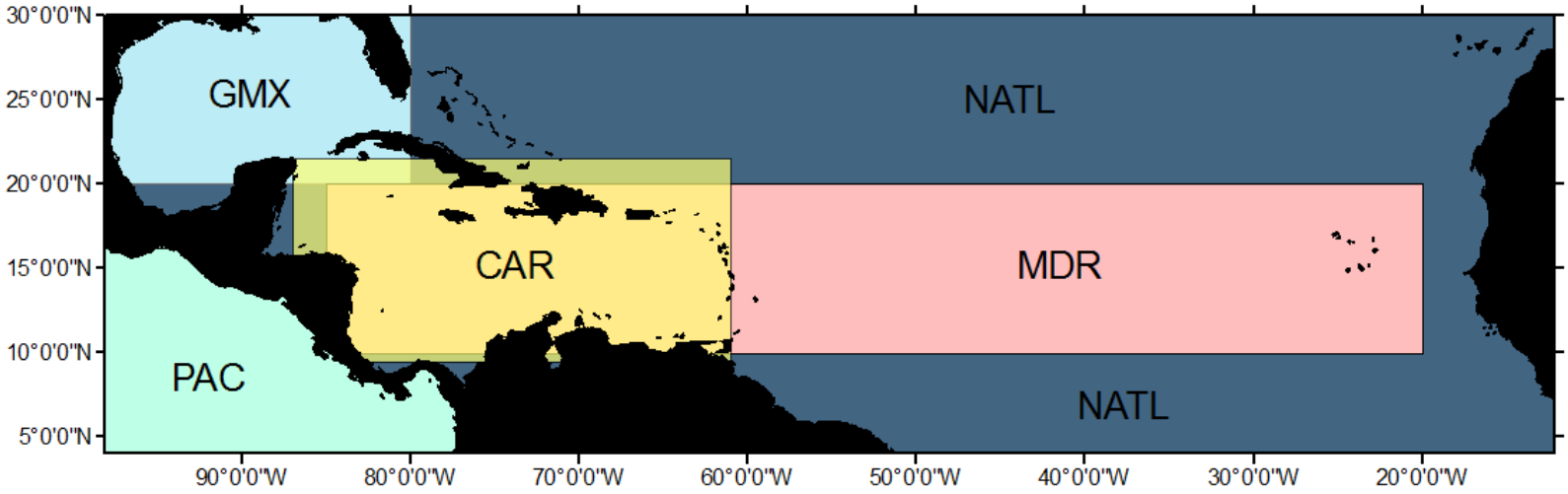

Figure 3.3. Spatial domain for independent variables used for TCP modeling: North Atlantic (NATL), Main Develop Region (MDR), Caribbean (CAR) and Gulf of Mexico (GMX).

The global scale predictors include indices representing signals of ENSO, NAO, QBO, and PDO. ENSO influences the global circulation and vertical shear in the Atlantic, so a variety of different ENSO indices are included. These include SST and Relative Sea Surface Temperature (RSST) for Niño 3, Niño 4 and Niño 3.4 regions in the Pacific, and Southern Oscillation Index (SOI). RSST was calculated by taking the differences between the average SST in Niño regions and the whole tropical ocean. The idea of Niño RSST is based on the concept of Atlantic RSST defined by *Vecchi et al.* [2008]. Niño RSSTs share very similar information with the original Niño SST, but they improve the predictive skill of the TCP models. NAO describes the sea level pressure differences in the North Atlantic and it influences hurricane tracks in the North Atlantic [*Elsner and Kocher*, 2000; *Kossin et al.*, 2010]. QBO is the quasi-biennial oscillation of upper-level winds and it was found to be highly correlated with Atlantic hurricane activity [*Gray*, 1984a]. However, the relationship is now under debate because of its disappearance after the 1990s [*Camargo and Sobel*, 2010]. Pacific Decadal Oscillation (PDO) is a sea surface temperature pattern in the Pacific that can intensify (attenuate) the ENSO's influence on Atlantic hurricane activity when they are in (out of) phase [*Klotzbach and Gray*, 2003].

The regional variables consist of oceanic and atmospheric variables and the thermo-dynamic variables derived from them. SST is considered to be the most important driver of all TC systems because it is highly related to the genesis, track and intensity of TCs [*Gray*, 1984b; *Emanuel*, 1991]. RSST is defined as the SST difference between the North Atlantic and the tropical mean (30 °N to 30 °S). There is a very

strong relationship between RSST in the Atlantic and the TC frequency in the North Atlantic [*Vecchi et al.*, 2008]. Here the original Atlantic RSST and RSST of other spatial averaging domains are both used to obtain additional predictors. Vertical shear (VSHR) is another important predictor since reduced vertical shear is associated with enhanced TC activity [*DeMaria*, 1996; *Vecchi and Soden*, 2007]. VSHR is calculated as the difference between the winds at 200 mb and 850 mb. TCs are not able to form with a zero vorticity of the air flow because it helps TCs to keep on spinning [*Emanuel*, 2003]. Low level vorticity may influence TC's destruction power (highly related to the maximum wind speed) [*Emanuel*, 2007] and the motion (track) [*Flatau et al.*, 1994; *Emanuel*, 2003]. The TC vortices can alter their environmental vorticity distribution and induce a poleward and westward drift of the TC [*Davies*, 1948; *Rossby*, 1949]. The large background vorticity can also interact with vertical shears and produce beta gyres with profound influences to TC tracks [*Shapiro*, 1992; *Wu and Emanuel*, 1995; *Smith et al.*, 2000]. Low level vorticity is frequently used in the seasonal TC genesis prediction [*Camargo et al.*, 2009; *Belanger et al.*, 2010] and the power dissipation index estimation [*Emanuel*, 2005; 2007]. *Emanuel* [2005] also mentioned that the potential intensity, low-level Vortices and vertical wind shear are highly correlated with each other. The maximum potential velocity (MPV) was included because it describes the theoretical maximum wind speed that storms can attain [*Emanuel*, 1995; *Holland*, 1997]. It is calculated from the interactions between sea surface temperature and atmospheric thermodynamic profiles [*Emanuel*, 1991; *Holland*, 1997]. Emanuel's version of MPV (maximum wind velocity) is used as a predictor. A TC system is characterized by a low-

pressure convection center [*Landsea et al.*, 1999], so sea level pressure (SLP) has been used in many seasonal TC counts forecasting models and is also included here.

Since TCs can interact with the land surface after they make landfall, a number of local predictors are also evaluated [*Bosart et al.*, 2000; *Wu et al.*, 2006; *Matyas*, 2008]. Air temperature, specific and relative humidity, precipitable water, and soil moisture have all been included as potential predictors. SLP and zonal and meridional winds have also been included as potential predictors since they may impact the movement and duration of TCs. All of these local variables are obtained by averaging over Texas. All independent variables mentioned above are standardized into z scores before fitting to the model. All the dependent variables are kept in their original unit.

3.2.3 USGS Historical Discharges and Land Use/Cover Change Data

The San Jacinto River basin is the study area for objective 3. It is located in southeastern Texas (Figure 3.2) and includes watersheds covering the metro and suburban area of Houston. They are either dominated by intensely developed land or have been undergoing rapid urbanization. The eight selected river gauges have complete data record (Table 3.3) and covers different types of watershed characteristics (size, shape, and land use condition). Watersheds for gauges 8045000, 8076500, 8073500, 8075000 (Whiteoak Bayou, Halls Bayou, Buffalo Bayou, and Brays Bayou) are located near the center of Houston. The remaining four watersheds are located in suburban areas north of Houston, which are undergoing rapid urbanization. Daily stream discharge for all eight watersheds was extracted from the U.S. Geological Survey (USGS) database (http://nwis.waterdata.usgs.gov/nwis/) from 1950 to 2009.

Table 3.3. Summary of the stream flow data and watershed characteristics associated with the selected USGS stations.

Station	Lat	Lon	Contributing Area (km^2)	Record Length (yrs)	Station Name
8074500	29.78	-95.40	242.7	60	Whiteoak Bayou at Houston, TX
8076500	29.86	-95.33	88.4	55	Halls Bayou at Houston, TX
8073500	29.76	-95.61	724.2	60	Buffalo Bayou nr Addicks, TX
8075000	29.70	-95.41	276.8	60	Brays Bayou at Houston, TX
8070500	30.26	-95.30	271.6	60	Caney Ck nr Splendora, TX
8068000	30.24	-95.46	2147.3	60	W Fk San Jacinto Rv nr Conroe, TX
8068500	30.11	-95.44	1054.3	60	Spring Ck nr Spring, TX
8069000	30.04	-95.43	725.2	60	Cypress Ck nr Westfield, TX

Daily precipitation data are from 27 Cooperative rain gauges (black dots in Figure 3.2), a subset of the 220 gauges selected for objective 1. They all have a complete 60 year observation record. Gauge precipitation is interpolated using Thiessen polygons [*Thiessen*, 1911]. Thiessen polygons were then used to calculate the weighted surface precipitation for each selected watershed.

Historical Land Use/Cover data from four periods (1980, 1992, 2001 and 2006) were used to evaluate the influence of urbanization on discharge in selected watersheds. The 1980 land use data are from the 'Enhanced Historical Land-Use and Land-Cover Data Sets of the U.S. Geological Survey'. It has a 30 by 30 meter resolution and it demonstrates the Land Use/Cover information from the 1970s and 1980s [*Price*, 2006]. The 1992, 2001 and 2006 land use/cover raster are obtained from the USGS Multi-Resolution Land Characterization (MRLC) Consortium with the same 30 by 30 meter resolution (www.mrlc.gov/). The original classifications have been reclassified into 5 major classes (Table 3.4) for better interpretation of major changes in the Land Use/Cover.

3.3 Methods and Models

3.3.1 TCP Extraction, Interpolation and Statistical Analysis for Objective 1

Typically a 500 km buffer has been used as the search radius in previous TCP studies [*Kunkel et al.*, 2010; *Larson et al.*, 2005] because the radius of outer closed isobar (ROCI) in the Atlantic is typically less than 550 km [*Merrill*, 1984]. The ROCI is defined as the average of distance from the TC center to the closed isobar in four

Table 3.4. Rules and Land Use/Cover Classification

Year	Developed Land	Grass and Agriculture Land	Forest	Water	Wetland
1980	11.Residential 12.Commercial and services 13.Industrial 14.Transportation,communication, utilities 15.Industrial and commercial complexes 16.Mixed urban or built-up land 17.Other urban or built-up land	21.Cropland and pasture 22.Orchards,groves,vineyards, nurseries, and ornamental horticultural 23.Confined feeding operations 24.Hther agricultural land 31.Herbaceous rangeland 32.Shrub and brush rangeland 33.Fixed rangeland	41. Deciduous forest land 42. Evergreen forest land 43. Mixed forest land	51.Streams and canals 52.Lakes 53.Reservoirs 54.Bays and estuaries	61.Forested wetland 62.Nonforested wetland
1992	21. Low Intensity Residential 22. High Intensity Residential 23.Commercial/Industrial/Transportation	51.Shrubland 61.Orchards/Vineyards/Other 81.Pasture/Hay 82.Row Crops 83.Small Grains 85.Urban/Recreational Grasses	41.Deciduous Forest 42.Evergreen Forest 43.Mixed Forest	11.Open Water	91. Woody Wetlands 92.Emergent erbaceous Wetlands
2001	21.Developed, Open Space 22.Developed, Low Intensity 23.Developed, Medium Intensity 24.Developed, High Intensity	52.Shrub/Scrub 71.Grassland/Herbaceous 81.Pasture/Hay 82.Cultivated Crops	41.Deciduous Forest 42.Evergreen Forest 43.Mixed Forest	11.Open Water	90.Woody Wetlands 95.Emergent Herbaceous Wetlands
2006	21.Developed, Open Space 22.Developed, Low Intensity 23.Developed, Medium Intensity 24.Developed, High Intensity	52.Shrub/Scrub 71.Grassland/Herbaceous 81.Pasture/Hay 82.Cultivated Crops	41.Deciduous Forest 42.Evergreen Forest 43.Mixed Forest	11.Open Water	90.Woody Wetlands 95.Emergent Herbaceous Wetlands

directions (north, east, south and west) [*Merrill*, 1984]. However, using a uniform ROCI radius (500 km) to search for the TCP region can be problematic because it may underestimate or overestimate the entire region where TC-related precipitation is occurring. About 10% of TCs have an ROCI larger than 550 km [*Kimball and Mulekar*, 2004]. Although the average TC size in the Atlantic Ocean is smaller than in the Pacific Ocean [*Merrill*, 1984], TCs in the Gulf of Mexico tend to have larger ROCI and smaller eyes [*Kimball and Mulekar*, 2004] and their sizes are more variable than other regions within the Atlantic [*Quiring et al.*, 2011]. Translation speed defines how fast the TC moves and it also vary greatly in different TCs [*Rego and Li*, 2009]. TCP can extend beyond a distance of 500 km even when considering an average size TC moving at an average speed over a 24 h period. Therefore, this study used a new method called the Moving ROCI Buffer Technique (MRBT) to identify daily TC precipitation from a network of rain gauges.

The Moving ROCI Buffer Technique (MRBT) used in this study was inspired by the Objective Synoptic Analysis Technique (OSAT) developed by *Ren et al.* [2007]. The OSAT was first applied to TCs in China and it produced results that are comparable to TCP partitioning done by weather forecasters [*Ren et al.*, 2006]. The OSAT procedure was tested in Texas and it was found that the original parameters used by *Ren et al.* [2007] are not appropriate in Texas because of differences in gauge density and TC size. In addition, both the OSAT and the standard approach of using a set radius (e.g., 500 km) are not ideal for identifying TCP because they fail to consider the TC translation speed. Both methods use only one location for the TC each day. This may result in an

underestimation of TCP if the TC is very large and/or the TC is moving rapidly. Most previous studies have also not considered the difference between the time when the rain gauges are read (time of observation) and when the position of the TC is recorded. HURDAT records the location of the center of circulation four times/day at 0:00, 6:00, 12:00 and 18:00 Coordinated Universal Time (UTC), while precipitation measurements for the Cooperative Observing Network are primarily made in the morning (e.g., 7 a.m. local time). These shortcomings in the methodologies that have previously been applied to extract TCP from a network of rain gauges motivated the development of MRBT. The MRBT approach is accurate, straightforward to apply and is easily transferable to other regions.

The radius of outer closed isobar (ROCI) was used for identifying locations receiving TCP because *Matyas* [2010] found that the ROCI encompasses the entire rain field in 90% of the cases they examined. HURDAT provides relatively complete information about ROCI for most of TCs examined in this study (ROCIs are available for 71% of the storms). For those observation times where the ROCI is missing, it is replaced with the median ROCI (333 km) calculated using all TCs with ROCI available in the study region. Since most of COOP stations recorded precipitation in the morning, the HURDAT observations times were converted from Coordinated Universal Time (UTC) to the Central Standard Time (CST). Then 12:00 (day -1), 18:00 (day -1), 0:00 (day 0), and 6:00 (day 0) CST have been selected as the HURDAT observations for measuring daily TCP. This accounts for the position and movement of the TC from the afternoon of the previous day (day -1) through the morning of the current day (day 0).

This is a better method to match the position of the TC with the COOP observations since it assumes all of the gauges measure precipitation in the morning. The MRBT uses the HURDAT information on the location of the center of the TC to construct four circles whose radii are based on the HURDAT ROCI. The four circles are then merged and the combined area is used to identify COOP gauges that may be receiving TCP (Figure 3.1b). This approach is repeated for each TCP day, so that the size of the contributing area varies as a function of the location and forward speed of the TC and as a function of the ROCI associated with the TC. All of the gauges that are located within this area on a given TCP day will be considered for calculating the TCP metrics. The spatial analysis includes a slightly larger number of TCP days than the temporal analysis because it is based on 353 gauges while the temporal analysis is only based on 220 gauges. Therefore, some of the TCs that only influence a small area of Texas (e.g., they graze the western boundary of the state) are not captured by the less dense gage network used for the temporal analysis. The spatial and temporal results will be interpreted and presented separately for this reason.

Daily TCP data from gauges were interpolated to a 0.25° grid covering Texas using Inverse Distance Weighting. This grid size was selected because it is commonly used for many precipitation products (e.g., Tropical Rainfall Measuring Mission (TRMM) Multisatellite Precipitation Analysis, or TMPA) [Huffman et al., 2007], and modeling studies [Chen and Knutson, 2008; Shepherd et al., 2007; Vorosmarty et al., 1996]. A gridded field was generated for every TCP day and the daily fields were aggregated for the monthly and annual analyses. The annual TCP metrics that were

considered in this study include: TCP depth, TCP's contribution to the total precipitation and TCP volume. Daily TCP depth, area, and annual maximum event TCP were also calculated by determining the mean based on all of the TCP days within a given year.

Since the size of the region receiving TCP varies significantly from day to day, it is necessary to use an area-weighted approach when calculating the annual TCP depth. For each TCP day a coefficient was calculated as the TCP area for that day divided by the annual averaged daily TCP area for the year. Area-weighted daily TCP is obtained by multiplying the daily coefficients with corresponding daily TCP depths (calculated by averaging the daily TCP across the grid cells with rainfall). Finally, annual TCP are based on summing the area-weighted TCP for all days. The area-weighted aggregation helps to account for variations in the area that receives TCP. Seven metrics were calculated for objective 1 on a annual basis: annual TCP (mm), annual TCP volume (km^3), TCP within 100 km of the center of the TC (mm), annual TCP days (number of days), mean daily TCP area (km^2), mean daily TCP (mm), and maximum daily TCP (mm). The timeseries of each metric is evaluated to identify linear trends and low frequency variability (9-year moving average).

Some statistical tests were utilized to analyze the time series in objective 1. The Mann-Kendall test [*Mann*, 1945; *Kendall*, 1975] is a nonparametric method of trend detection that has been applied in climatology and hydrology studies [*Kunkel et al.*, 2010; *Mattar et al.*, 2011; *Morin*, 2011]. It is based on the correlation between ranks of a time series and their time order [*Hamed*, 2008]. The significance of the trends in all possible time series larger than 10 years for all gauges (will be discussed in section 4)

was evaluated using α=0.05. One issue with the Mann-Kendall test is the influences from the serial correlations in the time series [*Hirsch et al.*, 1982; *Hamed and Ramachandra Rao*, 1998; *Villarini et al.*, 2009]. Although most of the TCP time series are annual extreme values that can be categorized as stochastic processes, the modified Mann-Kendall test proposed by *Hamed and Ramachandra Rao* [1998] was still applied. The modified approach computes the new variance of the Mann-Kendall trend test statistic by considering the effects from the autocorrelation in the time series. An autocorrelation analysis was also applied to test whether the annual values of the 7 metrics are serially correlated.

Finally, the de-trended time series was analyzed with the multitaper spectral analysis method [*Thomson*, 1982]. This methodology reduces the variance of spectral estimates by using small set of tapers [*Thomson*, 1982; *Ghil et al.*, 2002]. The approach of *Mann and Lees* [1996] was used to implement this method. The autocorrelation coefficients (ρ) were estimated for each of the TCP time series and the AR(1) "red" noise background signals were generated from the autocorrelations. The spectra were compared between the original TCP time series and their corresponding AR(1) "red" noise background. The "red" noise represents the simplest null hypothesis of stochastic processes in the atmosphere [*Frauenfeld et al.*, 2005] and it allows me to test whether the TCP spectra are statistically significant relative to the null hypothesis of stochastic variability.

3.3.2 Multiple Regression Model for Objective 2

There are many different types of statistical models that have been employed for modeling TC activity. Linear models are used in many studies for skillful forecasting of seasonal TC counts [*Gray*, 1984a; *Gray et al.*, 1993; 1994; *Klotzbach and Gray*, 2003] and TC size [*Quiring et al.*, 2011]. However, strict linear regression model requires the response variables to be normally distributed, which is sometimes not true for the highly stochastic TC datasets. Non-linear models, such as the Poisson series and regression trees have also successfully been applied in several TC activity modeling studies. For example, Poisson models have been used to predict TC frequency and intensity [*Jagger and Elsner*, 2006; *Villarini et al.*, 2010] because of their strengths in fitting extreme value distributions such as the hurricane occurrence. The regression tree model has no prerequisite for the distribution of data and sometime has very good prediction skills. *Konrad and Perry* [2010] used the regression tree model to describe impacts from TC characteristics (speed of movement, size, and strength) and the synoptic features to the amount of TCP in individual storms for the Carolina region.

Both the linear and the Poisson series models have been tested for this study. They finally ended up with very similar predictive skills with same number of independent variables. The regression tree model has also been tested. They can attain more fitting accuracy but with more independent variables, which make the models very complex. And pruning those regression trees into several predictors (~3) will reduce the predictive power significantly, even worse than the linear and Poisson series models. In this dissertation, only results from linear models will be presented because of their

simpler structure and the available knowledge about the physical mechanisms for the model parameters.

Three response variables selected for this study are the annual TCP, annual TCP's contribution and annual TCP events. Probability curves were constructed for all three response variables in comparison with their corresponding normal distributions (Figure 3.4). The response variables basically fit the normal distribution fairly well. Some deviations are evident in both tails of the distribution. The deviations at the low ends are caused by the 6 years with no TCs. Zeros are difficult to predict in multiple linear models. The higher end deviations are mainly due to the highly stochastic nature of TC genesis, tracks and variability in the precipitation generated by individual storms. Those values are kept in the linear models although removing them can improve model predictive skills. The integrity of the response variables was kept because they basically fit the normal distribution as shown by Figure 3.4.

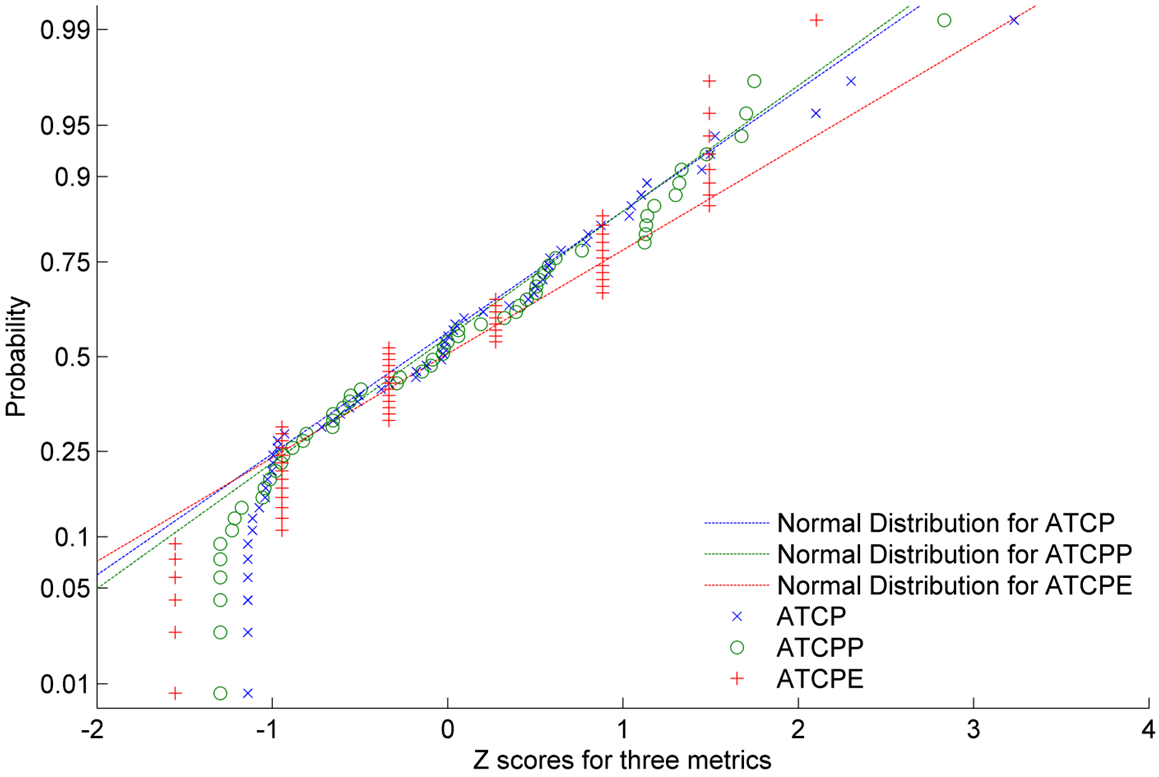

Figure 3.4. Probability of annual TCP (ATCP), TCP percentage(ATCPP) and TCP events (ATCPE) compared with probability of their associated normal distribution (ATCP, ATCPP and ATCPE are normalized to fit in the same scale).

There are 400 potential predictors, so a data mining approach was adopted to select the most appropriate combination of variables that fits the model. During that process, the physical meaning of the predictors was considered. The "leaps" function (freely available from the R statistical package) uses an efficient branch-and-bound algorithm [*Miller*, 2002] to select variables that best fit the regression model. The rationale is to exhaustively search combination of variables attaining the largest adjusted R^2 for each model. A maximum of 3 variables were allowed in the final models in order to avoid over-fitting and to make it possible to explain the physical meaning of the model. Final models were evaluated based on both statistical performance and physical interpretations. I have assessed goodness of fit by calculating both modeled and cross validation mean absolute error, R^2 and adjusted R^2. A leave-one-out cross validation [*Gray et al.*, 1992] was applied for all the selected models to test their stability and predictive skill.

3.3.3 Statistical Tests for Objective 3.

Different statistical tests were used to examine the variability and trends in the time series of maximum annual precipitation, TCP, daily discharge and TCP-related discharge. Daily discharge ratios were calculated by dividing the measured discharge by the area of individual contributing watersheds. Annual maximum discharge ratios were compared with the annual TCP related maximum discharge ratios during 60 years. The TCP related maximum discharge is defined as the maximum daily discharge between day -1 and day +3 of all TCP days during a year. Some studies used a day -3 to day +7 window to select maximum TC-related daily discharge in the eastern U.S [*Waylen*,

1991; *Hart and Evans*, 2001; *Villarini and Smith*, 2010a]. Considering the smaller size of contributing area of the watershed and the local land use [*Rose and Peters*, 2001], the selection of shorter screening window is believed to be more appropriate and accurate.

The Pettitt test [*Pettitt*, 1979] is applied in change point detection for many annual hydrological time series [*Tomozeiu et al.*, 2000; *Zhang et al.*, 2008; *Smith et al.*, 2010; *Villarini and Smith*, 2010]. The method uses a rank-based Mann-Whitney statistics to test whether the means of two samples are different. It is a non-parametric test and so it has fewer constraints regarding the distribution of data [*Pettitt*, 1979; *Reeves et al.*, 2007; *Villarini and Smith*, 2010a]. The TC related extreme precipitation and discharges have skewed time series with outliers, so the Pettitt test is appropriate for identifying change points. The purpose of the change point detection is to compare the happening year of abrupt changes in the hydrological extreme time series and the land use/cover changes. For example, if abrupt changes are detected simultaneously, it may indicate that the severe changes in land use/cover change have major impacts on the hydrological extremes. The change points have been tested for both the mean and variance in the time series for annual maximum discharge, the 90 percentile precipitation and the 90 percentile discharge, which are all continuous time series (no zero-inflated). The variance is also tested because it reveals the changes in the oscillation magnitude in the time series of extreme values [*Katz and Brown*, 1992; *Meehl et al.*, 2000]. The method of variance calculation was adopted from *Villarini and Smith* [2010a]: the squared residuals to the means of a local polynomial "loess" (Local regression) function with a span of 0.75 [*Cleveland*, 1979].

The Mann-Kendall test [*Mann*, 1945; *Kendall*, 1975] was selected to examine the monotonic trend in all the time series at the 95% significance level. I also used the Kwiatkowski–Phillips–Schmidt–Shin (KPSS) [*Kwiatkowski et al.*, 1992] tests whether the time series is stationary around a deterministic trend by examining whether the random walk has zero variance. Since there are 60 years of data, the KPSS test provides some knowledge about whether the trends are stationary.

Finally, some ensemble analyses were undertaken to investigate the relationships between the dynamics of land use/cover and extreme precipitation and discharge (especially related to TCs). Since only four discrete time steps are available for the land use change (1980, 1992, 2001 and 2006), the precipitation and discharge information were also averaged into four periods (1970-1979, 1980-1989, 1990-1999 and 2000-2009).

4. TEMPORAL AND SPATIAL VARIATIONS IN TCP IN TEXAS*

4.1 Spatial Variation of TCP

4.1.1 Daily TC Characteristics and TCP

TC characteristics are summarized in Figure 4.1a since they have a significant influence on the spatial distribution of daily TCP. Figure 4.1a summarizes the direction of movement for all TC days that are considered in Texas. The direction is defined as the angle from the vector of TC movement (black arrow in Figure 3.1b) to the north (clockwise). Since the direction of movement commonly changes during each TCP day, the direction of movement was determined using the first and last observations of TC position recorded in HURDAT for each TCP day. Most of the TCs that contribute TCP to Texas moved towards the north or west when they make landfall. As the TCs continue to move further inland they are influenced by both the Coriolis force and the increased jet stream and upper-level westerlies, therefore they tend to be moving towards the north and east as they exit the state. This typical path is illustrated by Hurricane Ike (Figure 3.1b). During the first TCP day associated with Hurricane Ike the TC moved towards the west.*

---

* Part of this section is reprinted with permission from "Variations in Tropical Cyclone Precipitation in Texas (1950 to 2009)" by Zhu and Quiring, 2012. *Journal of Geophysical Research-Atmospheres*, in press, Copyright [2012] by John Wiley & Sons, Inc.

On the second TCP day the direction of movement shifted to the northwest and during the third day Ike was moving in a northeasterly direction when it exited the state. Of course there is a large amount of variability in TC tracks and direction of movement. In Texas, some TCs can stall and move back towards the south. These cases are important because they are often associated with slow moving systems that generate extreme precipitation. Figure 4.1b is a histogram of daily TC translation speed. There is a large range in the translation speed of TCs in Texas, although most of the TCs travel at <30km/h. This variability illustrates why it is important to consider TC translation speed in the TCP extraction method developed for this paper. The translation speeds have been averaged for each storm and compared with the total TCP volume generated in Texas for each storm (Figure 4.2). Many of the storms that generated large amounts of TCP (e.g., >25 km^3) are associated with relatively slow translation speeds (<10 km/hr). However, there are also many smaller TCP events that are associated with slow moving storms, making the sample size for the first box (storms with translation speed <10 km/hr) very large (71 out of 152 events). Only 3 of the storms with a translation speed greater than 20 km/h had larger than normal TCP (two had < 30 km^3 of TCP). However, there are fewer TC events associated with higher translation speeds (only 45 events had a translation speed >15 km/hr).

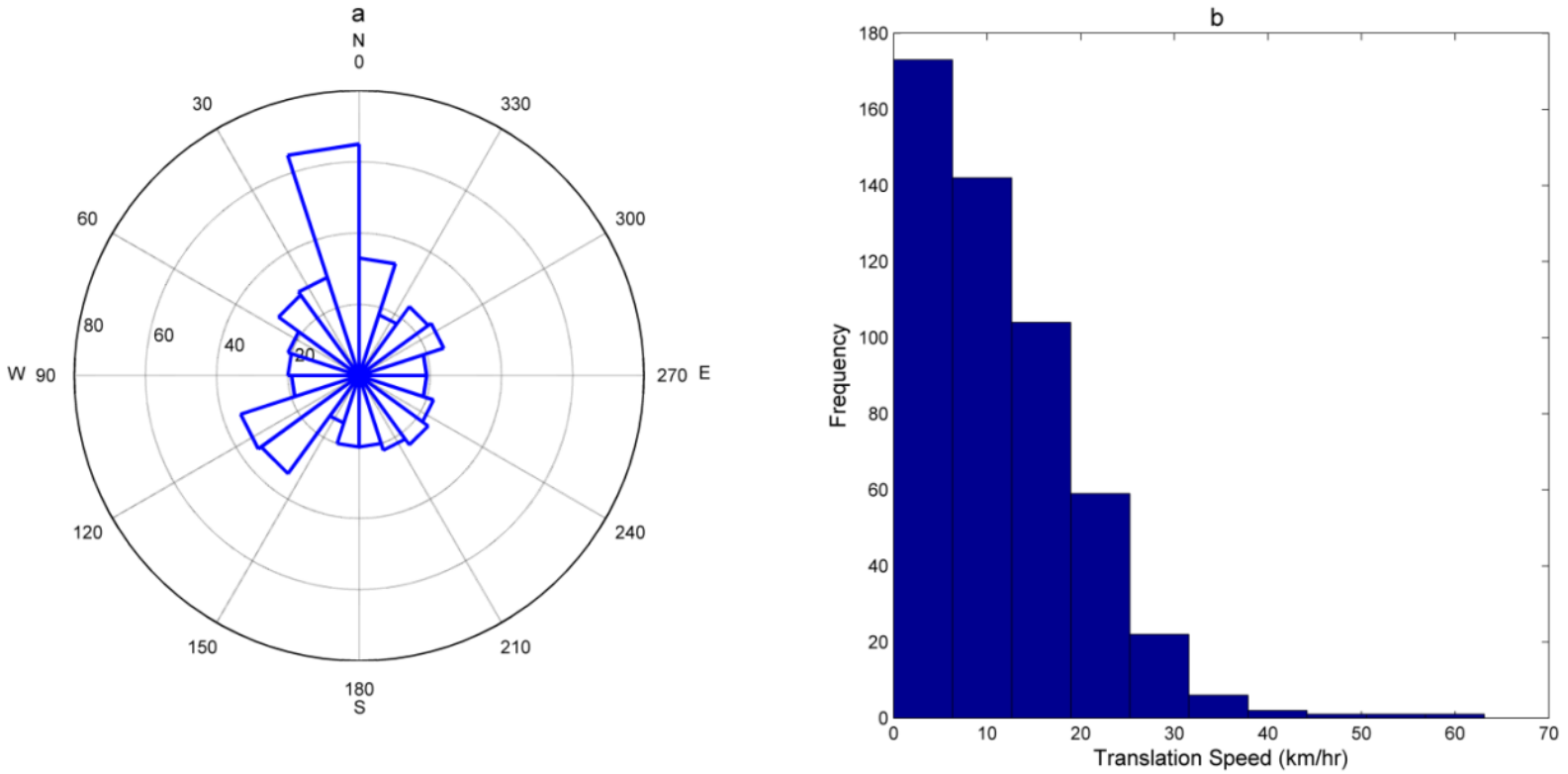

Figure 4.1 a. Distribution of daily TC direction of movement, b. Histogram of TC translation speed for all TCs that influenced Texas between 1950 and 2009.

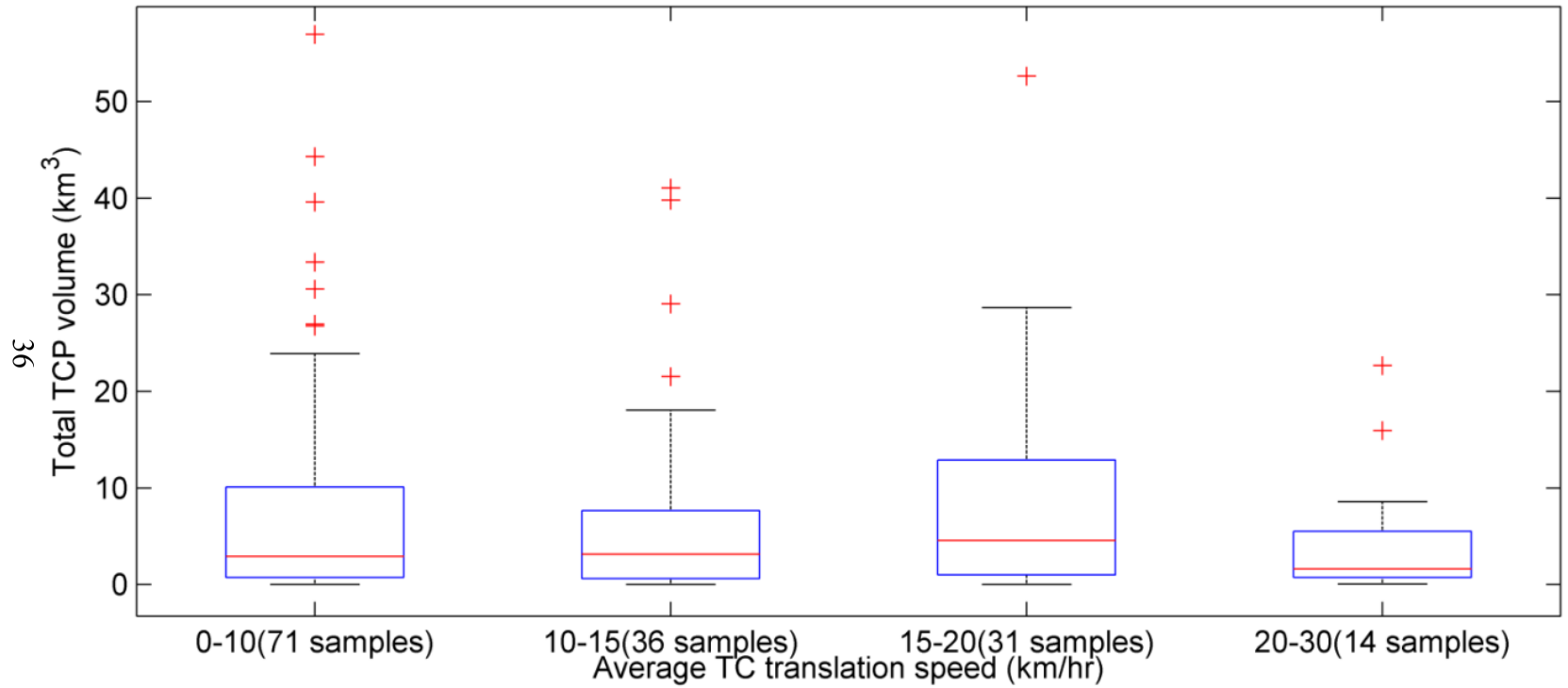

Figure 4.2. Box-Whisker plot of total TCP volume for 4 groups of TC events divided by average TC translation speed. Boxes represent 25th and 75th percentile inter-quartile ranges. Median extents are shown by the red line in each box. Whiskers (black horizontal lines) represent approximately +/–2.7σ and 99.3% coverage if the data are normally distributed. Extents larger (smaller) than the whiskers are shown as individual red crosses.

Figure 4.3 shows the variation of daily TCP as a function of distance from the center of the storm and it is separated into quadrants (e.g., left front, right front, left rear, right rear) based on the TC's direction of movement. The gauge and grid-based TCP data both show a similar pattern. Most daily TCP are below 200 mm, but there are some extreme cases ranging from 300 to 700 mm. The locations that receive less than 100 mm of daily TCP are distributed over a broad area that ranges from 0 to ~1000 km from the storm center. However, TCP is most highly concentrated within 400 km of the storm center. Locations that receive extreme daily TCP (>300 mm) are almost found within 200 km of the storm center. This agrees with previous studies that have identified that precipitation is closely related to hurricane intensity and extreme TCP mostly occurs within ~100 km of the center of circulation [*Molinari et al.*, 1999; *Matyas*, 2010]. The asymmetrical structure of TCs is evident from the spatial distribution of daily TCP and the results conform to those from other TCP studies [*Lonfat et al.*, 2004; *Atallah et al.*, 2007; *Jiang et al.*, 2008; *Villarini et al.*, 2011a]. The front half of TCs is typically associated with more TCP than the rear half because storm motion causes heavier precipitation ahead and to the right of the storm [*Matyas*, 2010]. More locations receive >200 mm on the right side (right-front and right-rear) of the TC than on the left side. Vertical wind shear influences the distribution of the convection in TCs [*Corbosiero and Molinari*, 2002], so the down-shear part (right side in this case) of the

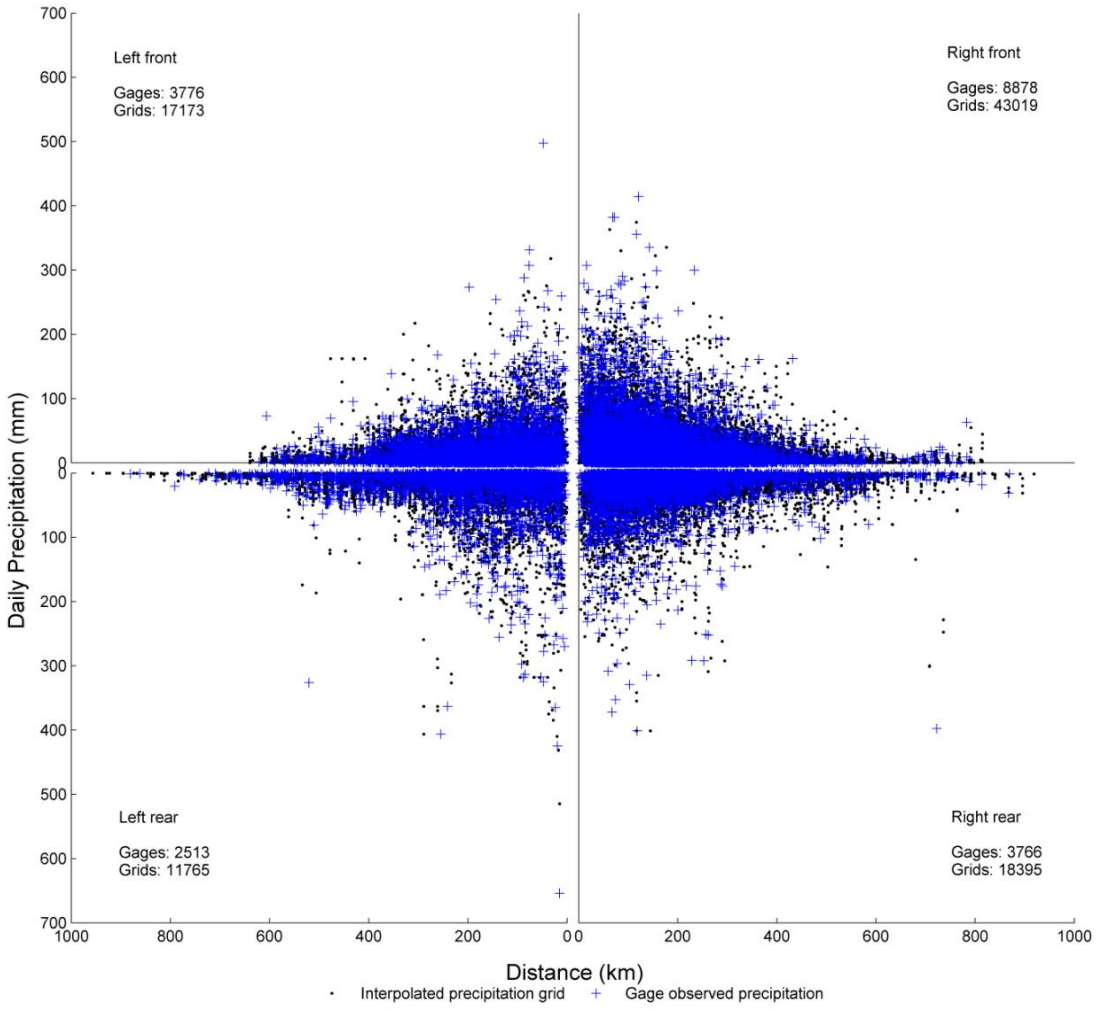

Figure 4.3. Distribution of daily precipitation (mm) (interpolated and gage-based) by quadrant with respect to the direction of movement and center of the TC.

storm is associated with greater precipitation intensity. Many extreme daily TCP events (>300 mm) are all located in the left-rear or right-rear quadrant. Many of these cases (including the historical event with >650 mm daily TCP) were associated with TCs stalled by troughs of cold air mass from the north. These TCs were sometimes pushed back towards the south or were relatively stationary (TS Alison 2001 and TS Claudette 1979).

4.1.2 Monthly TCP

Mean TCP was calculated for each month of the Atlantic hurricane season (June - October) based on 60 years of data from 353 gauges (Figure 4.4. Texas has 65 TCP days in June, coastal Texas receives ~10 mm TCP and the locations with the highest TCP are found in eastern Texas. Although July has 67 TCP days, TCP decreases in terms of the area affected and amount. In August as the TC activity increases (125 TCP days), TCP spreads deeper inland and shows two TCP maxima in eastern and southern Texas. September is the peak of the hurricane season (174 TCP days) and Texas receives the most TCP in September. The spatial pattern of precipitation is dominated by decreases in TCP as one moves inland from the coast. There is a ~100 km wide belt formed along the coast that, on average, receives >30 mm of TCP during September. The amount of TCP decreases greatly in October because of the sharp decrease in TC activity (52 TCP days). Only a few locations in southern and eastern Texas receive ~10 mm of TCP. When the monthly TCP is aggregated for the whole state, September ranks first in monthly mean, maximum and minimum TCP (Table 4.1). Monthly TCP in Texas is basically in phase with variations in Atlantic hurricane activity, which peaks in August

and September [*Hart and Evans*, 2001]. The monthly TCP variations described here basically match with long-term monthly variations in hurricane frequency in Texas shown by *Islam et al.* [2009]. Monthly TCP in Texas is primarily controlled by TC frequency. On average, months with more TC activity receive more TCP.

4.1.3 Annual TCP

A total of 495 days were identified as TCP days between 1950 and 2009. On average there are ~8 TCP days/year. Mean annual TCP (Figure 4.5a) shows a pronounced coast-to-inland gradient. Locations near the coast typically receive much more TCP than inland locations. Those spatial patterns basically agree with the Texas portion of the analysis of annual TCP completed by *Knight and Davis* [2009]. Locations in southeastern corner of Texas receive >80 mm annual TCP, which is the maximum in Texas. However, even regions in far western and northern Texas receive some TCP (<20 mm). TCP's contribution to the annual precipitation is calculated for each location by dividing mean annual TCP by mean annual precipitation (i.e., all sources of precipitation). Generally, TCP contributes >3% to mean annual precipitation in more than half of Texas (Figure 4.5b). Figure 4.5b shows a similar pattern as Figure 4.5a (e.g., influence of TCP decreases as you move further inland), but there is more spatial variability. TCP contributes ~8% of annual precipitation in coastal areas. TCP contributions to annual precipitation are higher in southern Texas than in eastern Texas

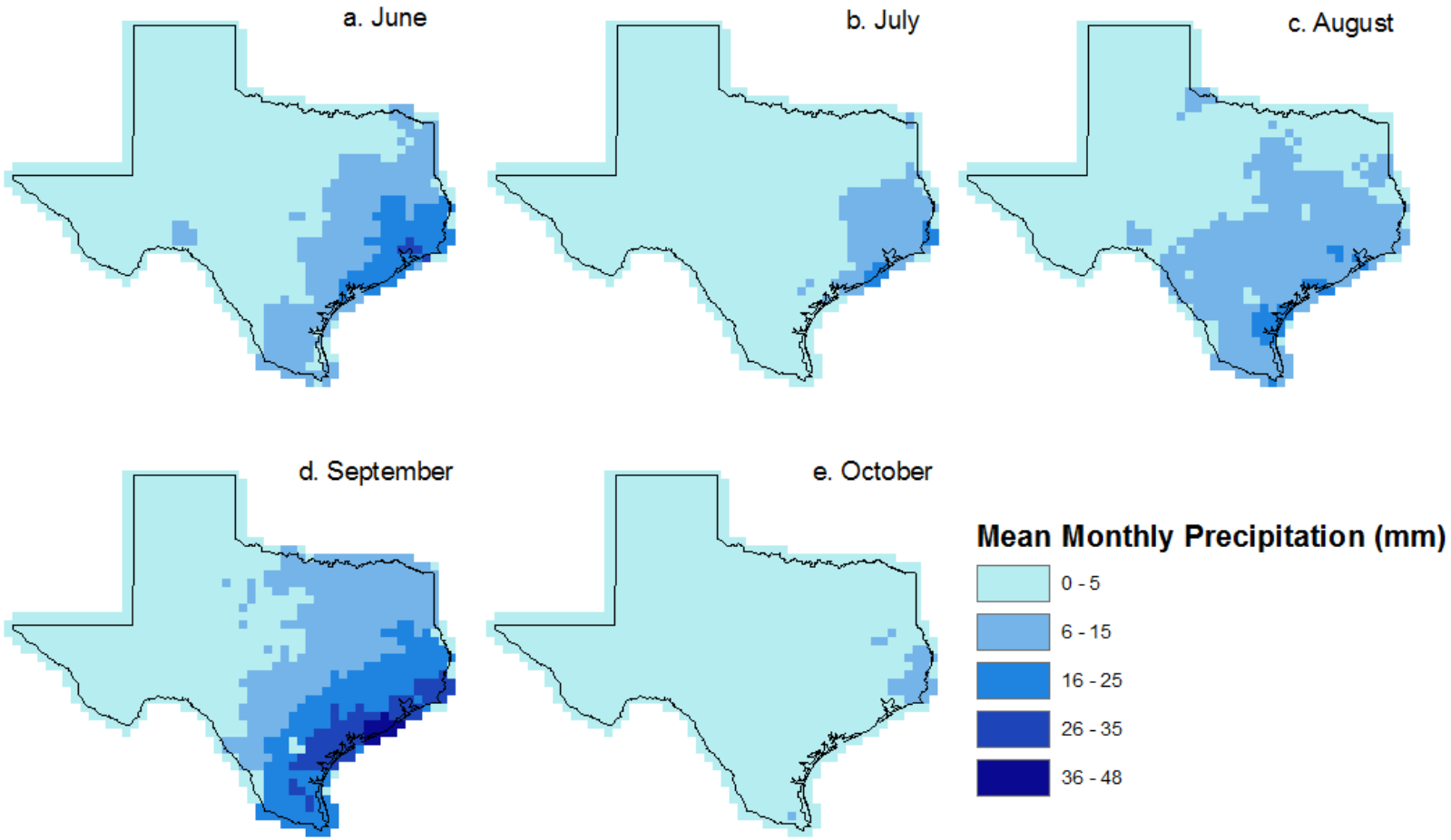

Figure 4.4. Spatial distribution of mean monthly TC precipitation (mm) (1950-2009): a. June, b. July, c. August, d. September, e. October.

Table 4.1. Monthly TC precipitation (mm) based on the entire rainfall region.

	June	July	August	September	October
Mean	10.1	5.6	10.9	18.5	3.6
Maximum	92.8	82.7	54.5	137.6	44.7
Standard Deviation	22.2	13.6	14.8	27.7	8.4

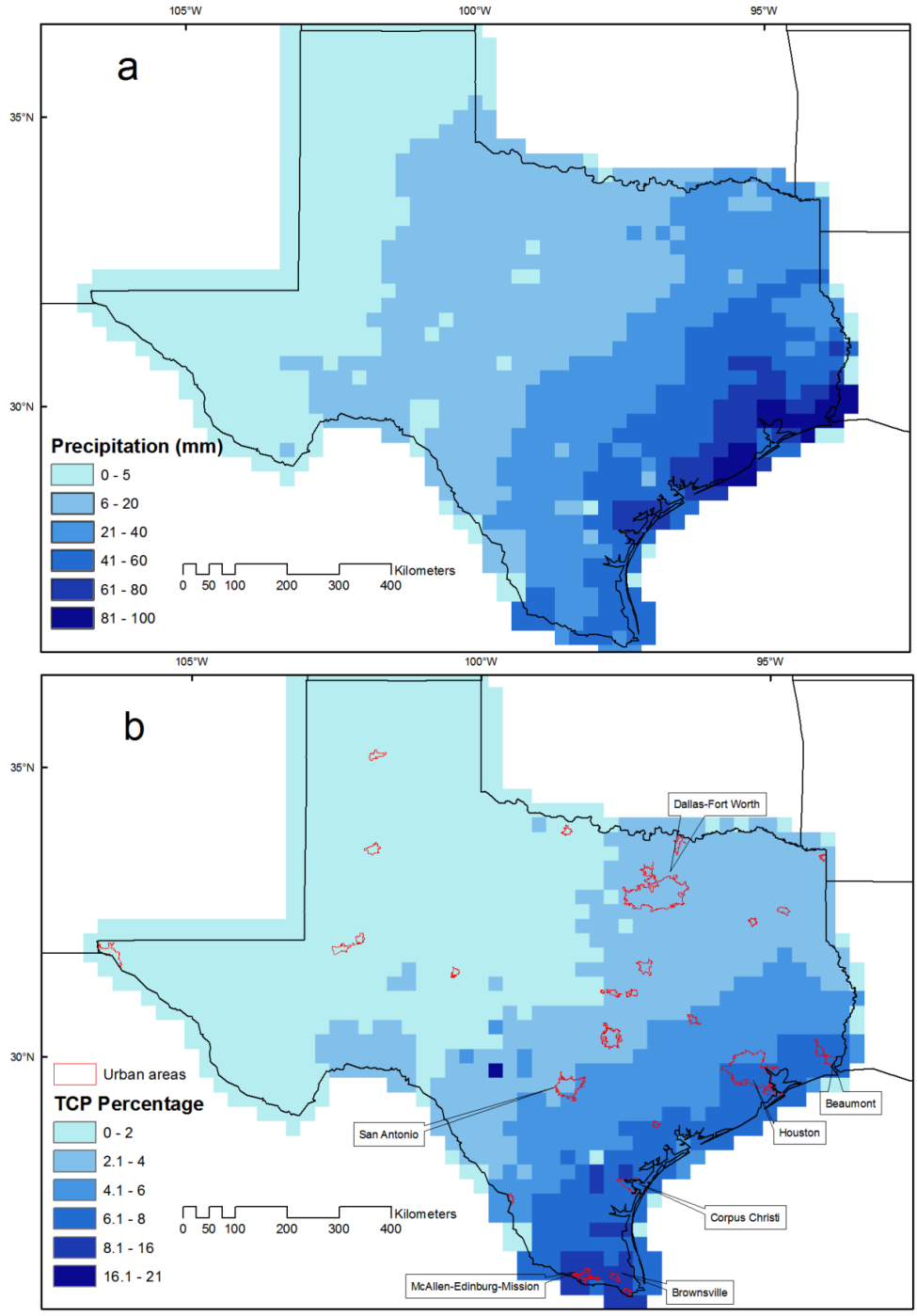

Figure 4.5. Spatial distribution of a. Mean annual TC precipitation (mm), b. Contribution of TC precipitation to annual precipitation (%).

partly because mean annual precipitation is lower in southern Texas. The maximum TCP's contribution in total precipitation in Texas is somewhat greater than previously reported by *Knight and Davis* [2007] (>15% vs. ~12%). The results also show some differences in the spatial pattern of the contribution of TCP to annual precipitation. For example, larger area can be identified in southern and central Texas than shown by *Knight and Davis* [2007] where the contribution of TCP was >8%. In addition, TCP's contribution in the southern and eastern Texas from *Knight and Davis* [2007] is ~3%-4% smaller than the 1931-1961 estimation by *Cry* [1967]. Finally, none of the previous studies have captured the contribution of TCP in western and central Texas. The signal in this region is likely due to several rare TCs that caused extreme precipitation.

4.2 Temporal Variation

The trend in annual TCP was evaluated for each of the 220 gauges by considering all possible combinations of >10 year periods [*McCabe and Wolock*, 2002b]. The number of significant trends for each starting and ending year combination are summarized and displayed (Figure 4.6 and 4.7). There are 1250 time periods between 1950 and 2009 that are >10 years. The number of gauges with significant trends (Mann-Kendall, $p \leq 0.05$) is counted for each period. The analysis was repeated for three of the most important TCP metrics, namely: annual TCP, mean daily TCP and maximum daily TCP.

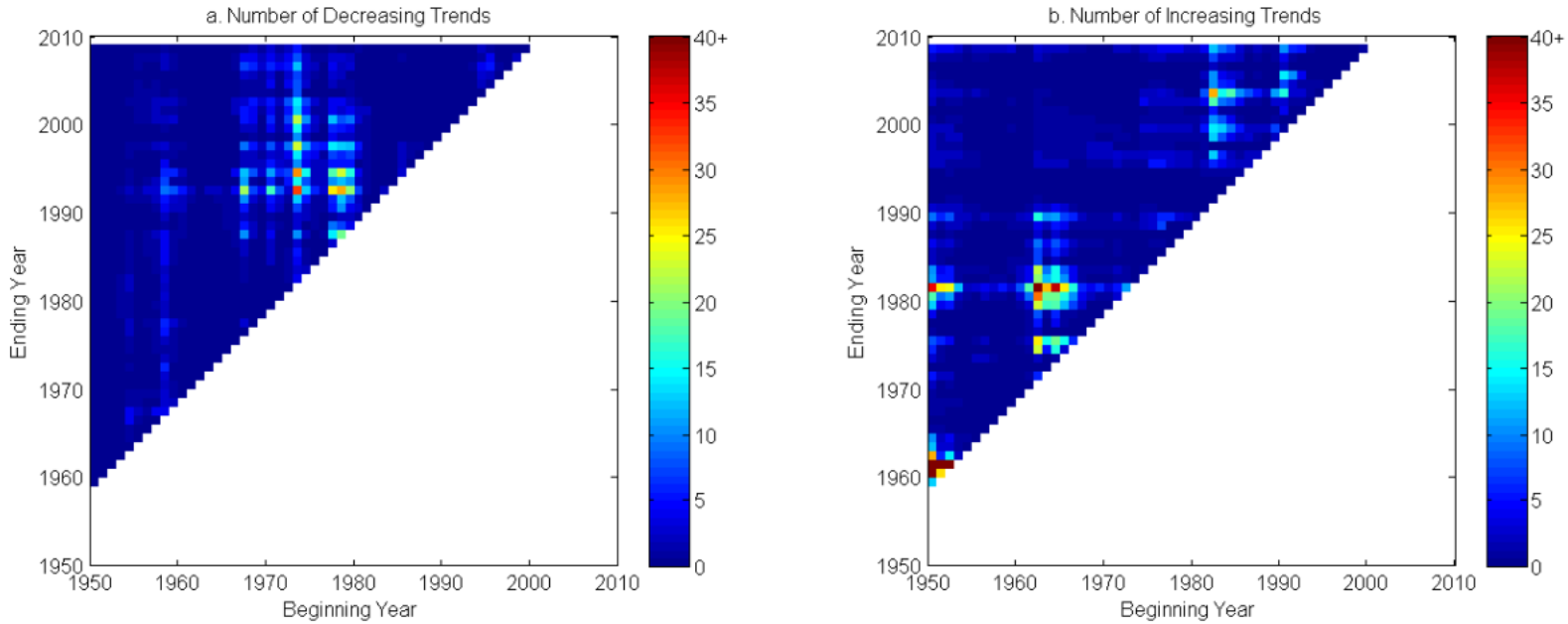

Figure 4.6. Number of stations with statistically significant (95% confidence, Mann-Kendall) decreasing and increasing trends in annual TCP.

There are relatively few statistically significant decreasing and increasing trends for annual TCP (Figure 4.6). The highest concentration of decreasing trends is associated with the time period starting around 1975 and ending around 2000. A maximum of 28 stations (out of 220) have decreasing trends (approximately 13% of the stations). There are also a few decreasing trends starting around 1960. Generally, there are more statistically significant increasing trends (3232) than decreasing trends (1866). There are clusters of statistically significant increasing trends for time periods that start in 1950, 1965 and 1985. Most of those trends have durations less than 30 years. There are only 3 gauges (out of 220) that have statistically significant increasing trends when considering the entire 60 years. The maximum number of stations with increasing trends are found during the period from 1950 to 1961 (12 years of duration) when 90 gauges (41%) have a statistically significant increasing trend.

The trends in the daily TCP metrics (Figure 4.7) are similar to those found in the annual TCP metrics. There is a relatively high concentration of statistically significant decreasing trends for time periods starting between 1970 and 1980. Similar to Figure 4.6, increasing trends for daily TCP metrics in Figure 4.7 are concentrated in three clusters with starting years around 1950, 1965 and 1985, respectively. These results indicate that TCP in Texas is most strongly influenced by intra-decadal variability and that there is no evidence of a statistically significant long-term trend in TCP.

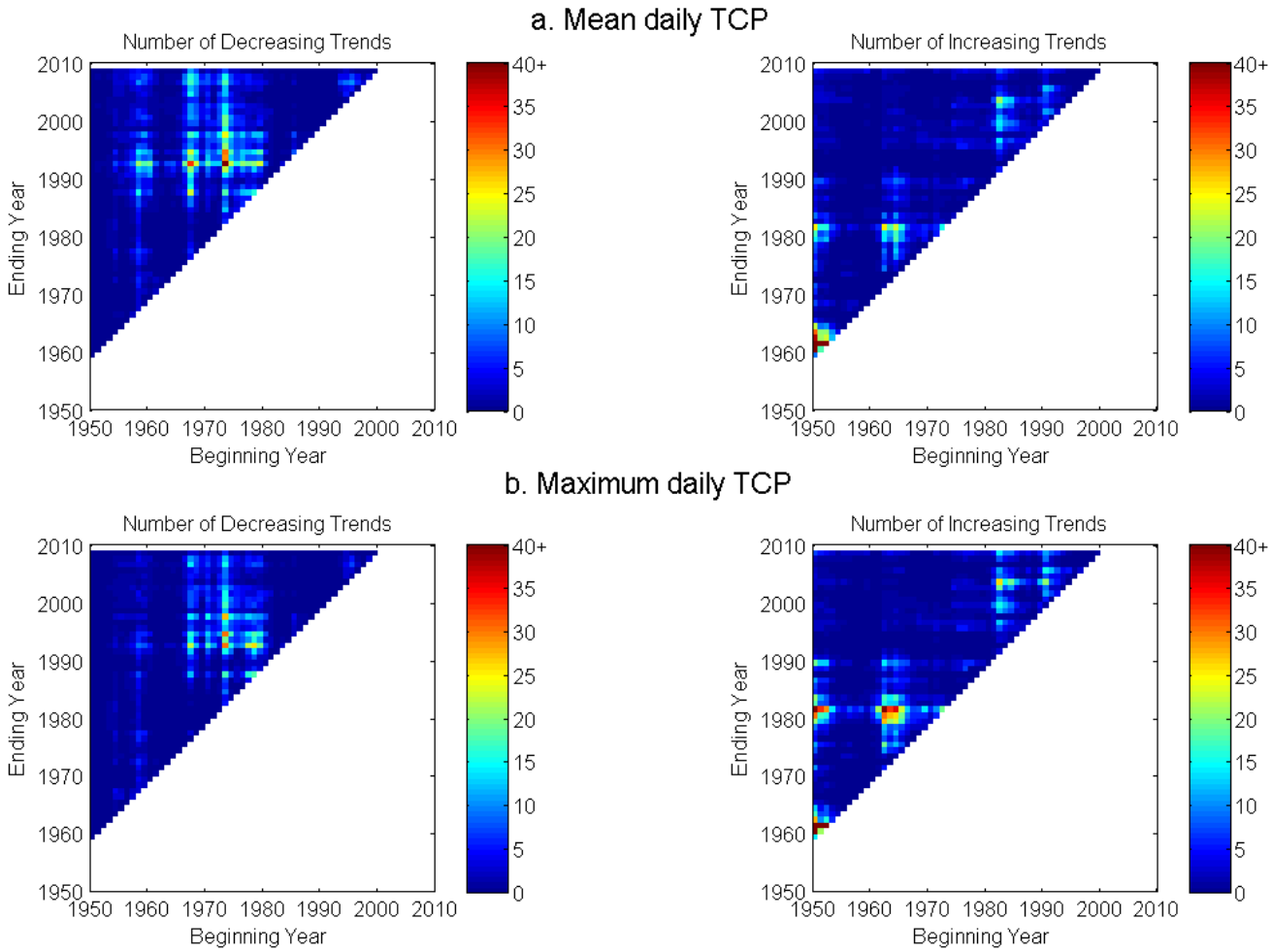

Figure 4.7. Number of stations with statistically significant (95% confidence, Mann-Kendall) decreasing and increasing trends in mean daily TCP (a) and maximum daily TCP (b).

TCP metrics are displayed as black lines in Figure 4.8, the 60-year linear trend (red solid line) and the 9-year moving average (blue solid line) are also shown. There is substantial interannual variability in the TCP metrics (Figure 4.8a & b). The annual average TCP is 123.5 mm with the maximum of 537.4 mm obtained in 1979 (Figure 4.8a). The TCP volume accounts for variations in the number of TCP days, daily TCP area and depth and so it serves as an integrative metric (Figure 4.8b). Large interannual variability is also observed in the annual TCP volume, with a mean of 17.8 km^3 and a maximum 77.6 km^3 also reached in 1979. Therefore, Texas accounts for ~1/5 of the TCP volume in the U.S. since *Noguira et al.* [2010] showed that the mean annual TCP in the U.S. is 107 km^3.

No statistically significant ($p < 0.05$) trend exists when considering the entire 60-year time series for annual TCP and TCP volume. This agrees with the results shown in Figure 4.6. I also tested the auto-correlations in the annual TCP time series and no significant (95% level) auto-correlation lag is observed. The 9-year moving average removes the strong interannual variability and emphasizes the inter- and multi-decadal signals.

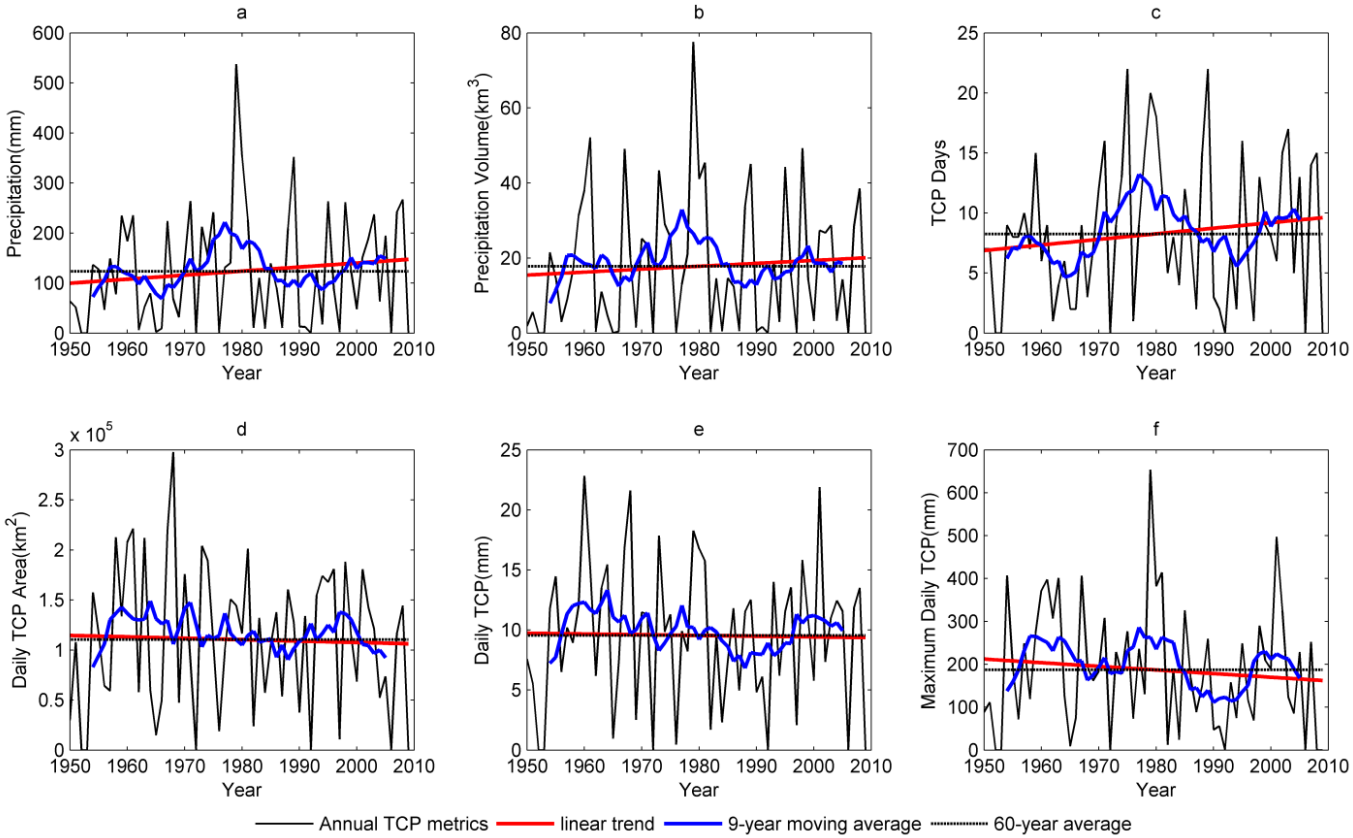

Figure 4.8. Original time series (black line), linear trend (red line), and 9-year moving average (blue line) for the following TCP metrics: a. Annual TCP, b. Annual TCP volume, c. Annual TCP days, d. Mean daily TCP area, e. Mean daily TCP, f. Annual maximum daily TCP.

Both annual TCP depth and volume are determined by daily precipitation depth, TCP area and the annual TCP days. These metrics still have large interannual variability shown in their time series (Figure 4.8c, 4.8d, 4.8e, and 4.8f) and standard deviations (Table 4.2). Since they are showing different information about daily TCP, the signals share less similarity when compared with the signals for annual TCP. The annual TCP days (Figure 4.8c) show good correspondence with the annual TCP, which suggests thatthe TC frequency and duration are important factors for annual TCP in Texas. The daily TCP area (Figure 4.8d) and depth (Figure 4.8e) correspond with each other relatively well, indicating that larger storms may produce more cases of intense daily TCP. The time series for the maximum daily TCP demonstrate abrupt changes, such as the extreme case in 1979 (TS Claudette) and 2001 (TS Allison) (Figure 4.8f). However, the year with the maximum daily TCP intensity is not the year with annual average daily TCP depth and area. The time series for daily TCP metrics also do not show significant autocorrelation.

I have also compared the spectra for all TCP metrics and their associated red noise backgroud (Figure 4.9). Although there are peaks in spectral power that are above the red noise threshold at interannual, biennual, 5-8 year, and >10 year cycles, none of these peaks are statistically significant at the 95% confidence level. The physical mechansims responsible for these patterns are beyond scope of this study.

Table 4.2. Summary of annual and daily TC precipitation metrics.

	Annual TCP (mm)	Annual TCP Volume (km^3)	Annual TCP within 100 km (mm)	Annual TCP Day (Days)	Annually averaged Daily TCP area (km^2)
Mean	123.5	17.8	107.1	8	110416
Maximum	537.4	77.6	629.9	22	297920
Standard Deviation	113.3	17.9	114.1	6	71973

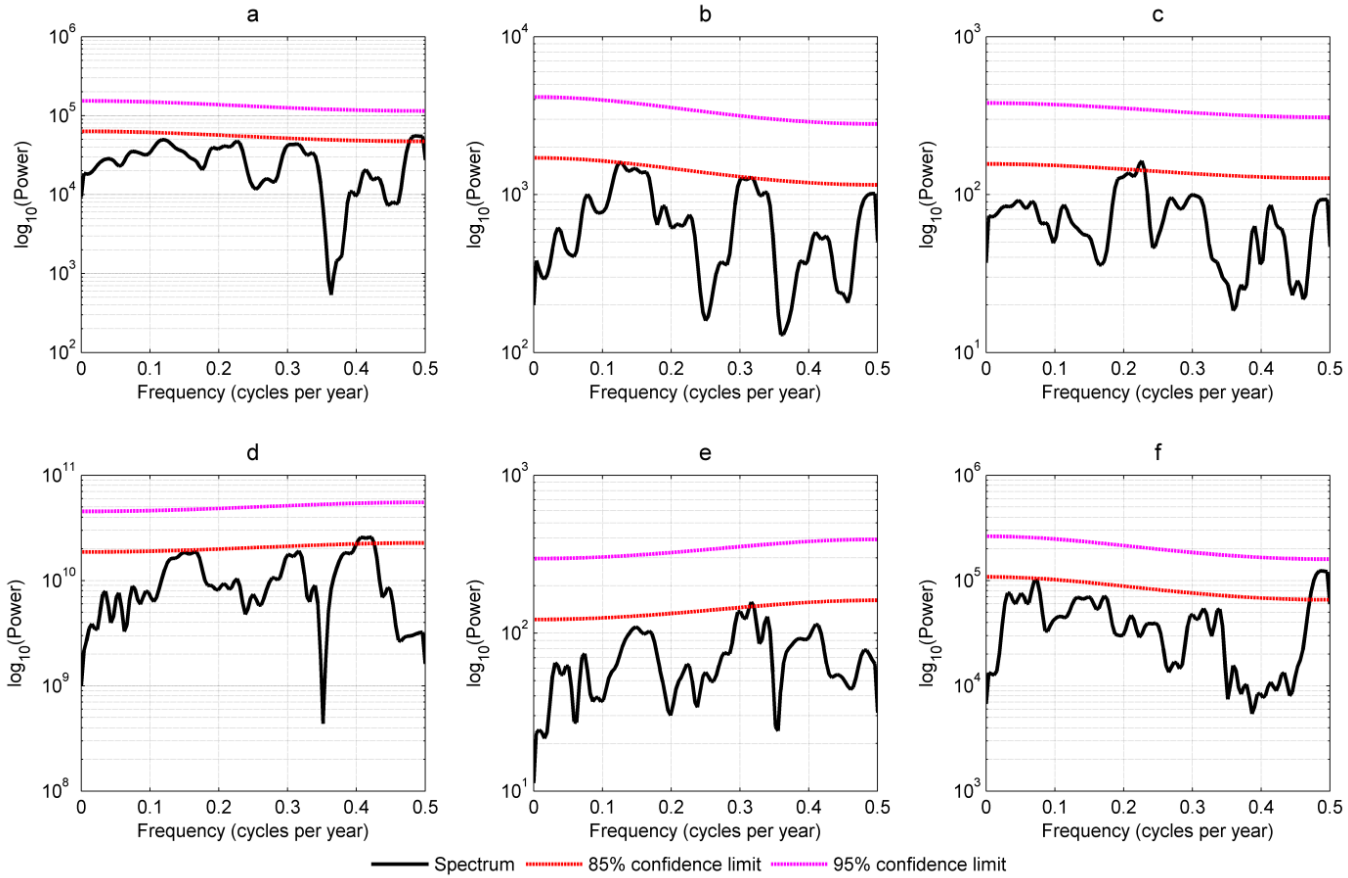

Figure 4.9. Power spectra for annual TCP metrics (black line) compared with the 85% and 95% confidence limit of the "red" noise references: a. annual TCP, b. annual TCP volume, c. annual TCP day numbers, d. annual average daily TCP area, e. annual average daily TCP, f. annual maximum daily TCP.

4.3 TCP Extremes

4.3.1 Probability of Extreme TCP Events

The probability of extreme TCP events is determined by counting the number of times that TCP has exceeded 50 mm (~2 in.) and 100 mm (~4 in.) at each location. The 50 mm and 100 mm have been chosen as extreme daily precipitation thresholds based on previous studies [*Easterling et al.*, 2000]. Daily TCP >50 mm has occurred at least once in most locations in Texas during the last 60 years (Figure 4.10). Not surprisingly, many of the locations with higher frequencies (e.g., >0.10) are in coastal areas. The highest frequencies are located in eastern Texas, where >50 mm daily TCP occur nearly once every two years (>0.5 frequency).

Days with TCP >100 mm are far less frequent (Figure 4.10b). Regions within 150 km to the coastline have frequencies ranging from 0.1 to 0.2. The highest frequency areas are also located in eastern Texas with a frequency of ~0.3. There are a few inland locations that show higher than expected frequencies. These locations are associated with TCs that may re-intensify from interacting with local conditions (e.g., topography or soil moisture), or interacting with extra-tropical frontal systems. Although these situations are relatively rare, they can produce very intense precipitation locally. The frequency analysis generally confirms the findings of *Kunkel et al.* [2010] given that they also found coastal areas are associated with higher probabilities of extreme TC precipitation.

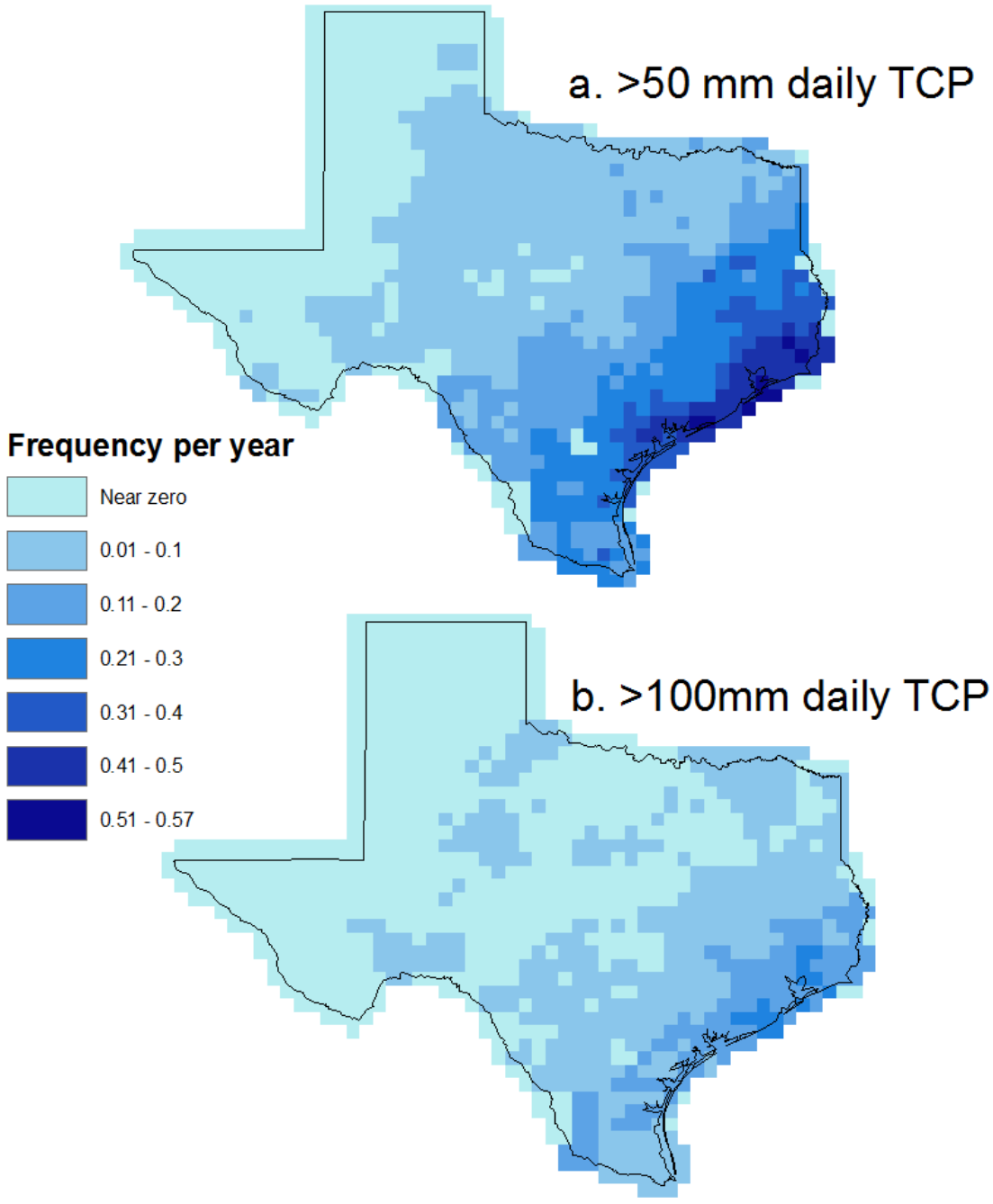

Figure 4.10. Spatial distribution of annual frequency of a. Daily TCP >50 mm, b. Daily TCP >100 mm (calculated from stations with 50+ years of data).

4.3.2 Historical Maximum Events

Historical maximum daily TCP events are associated with a relatively small number of TCs. The historical maximum daily TCP value was selected for each location in Texas and the specific storm that produced it was identified (Figure 4.11). Tracks are shown for 10 TCs that covered the greatest area in Texas (Figure 4.11a). A strong coast-to-inland decreasing pattern is evident (Figure 4.11a). Many coastal locations have daily TCP extremes >350 mm (maximum = 515 mm). However, there is a great deal of variability in the spatial pattern. There are numerous locations of high TCP in central Texas that are associated with these high impact TCs (Figure 4.11b). Together, these 10 TCs cover 2/3 of Texas. The three most important storms, in terms of area affected, are TS Dean (1995), TS Deila (1973) and TS Erin (2007). Many TC systems travel towards the north and west after landfall. Typically TCP intensity gradually decreases as the TC moves inland. However, sometimes TC re-intensify because of interactions with other weather systems or local conditions. These inland TCP events can generate large amounts of precipitation in western and northern Texas, such as the >500 mm/day of TCP that fell in western Texas from Hurricane Alice (1981), or the clusters of TCP extremes (~250 mm/day) in northern Texas associated with TS Dean (1995) and TS Erin (2007). Antecedent soil moisture conditions are one of

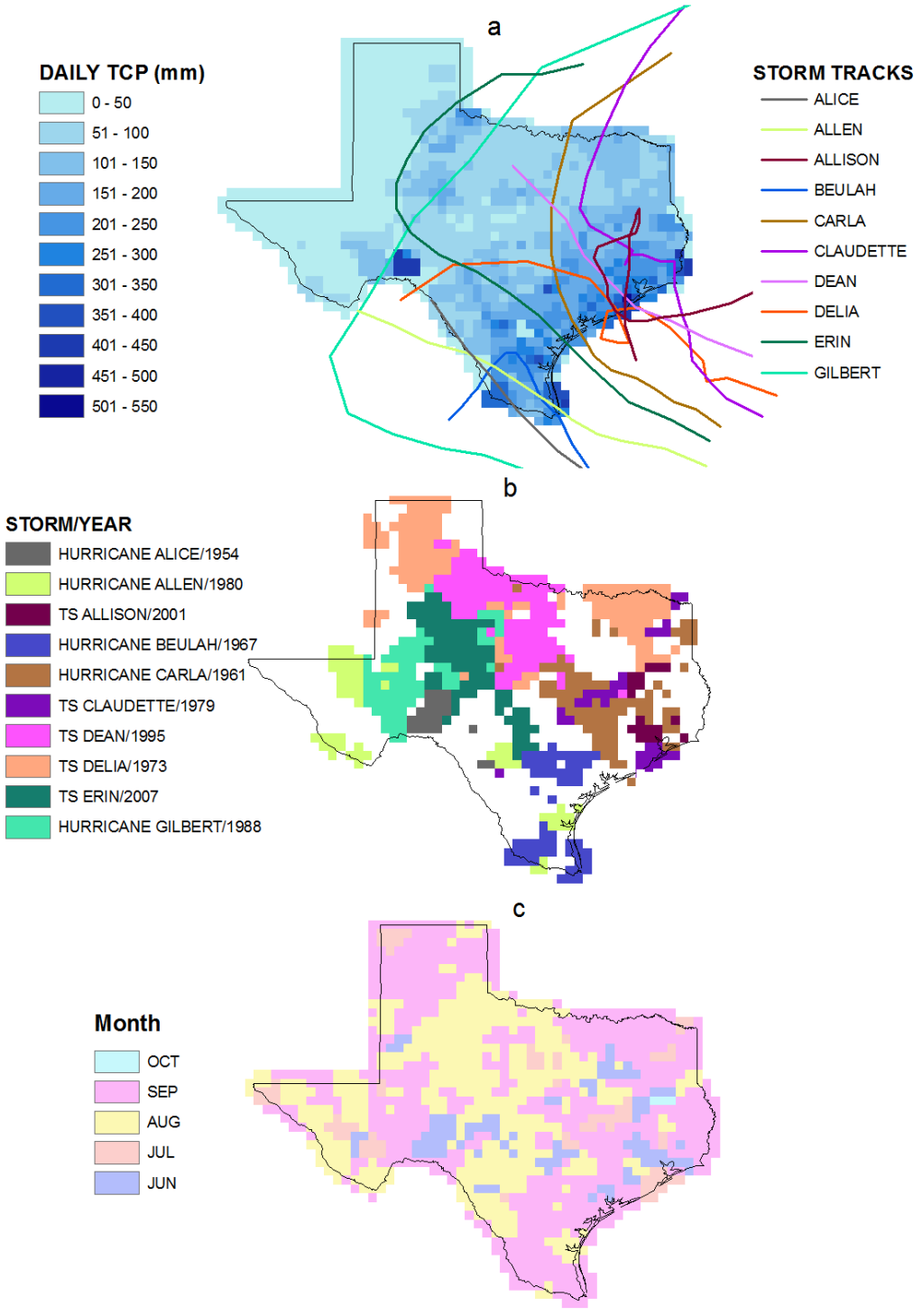

Figure 4.11. a. Spatial distribution of maximum daily TC precipitation (mm), b. Ten extreme TCs that influenced the greatest area in Texas for the maximum daily TCP, c. Month of occurrence of the maximum daily TCP value at each grid point.

the factors that led to the re-intensification of TS Erin (2007) [*Evans et al.*, 2011]. In other cases inland TCP maxima are associated with TCs that become stalled due to weak steering winds or interactions with mid-latitude weather systems (TS Claudette in 1979 and TS Delia in 1973). Other TCs that generated extreme amount of precipitation did so because they reversed course (TS Alison in 2001 and Hurricane Beulah in 1967). TS Claudette and TS Alison are associated with the record daily TCP in Texas (~1000 mm) and the heavy precipitation and slow movement caused major inland flooding. These events have occurred most commonly in August and September (Figure 4.11c). In August, locations with TCP maxima are mostly distributed across inland areas of north, central and west Texas. In September, the TCP maxima are concentrated on the eastern and southern Gulf coast. This also agrees with the spatial pattern shown for mean monthly precipitation in these months (Figure 4.4c & d).

4.4 Conclusions

Sixty years of tropical cyclone precipitation data were extracted from the rain gage data using the MRBT automated extraction method. The new MRBT method provides more complete and accurate estimations of daily TCP rain regions by considering both the TC size and TC translation speed from observations. The spatial pattern of daily TCP field generally agrees with previous studies [*Molinari et al.*, 1999; *Lonfat et al.*, 2004; *Matyas*, 2010]. TCP is widely distributed and can occur up to 1000 km from the center of circulation. However, most extreme TCP (>300 mm) occurs within 200 km of the TC. Generally, the front half and right side of the TC receive more

frequent and intense precipitation than the rear half and the left side. The largest TCP events in Texas are associated with slow moving or stalled TC systems.

August and September are two months with the most extensive and heaviest TCP in Texas since this is when TC landfalls are most frequent [*Islam et al.*, 2009]. Monthly TCP, annual TCP and its contribution to annual total precipitation all decrease with distance from the coast, but there are exceptions at several locations where TCs re-intensified or stalled. Coastal areas also generally have a higher probability of experiencing extreme daily TCPs (>50 or >100 mm), and local maxima are located in southeastern Texas. The historical maxima for daily TCP (>300-mm) also occurred mostly in coastal locations in Texas. However, rare TCs can produce extreme daily TCP at some inland locations (Hurricane Gilbert, >400 mm) in western Texas. Maximum daily TCP occurs most commonly in August and September.

Texas has 123.5 mm and 17.8 km^3 of TCP annually. Texas TCP accounts for ~20% of all TCP that occurs in the U.S. These values are somewhat greater than those reported in previous studies [*Knight and Davis*, 2009; *Nogueira and Keim*, 2010]. This is partly because a denser network of stations was used, longer time period for the analysis, and a TCP extraction method that considers the translation speed of TCs.

The analysis considered all possible trends longer than 10 years for all stations. In contrast to previous studies, which tend to show positive trends in TCP both during recent years and over the long-term [*Knight and Davis*, 2009; *Kunkel et al.*, 2010], no statistically significant long-term trend (>50 years) can be observed in the annual and daily TCP metrics. There are statistically significant increasing and decreasing trends at

some gauges over shorter time periods (10-30 years), but most gauges (>75%) do not have any statistically significant trends.

Many of the annual and daily TCP metrics have spectral power at interannual, biennual, 5-8 year, and >10 year oscillations, but none of these are statistically significant at the 95% confidence level. There is more variability in the spectra for the daily TCP metrics than the annual metrics. The results demonstrate that Texas TCP is dominated by interannual oscillations and there is no evidence of long-term trends in TCP.

5. STATISTICAL FORECASTING MODELS FOR SEASONAL TCP IN TEXAS

5.1 Model Comparison

Three dependent variables have been calculated to describe the seasonal TCP in Texas. The annual TCP is calculated by summing the TCP within each grid cell throughout a hurricane season and then averaging all grids with none-zero seasonal TCP. It provides information about the average amount of TCP in Texas within a year. The second variable is the TCP percentage. It calculates the ratio of seasonal TCP in total annual precipitation for each rain station and then takes the average for all stations with non-zero seasonal TCP. The annual TCP event summarizes the number of TCs with the precipitation impacts in Texas.

Three models (red, green and blue lines) have been constructed for each of the three response TCP variables (Figure 5.1a, b and c). The comprehensive models (redline, models with c) are constructed from all 400 variables including all basic and thermo-dynamic atmospheric and oceanic conditions at all different scales (Table 3.2). The independent variables are separated as basic and thermo-dynamic. The basic variables are scalar and vector variables directly measured by the instruments, such as the temperature, pressure, humidity, wind speed, etc. Two thermo-dynamic variables are used in our models, they are either calculated to represent the dynamical interactions between the SST and the atmosphere (Maximum Potential Velocity) or fluid dynamics of the atmosphere on the earth (vorticity).

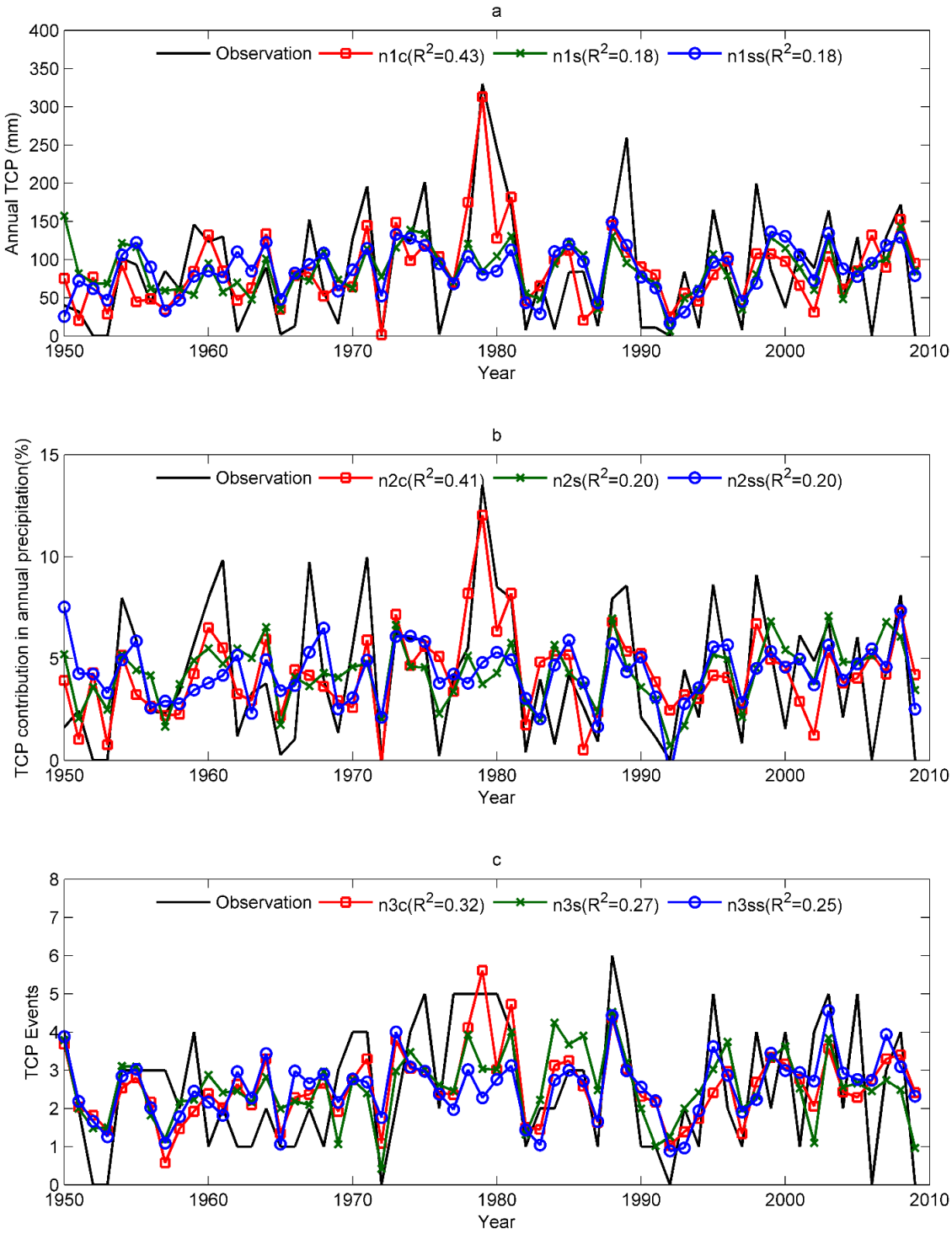

Figure 5.1. Observed and modeled TCP: (a.) annual TCP (models with n1), (b.) TCP percentage (models with n2), (c.) TCP events (models with n3). The black line is for observation, the red line is for the comprehensive model ('c' series), and the green and blue represent two simple models ('s' and 'ss' series).

The simple models are based on basic predictors used by previous TC frequency and intensity forecasting studies [*Gray*, 1984a; *Gray et al.*, 1994; *Elsner and Jagger*, 2006]. Two simple models have been generated for each of annual TCP metric: models (with "s" in their names, green line) based on one regional variable (SLP) and one global scale signal (ENSO), and models (with "ss" in their names, blue line) constructed on only global scale variables (NAO and ENSO signals).

The parameter information for all models are shown in Table 5.1. The statistics of model accuracy and cross validation error are shown in Table 5.2. Basically, the models for the TCP events have the best skills in the modeled and cross validated (CV) MAE (all < 50% of the observed mean). The annual TCP models have the second best skill in terms of modeled and CV MAE (48.2% to 57.4% of the observed mean). The models for the TCP percentage have the most unstable prediction modeled and CV MAE ranging from 52.7% to 73.3% of the observed mean. The comprehensive models ("c" series) have significant improvements in the explained variance when compared with the simple models ("s" and "ss" series). With one more predictor, the comprehensive models for the annual TCP and TCP percentage have ~0.20 larger R^2 than the same series of simple models. Figure 5.1 reveals that much of the improvement is from the high value years. Simple models for the TCP events have less cross validation error when compared with simple models for other two TCP metrics (Table 5.1c). The simple models for TCP events also have good and stable MAE, R^2, and adjusted R^2. In contrast, simple models for the annual TCP and the TCP percentage (Table 5.2a&b) have big drops from the modeled R^2 to the CV R^2. Some simple models for the annual TCP and the TCP

Table 5.1. Model parameters and coefficients.

Dependent variable	Model Name	Parameters	Coefficient	t value	P value
(Annual TCP, mm)	n1c	CONSTANT	86.1	11.43	<0.001
		MAY_VOR_MDR	-23.1	-2.85	0.006
		D2M_MPV_GMX	-42.3	-5.41	<0.001
		M2M_SOI	18.7	2.24	0.029
	n1s	CONSTANT	86.1	9.80	<0.001
		MAY_SLP_GMX	-23.9	2.48	0.016
		MAY_RSST_NIÑO34	-36.7	-3.80	<0.001
	n1ss	CONSTANT	86.11	9.60	<0.001
		D2M_SST_NIÑO4	18.67	1.89	0.06
		MAY_RSST_NIÑO34	-34.75	-3.52	0.001
(TCP percentage, %)	n2c	CONSTANT	4.25	12.76	<0.001
		MAY_VOR_MDR	-1.29	-3.78	<0.001
		D2M_MPV_GMX	-1.40	-4.12	<0.001
		MAY_SOI	0.72	2.10	0.04
	n2s	CONSTANT	4.25	11.07	<0.001
		D2M_SST_CAR	0.89	2.26	0.027
		MAY_RSST_NIÑO34	-1.33	-3.40	0.001
	n2ss	CONSTANT	4.25	11.06	<0.001
		MAY_NAO	-0.87	-2.24	0.029
		MAY_RSST_NIÑO34	-1.23	-3.16	<0.002
(TCP Events)	n3c	CONSTANT	2.55	14.36	<0.001
		D2M_MPV_GMX	-0.60	-3.32	0.02
		MAY_RSST_NIÑO34	-0.76	-4.21	<0.001
	n3s	CONSTANT	2.55	14.14	<0.001
		MAY_SLP_GMX	-0.45	-4.62	<0.001
		MAY_RSST_NIÑO34	-0.73	-3.65	<0.001
	n3ss	CONSTANT	2.55	13.67	<0.001
		M2M_SST_NIÑO4	0.60	2.16	0.035
		MAY_RSST_NIÑO34	-1.16	-4.16	<0.001

Table 5.2. Observations and statistical measures of model fit and leave-one-out cross validation (CV) for a. annual TCP, b. TCP percentage, and c. TCP events.

(a) Model Statistics for annual TCP (mm)

		n1c		n1s		n1ss	
	Observed	Model	CV	Model	CV	Model	CV
Mean	86.1	86.1	85.3	86.1	86.2	86.1	77.7
SD	75.5	49.7	48.3	31.7	32.1	32.2	80.1
Max	330.1	312.9	291.7	157	171.4	148.6	148.8
Min	0	1.7	1.8	6.2	7.1	16.8	-483.7
MAE		45.4(52.7%)	48.5(56.3%)	52.2(60.6%)	54.7(63.5%)	52.9(61.4%)	63.1(73.3%)
R^2		0.43	0.36	0.18	0.11	0.18	0.05
Adj R^2		0.40	0.34	0.15	0.09	0.15	0.03

(b) Model Statistics for TCP percentage (%)

		n2c		n2s		n2ss	
	Observed	Model	CV	Model	CV	Model	CV
Mean	4.25	4.25	4.22	4.25	4.27	4.25	4.26
SD	3.28	2.10	2.03	1.48	1.49	1.47	1.51
Max	13.53	12.04	10.41	7.08	7.11	7.52	8.26
Min	0	-0.21	-0.24	0.72	0.81	-0.77	-0.99
MAE		2.05(48.2%)	2.19(51.2%)	2.31(54.4%)	2.42(56.9%)	2.32(54.6%)	2.44(57.4%)
R^2		0.41	0.34	0.20	0.14	0.20	0.13
Adj R^2		0.38	0.31	0.18	0.12	0.18	0.12

(c) Model Statistics for TCP events (ATCPE)

		n3c		n3s		n3ss	
	Observed	Model	CV	Model	CV	Model	CV
Mean	2.5	2.6	2.6	2.5	2.5	2.6	2.5
SD	1.6	0.9	1	0.9	0.9	0.8	0.8
Max	6	5.6	6.3	4.5	4.6	4.6	4.6
Min	0	0.6	0.3	0.4	0.5	0.9	0.9
MAE		1.1(45.2%)	1.2(47.6%)	1.1(45.6%)	1.2(48%)	1.1(44%)	1.2(46.8%)
R^2		0.32	0.27	0.27	0.23	0.25	0.19
Adj R^2		0.30	0.24	0.24	0.22	0.23	0.18

*Statistical measures of model fit include mean absolute error (MAE), coefficient of determination (R^2), and adjusted coefficient of determination (Adj R^2).

percentage also demonstrate several negative values in the modeled and CV predictions, which are physical impossible. So the simple models for the annual TCP and TCP percentage are not as stable as the simple models for the TCP events.

The annual TCP presents the major information about how much TCP has been generated in Texas every year. The n1c model stands for the comprehensive models for the annual TCP. It is the best model with ~7 mm less modeled MAE and 0.25 more in Modeled R^2 than other two simple models for the annual TCP (n1s and n1ss). Those simple models are very unstable for the annual TCP because their CV MAE and the R^2 deteriorate very fast. This is also demonstrated by their high CV standard deviation (SD) and the physically impossible negative CV minimum (Min) in n1ss.

The TCP percentage has the combined information from both the seasonal TCP and total annual precipitation amount. Similar to models for annual TCP, the comprehensive model fits better with the addition of thermo-dynamic variables (MPV and vorticity). Both the comprehensive and simple models are relatively stable, with relative less difference between the modeled and CV statistics (MAE, R^2 and Adj R^2, Table 5.2b). The two simple models are not able to accurately predict years with extreme values (Figure 5.1b) and have similar predictive skills and cross validation errors (Table 5.2b).

Generally all models for the TCP events have good skill and small CV error. The thermo-dynamical variable again provides better skills for the comprehensive (n3c) model than the simple models (n3s and n3ss), but the improvement is not as large as the models for annual and TCP percentage. Removing one predictor (2 compared to 3 in

other models, Table 5.1) reduced some skills in the n3c, but the simpler model still has strong predictive power and the CV is stable. On the other hand, there are significant improvements in both modeled and CV performance for the simple models (n3s and n3ss). The simple models for the TCP events are more stable than the simple models for annual TCP and TCP percentage because they have less differences between modeled and CV statistics. The n3ss has smaller modeled and CV MAE than its comprehensive model counterpart (n3c).

5.2 Parameter Analysis and Possible Physical Mechanisms

Seasonal TCP in Texas is a complex function of many interacting factors. However, the complex information can be divided into two basic parts. One important factor is how many TCs have made landfall and generated precipitation in Texas in each season. This information is directly modeled (TCP events) and it also influences the models of annual TCP and TCP percentage. Another important factor is how much precipitation is generated by each individual storm. This is highly variable, since each storm is different in terms of its type, size, translation speed, track, and interactions with the local environment. The constructed models have provided some useful and interesting information on TCs in Texas and have revealed some of the major physical mechanisms that control variations in TCP. For each of model, maps were generated for the spatial distributions of the correlations between the response variables (TCP metrics) and important predictors (climatic forcings) in the final models (Figure 5.2, 5.3, 5.4, 5.5).

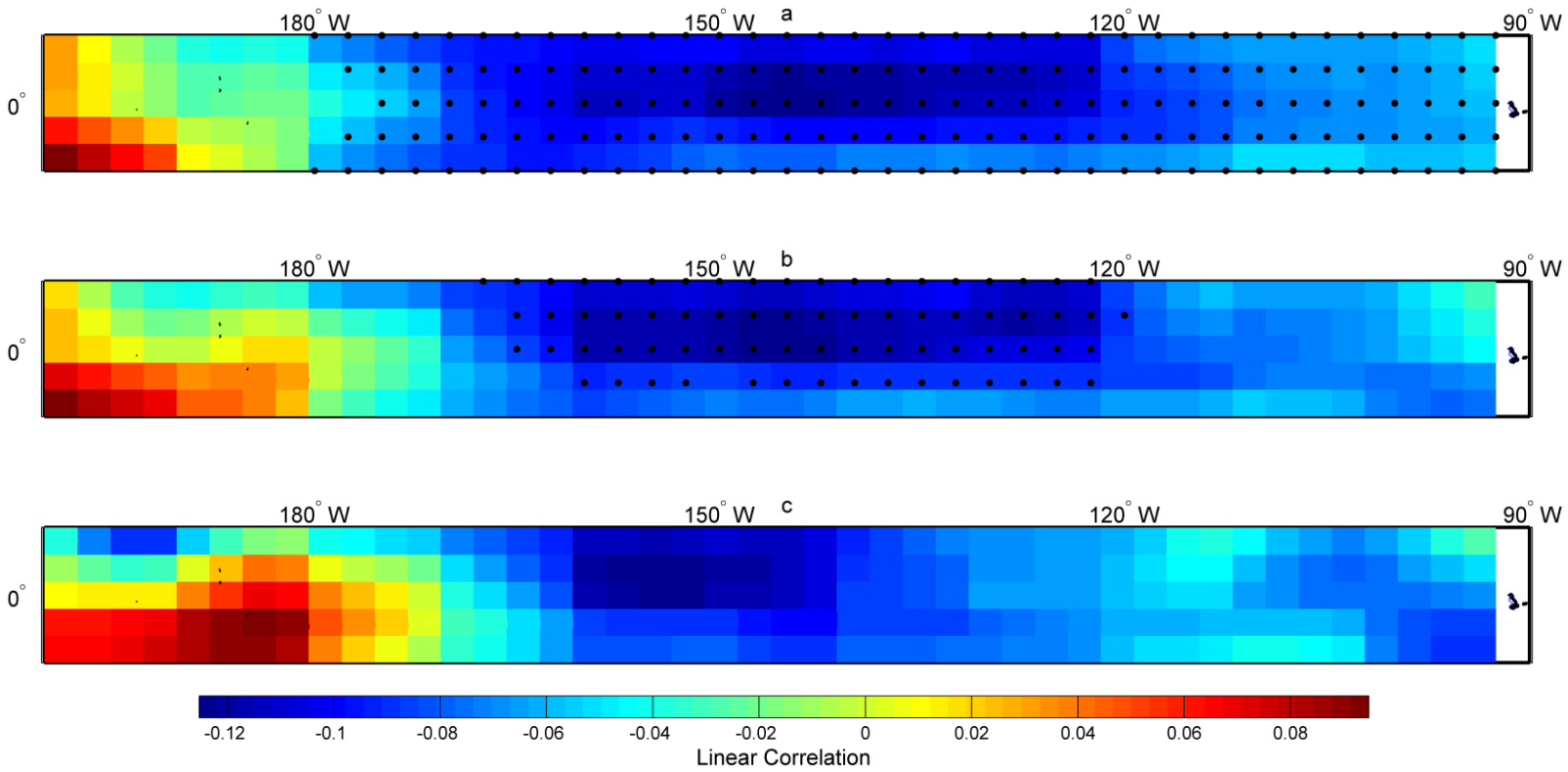

Figure 5.2. Pearson's correlations between SSTs in Nino 4 and 3 regions and annual TCP event (ATCPE): a. May Nino 3 and 4 SST and TCP events, b. March to May Nino 3 and 4 SST and ATCPE, c. December to May Nino 3 and 4 SST and TCP events. The black dots represent correlations with a 90% significance.

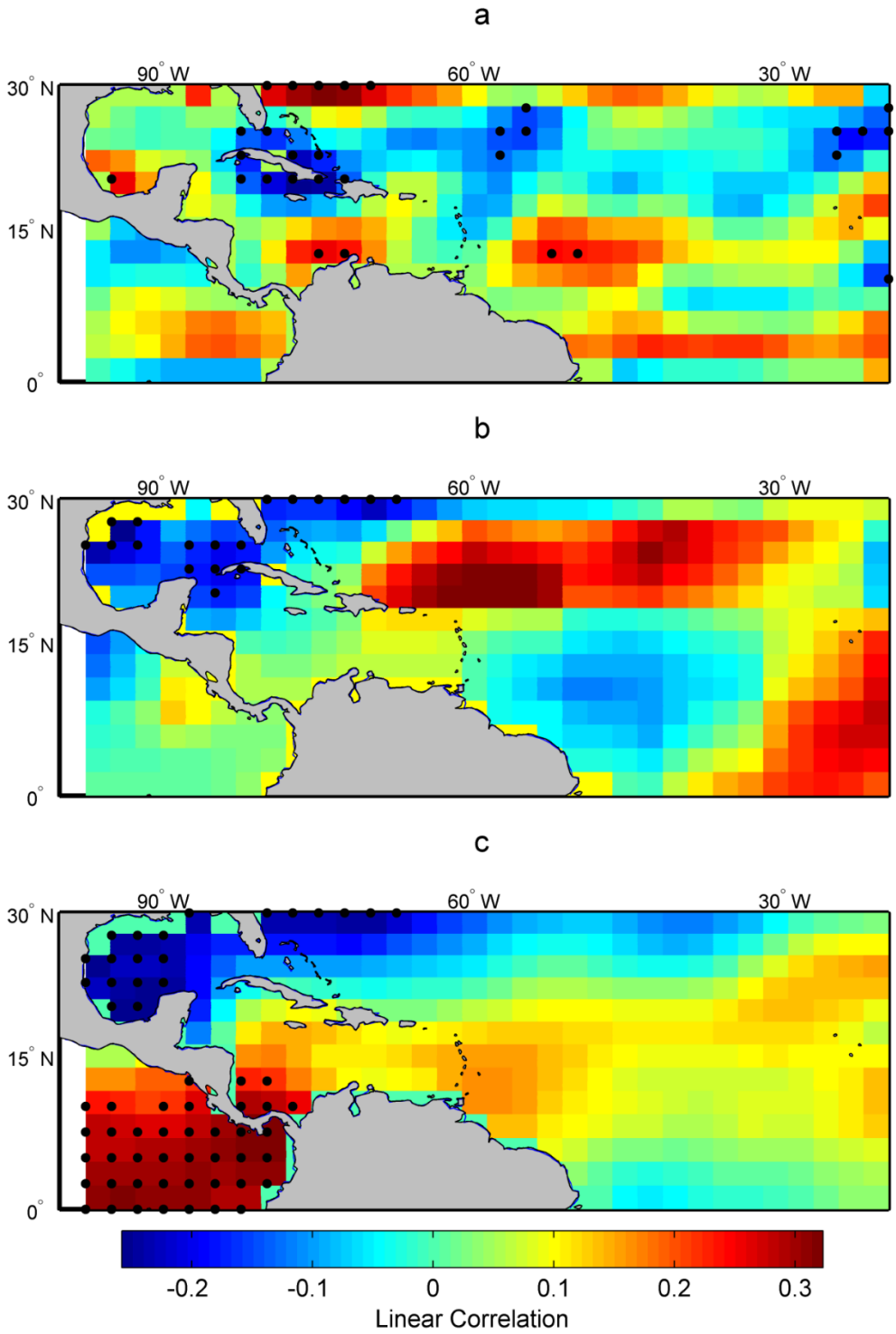

Figure 5.3. Pearson's correlations between regional predictors and the annual TCP (ATCP): a. May vorticity and ATCP, b. December to May Maximum Potential Velocity (MPV) and ATCP, c. May sea level pressure and ATCP, the black dots are points with correlation significant at 90% confidence level.

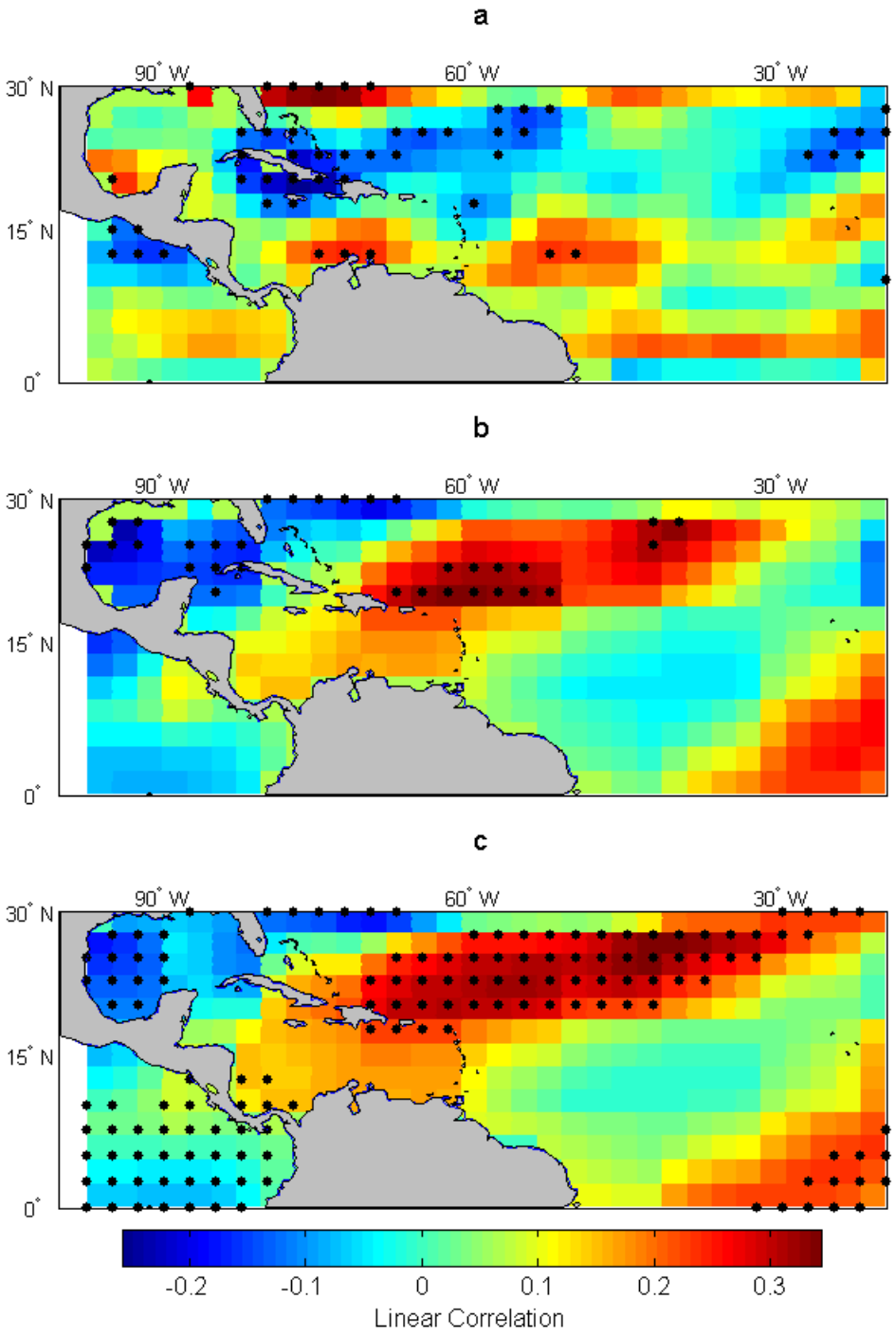

Figure 5.4. Pearson's correlations between regional predictors and TCP percentage (ATCPP): a. May vorticity and ATCPP, b. December to May Maximum Potential Velocity (MPV) and ATCPP, c. December to May SST and ATCPP, the black dots are points with correlation significant at 90% confidence level.

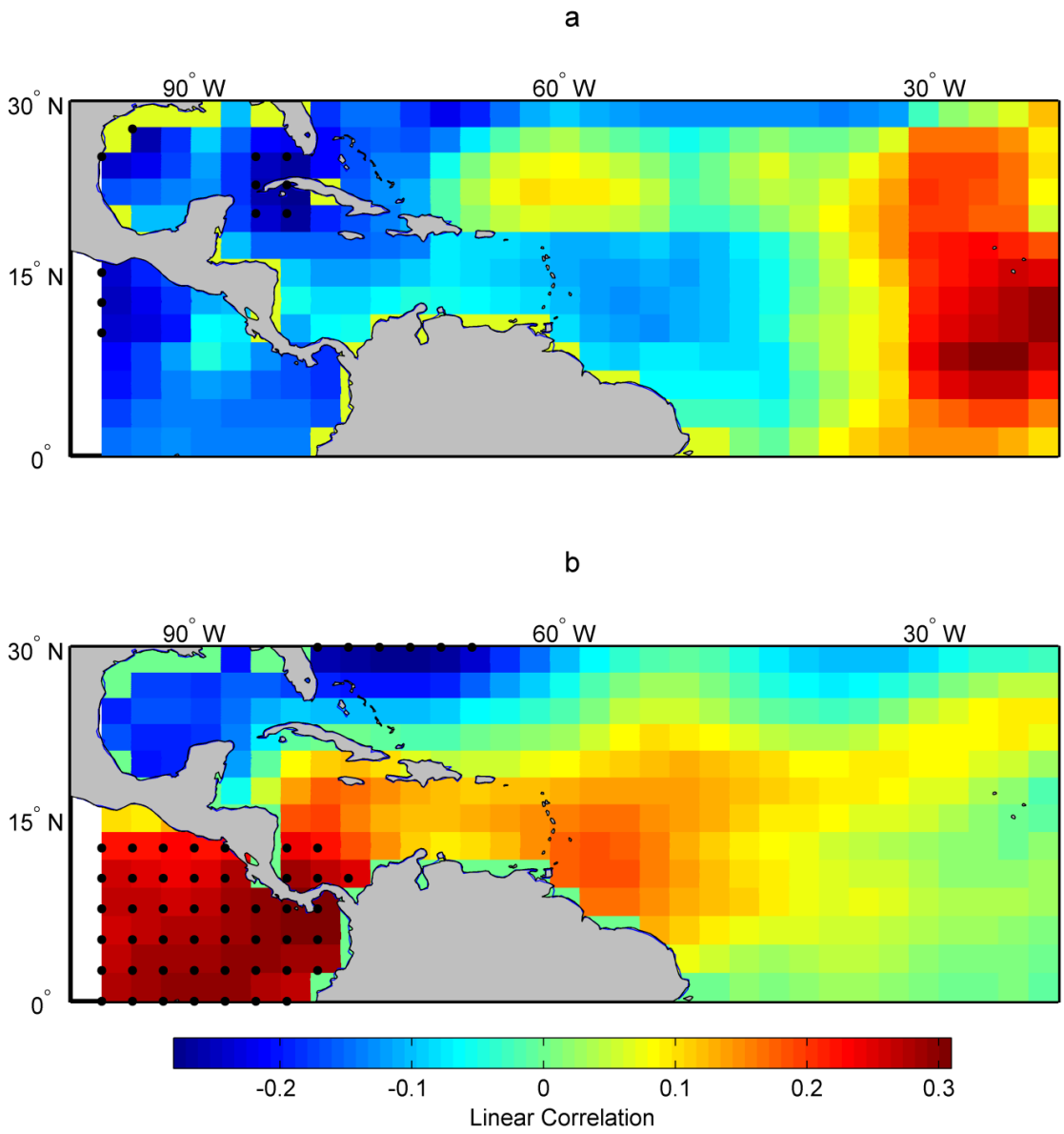

Figure 5.5. Pearson's correlations between regional predictors and the TCP events (ATCPE): a. December to May Maximum Potential Velocity (MPV) and ATCPE, b. May sea level pressure and ATCPE, the black dots are points with correlation significant at 90% confidence level.

5.2.1 ENSO

ENSO is the most importance variable in all of the models. In particular, La Niña (Niño 3.4 SST cooling) signal is the major control of Atlantic TC frequency. But the Niño 4 SST warming (Central Pacific Warming, CPW) signal was also mentioned to be positively related to the frequency of landfall TCs in the Gulf of Mexico and the Caribbean [*Kim et al.*, 2009]. Many studies [*Gray*, 1984b; *Gray et al.*, 1993; 1994; *Elsner et al.*, 1999; *Klotzbach and Gray*, 2003; *Klotzbach*, 2011] have demonstrated that ENSO has a major influence on seasonal TC frequency in the Atlantic by altering the Walker circulation. In typical ENSO warming events (Niño 3.4 SST warming), the weaker than normal Walker circulation makes an eastward shift, so there is an increased upper-level westerly wind over Caribbean and tropical Atlantic. The strong westerly may combine with lower-level easterly wave and generate a high vertical wind shear environment, which is not favorable to TC formation and movement [*Gray*, 1984a; *DeMaria*, 1996; *Goldenberg and Shapiro*, 1996; *Knaff et al.*, 2004; *Klotzbach*, 2011]. Therefore, in the negative phase of ENSO (La Niña), the environment conditions are more favorable for TCs in the Atlantic and Caribbean to develop, persist and make landfall. More TCs make landfall in the U.S. during La Niña years than El Niño or neutral years [*Pielke and Landsea*, 1999; *Smith et al.*, 2007; *Mann et al.*, 2009].

All the final models have one predictor pertaining to the La Niña signal, but taking different forms (Table 5.1). A La Niña signal here means cooler pre-hurricane season SST in the Niño 3.4 region will cause more TC activities and TCP in Texas. I believe this strong La Niña signal controls the TCP in Texas by influencing the annual

landfall TC counts. I computed the Pearson correlations between the TCP events and each gridded SST in the Niño 4 and Niño 3 regions (Figure 5.2). The spatial patterns of the La Niña signal (negative correlation between SST and TCP events) are pretty strong and dominate in the eastern central Pacific (Niño 3.4 region).

The Southern Oscillation Index (SOI) is the ENSO predictor used in the n1c and n2c models. The SOI is an important component of the ENSO cycle [*Deser and Wallace*, 1987; *Trenberth and Shea*, 1987; *Trenberth and Hoar*, 1996]. All SOI predictors in the models have positive signs, which are correspondent to the La Niña phase. Previous modeling [*Villarini et al.*, 2011b] also indicated that remote influences of SOI and tropical mean SST can explain part of the U.S. landfall hurricanes counts.

All Niño 3.4 RSST predictors have negative signs, meaning the Niño 3.4 cooling relative to the tropical mean SST are corresponding with more TCP in Texas. Those Niño 3.4 RSST signals are in the same direction with the La Niña signal.

Two simple models (n1ss and n3ss) are solely based on ENSO signals. Besides the La Niña signal, the positive sign of Niño 4 SST predictors indicates that the warm SST in the western central Pacific region (5S-5N, 160E-150W) may be favorable to more TCP in Texas. Several studies have already investigated the impacts from the shifting patterns of Pacific Ocean warming on the North Atlantic TCs [*Kim et al.*, 2009; *Lee et al.*, 2010; *Larson et al.*, 2012]. *Kim et al.* [2009] showed that the Gulf of Mexico coast and Central America will have above average TC frequency and increased TC landfall probability under the Central Pacific Warming (the Niño 4 region). I believe that

Central Pacific Warming is related to the inhomogeneous impact from the whole Niño 3 and Niño 4 SST to the Texas TCP events.

5.2.2 MPV and Vorticity

5.2.2.1 MPV, vorticity definition and their signals the models

MPV and the vorticity are two important thermo-dynamical variables that improved the performance of the comprehensive models significantly (~0.20 in R^2) when compared with the simple models (Table 5.2). Their coefficients are negative in all comprehensive models.

MPV stands for the maximum potential velocity, an index originally developed by *Emanuel* [1995] and *Holland* [1997] to describe the limit for the maximum wind velocity that is approachable in TCs based on the ocean and atmosphere energy conditions. Previous studies usually shows storms with stronger winds are associated with larger amount of precipitation [*Cerveny and Newman*, 2000], especially in the inner core area [*Rodgers et al.*, 1994]. However, the relationships between MPV and TCP metrics in our models are all negative, which indicates that larger TCP may be produced by weaker storms. And the negative correlations between MPV and the TCP metrics are pretty spatially consistent in the Gulf of Mexico as shown in Figure 5.3b, 5.4b, 5.5a, corresponding to the negative signs of D2M_MPV_GMX predictors in the models. Those previous analyses showing positive relationships were primarily based on individual or a group of TCs in the ocean, while our study is for the seasonal accumulated TCP metrics in Texas during 60 years. Many TCs with relative low

maximum wind speeds have generated large amounts of precipitation in coastal areas of the U.S. Tropical Storm Alison in 2001, Hurricane Irene (Category 1-3) in 2011, and Hurricane Isaac (Category 1) in 2012 are all recent examples of TCs with relatively low winds that produced large amounts of precipitation and caused severe inland flooding.

Low level (850 mb) MDR vorticity in May (MAY_VOR_MDR) is another thermo-dynamic predictor appeared in the comprehensive models for the annual TCP and TCP percentage. Vorticity is a numerical description for the rotational characteristics of the atmosphere movements [*Hoskins et al.*, 1985]. The TCs are vortex systems themselves and they are embedded in the large scale environmental vortex systems [*Emanuel*, 2003]. The environmental vorticity may influence the TC genesis, tracks and intensity [*Davis and Emanuel*, 1991; *Jones et al.*, 2003; *Emanuel*, 2007] [*Flatau et al.*, 1994; *Emanuel*, 2003]. It was more frequently used in the seasonal TC genesis prediction [*Camargo et al.*, 2009; *Belanger et al.*, 2010] and the power dissipation index estimation [*Emanuel*, 2005; 2007]. *Emanuel* [2005] also mentioned that the potential intensity, low-level vorticity and vertical wind shear are highly correlated with each other. So enhanced low-level vorticity prior to the hurricane season may be one of the contributors to high wind speed in TCs during the season. Most studies have shown that enhanced vorticity produces more convection, higher wind, and more intense precipitation. However, the models constructed by this study all show negative coefficients for the MDR May vorticity (Table 5.1). Spatially, those negative correlations are mostly located in western MDR near the Gulf of Mexico (Figure 5.3a&5.4a). One of reasons may be the same with the negative relationships found in

MPV; storms with weaker winds produced more precipitation because low vorticity basically means low wind speed. In addition, less vorticity in the western MDR may result in TCs with larger size and lower translation speed before they enter the Gulf of Mexico. It has also been suggested that a smaller TC radius is associated with larger values of vorticity [*May and Holland*, 1998]. Vorticity can also have complex impacts on TC movement based on the physical interaction between TC's own vorticity and the environmental flow [*Holland*, 1983; *Shapiro*, 1992; *Flatau et al.*, 1994]. The track and translation speed of a TC are important factors determining how much precipitation it will produce in Texas. It is possible that slower spinning storms may travel with lower speed and have more accumulated precipitation.

5.2.2.2 TCP and TC characteristics (size, intensity and translation speed)

MPV and vorticity significantly determine the TC characteristics including the wind intensity, spatial coverage and translation speed. The models show negative relations between MPV/vorticity and TCP metrics. Therefore, it is reasonable to test the relationships indicated by the statistical models: do storms with weaker winds and slower translation speeds generate more TCP in Texas historically? This study examined how the maximum wind speed, translation speed and TCP coverage are related to the amount of precipitation generated by individual TCP days in Texas. Daily TC maximum wind speed and translation speed were averaged from observations for each TCP day from the 6 hour observations. The daily TCP volume is calculated for each TCP day by aggregating all precipitation amounts from the non-zero grids. There are 30 TCP days out of the whole sample (495 days) with only one observation of spatial position. They

were not used in the analysis because they had very minor precipitation impact in Texas and treating their traveling speed as 0 km/hr will introduce bias in the analysis. The remaining 465 TCP days were divided into two equal parts: the first 233 TCP days all have TCP covering less than 13% of Texas and account for only 8% of the TCP volume; while all remaining 232 TCP days have covered 13-64% of Texas and together account for 92% of the TCP volume.

The Box-Whisker plots (Figure 5.6) were constructed for the relationships between daily TCP volume and TCP maximum speed, and between the TCP volume and TC translation speed. In Figure 5.6a&b, The first two boxes (TCP days with maximum speed <14 m/s) have very large sample size (169 out of 232 days for Figure 5.6a, 180 out of 233 days for Figure 5.6b) with many cases of low precipitation storms. On the other hand, fewer TCP days are in the other two high wind speed boxes (63 for both 3rd and 4th box in Figure 5.6a, 52 for both 3rd and 4th box in in Figure 5.6b). For the extreme values, low wind speed boxes (<14 m/s) are associated with much more TCP days with outliers (e.g., > 1 km^3 for Figure 5.6a, >10 km^3 for Figure 5.6b) than the high wind speed boxes. The historical record of daily TCP (~ 28 km^3) is related to the rare storms with both heavy wind (22.4-67.1 m/s) and high precipitation. Overall, it indicates that TCs with slow or medium maximum wind speed account for most of the TCP because they occurred more frequently and contributed most of the large events. The means of the four boxes show no statistical significant difference in Figure 5.6a and 5.6b using the Bonferroni adjustment on a 95% significance level.

Similar relationships are demonstrated between the TC translation speed and the daily TCP in Figure 5.6c&d. Many TCP days with large amounts of precipitation (e.g., > 1 km^3 for Figure 5.6a, >10 km^3 for Figure 5.6b) are associated with very slow translation speeds (<10 km/hr). Sample size is still larger for the first two boxes. TCP days in those two boxes take most of the TCP outliers. In Figure 5.6d, the median precipitation in the first box is ~2 km^3 larger than the median of the 4^{th} box, although the first box has much larger sample size and is associated with many small TCP days. The historical high daily TCP is in the first box with lowest TC translation speed (<10 km/hr). Therefore, TCs with lower translation speed normally generate more extreme TCP events and account for a greater proportion of TCP in Texas. The means of the four boxes show no statistical significant difference in Figure 5.6c using the Bonferroni adjustment on a 95% significance level. However, the both 3rd and 4th box in Figure 5.6d are showing significantly smaller mean value than then 2rd box using the same test.

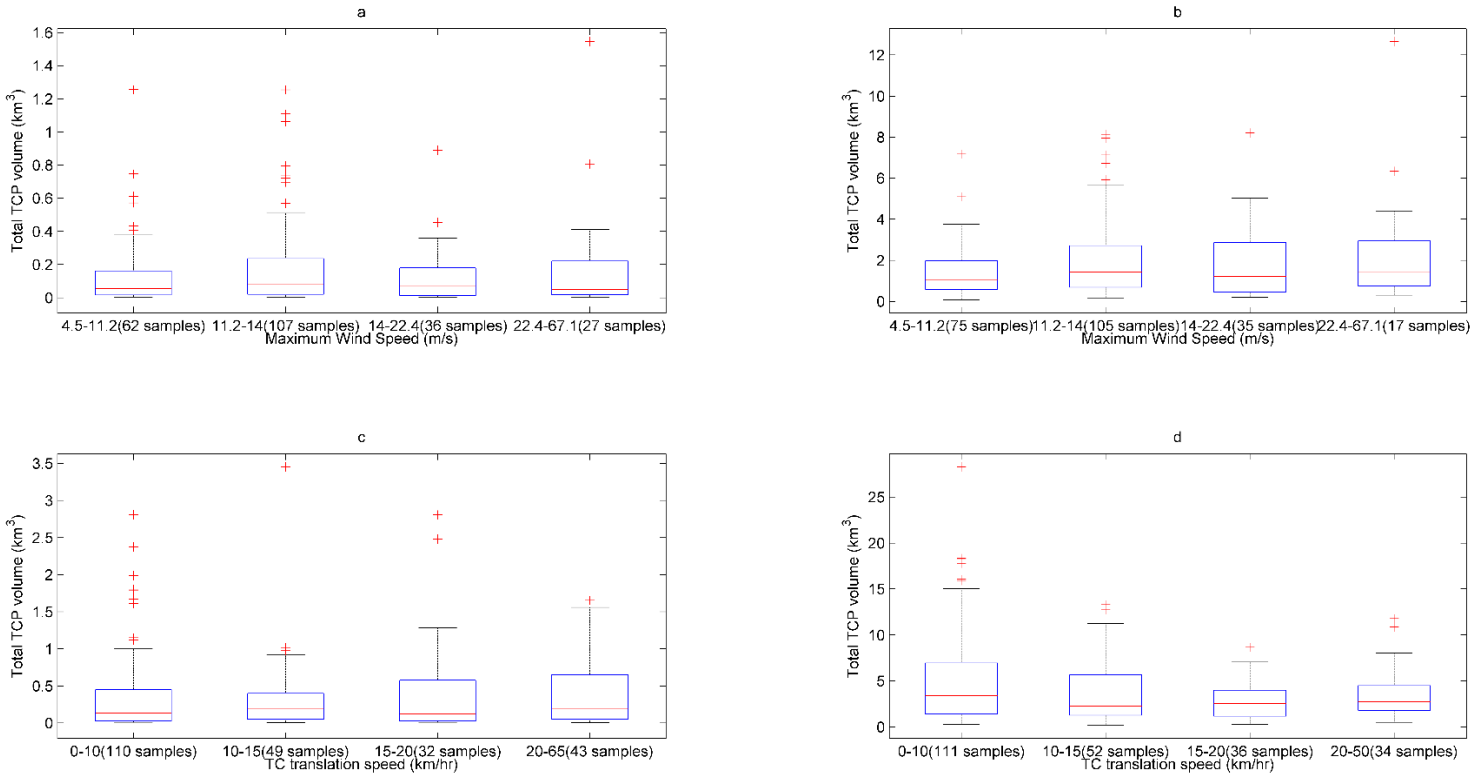

Figure 5.6. Box-Whisker plot of daily TCP volume for 4 groups of TC events divided by daily TCP characteristics (maximum wind speed and translation speed). Boxes represent 25th and 75th percentile inter-quartile ranges. Median extents are shown by the red line in each box. Whiskers (black horizontal lines) represent approximately +/–2.7σ and 99.3% coverage if the data are normally distributed. Extents larger (smaller) than the Whisker are shown as individual red crosses: a. TC maximum speed and TCP volume for TCP days with rainfall area covering < 13% of Texas (232 days). b. TC maximum speed and TCP volume for TCP days with rainfall area covering 13%-64% of Texas (233 days). c. TC translation speed and TCP volume for TCP days with rainfall area covering < 13% of Texas (232 days). d. TC translation speed and TCP volume.

Figure 5.7a and 5.7b are histograms of the maximum wind speed and the translation speed for all the TCP days. Quartiles are divided by the maximum wind speed and the translation speed. TCP amounts are accumulated in each quartile with the same number of TCP days. The TCP mean show no statistical significant difference in maximum wind speed quartiles (Figure 5.7a) using the Bonferroni adjustment on a 95% significance level. The TCP mean also show no statistical significant difference in TC translation speed quartiles (Figure 5.7a) using the Bonferroni adjustment on a 95% significance level. However the low wind speed quartiles have much less mean TCP than the high wind quartiles.

Both the Box-Whisker and quartile analysis have provided some interpretations for the physical mechanisms behind the negative signs of MPV and vorticity coefficients in our models. The TC events with lower or medium maximum wind speed and slower translation speed actually generated more big TCP events and therefore account a greater proportion of the total TCP in Texas. Therefore, the lower preseason regional MPV and vorticity are important factors for more of those weaker and slow moving TC systems in Texas.

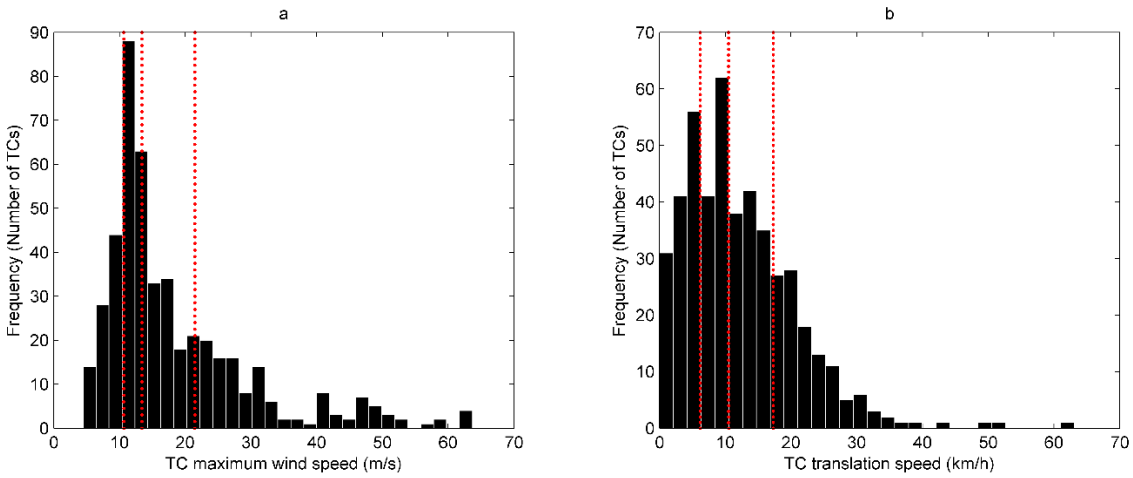

Figure 5.7. Histograms of daily TC maximum wind speed and translation speed and their quartile divisions.

5.2.3 Other Predictors

Besides ENSO, MPV and vorticity, some other climatic variables also appear in some of the models. May sea level pressure in the Gulf of Mexico (MAY_SLP_GMX) shows negative coefficients in two simple models for both annual TCP and TCP events. Sea level pressure was mentioned in many previous studies as an important predictor for hurricane frequencies [*Ray*, 1935; *Landsea et al.*, 1998; *Landsea et al.*, 1999; *Goldenberg et al.*, 2001]. *Gray et al.* [1993] showed that low June to July sea level pressure are corresponding to larger amount of TC activities in the Atlantic basin after August 1st. Another early study by Shapiro [1982] displayed a strong negative correlation (~-0.3) between the May-June-July sea level pressure in the Gulf of Mexico and the Autumn-September-October hurricane activities in the Atlantic Ocean from historical record from 1899 to 1978. *Gray et al.* [1993] explained that the low sea level pressure in the MDR strengthens the inter-tropical convergence zone (ITCZ) and is more favorable for cyclongenesis [*Gray*, 1968]. Figure 5.3c and 5.4b show that negative correlations for the sea level pressure are consistent in the Gulf of Mexico and north tropical Atlantic. *Knaff* [1997] indicated that the low regional sea level pressure is associated with deeper moist boundary, warmer middle level temperatures and weaker vertical wind shear. Therefore, the low sea level pressure in the Gulf of Mexico prior to the hurricane season might be more favorable to the formation and development of TCs in the Gulf of Mexico and so more TCP for Texas.

The December-May SST in the Caribbean (D2M_SST_CAR) shows a positive sign in model n2s for the TCP percentage. *Inoue et al.* [2002] argued that the

strengthened easterly trade wind may create low SST, high sea level pressure and more outgoing longwave radiation in the Caribbean in some years, which are unfavorable for development of TCs. In addition to that, warmer SST in the Caribbean is favorable to the traveling of TCs from the Atlantic [*Vecchi and Knutson*, 2008; *Kossin et al.*, 2010]

North Atlantic Oscillation (NAO) is defined as the large-scale alternation of atmospheric mass between subtropical high surface pressure (near Azores) and subpolar low surface pressure (extending to east of Greenland) in the Atlantic [*Lamb and Peppler,* 1987]. Some studies suggest that annual Atlantic and U.S. landfall TC frequencies are closely related to NAO [*Emanuel*, 2005; *Kossin et al*., 2010]. One of our models for the TCP percentage has the May NAO showing a negative coefficient sign. *Kossin et al.* [2010] indicated that the May-June NAO controls the position of the North Atlantic sub-tropical high, which modulates the tracks of the "straight moving" hurricanes during the season. The "straight moving" hurricanes is defined as ones that formed in deep tropics, travelled straight westward with little recurvature, and finally made landfall in the Caribbean or the Gulf coast [*Elsner*, 2003; *Kossin et al*., 2010]. Some of the TCs produced precipitation in Texas can be those "straight moving" hurricanes. In addition, negative NAO are related to the winter precipitation decrease in southeastern U.S [*Hurrell*, 1995]. Less winter precipitation may lead to less annual precipitation, and so more TCP's contribution. NAO was also mentioned to be negatively correlated with drought-busting Tropical Cyclones in the southeastern U.S [Maxwell et al., 2012]. All those support the negative NAO coefficient in the n2ss model for the TCP percentage.

5.3 Summary and Conclusions

Multiple linear regression models were built for forecasting annual TCP, the percentage of TCP, and TCP events in Texas. Three models were constructed for each of the TCP metrics: one comprehensive model including all thermo-dynamic and simple forcing variables, two simple models using only the simple forcing variables. The comprehensive models can explain 32%-43% of the variance of the seasonal TCP metrics, and the simple models can explain 18%-27% of their variance. Nearly all the parameters in the final models have statistical significant p values (<0.05). The modeled cross-validation statistics show that most of the models are stable and robust.

ENSO is the most important factor in the final models, but it takes different forms (RSST_NIÑO34, SOI, and SST_NIÑO4). The primary signal is related to La Niña, which reduces the upper tropospheric winds and so the vertical shear in the Caribbean and tropical Atlantic [*Gray*, 1984a; b]. The Central Pacific Warming (CPW) [*Kim et al*., 2009; *Lee et al*., 2010] related variables appeared in the models for the annual TCP and TCP events, but the signal is still weak.

The addition of thermo-dynamic predictors (MPV and vorticity) have significantly increased predictive skills and cross-validation accuracy of the comprehensive models for the annual TCP and TCP percentage. Pre-season MPV in the Gulf of Mexico and vorticity in the MDR are connected to the maximum wind speed, translation speed and size of the Texas landfall TCs. Their negative relationship between the two thermo-dynamic predictors and the TCP metrics in Texas can be validated by patterns in TC characteristics and TCP amounts.

Other predictors in models all have physical connections to seasonal TCP in Texas. Low sea level pressure in the Gulf of Mexico is favorable to the formation and development of TCs in the Gulf of Mexico and it produces more TCP in Texas. Warmer than normal SSTs in the Caribbean enhance TC genesis and also support TCs that formed in the Atlantic and then move through the region. The negative NAO may produce more westward "straight moving" TCs and less winter precipitation, and therefore make more TCP's contribution in annual precipitation of Texas.

This is the first regional study using multiple linear regression models to predict seasonal TCP in Texas. Statistically robust models can be constructed using ≤ 3 independent variables (many just have two) with both statistical skills and physical interpretations. An important finding is that thermo-dynamic variables can improve the performance of the TCP models significantly when working together with ENSO signal and other signals. The negative relationships between the thermo-dynamical variables and TCP can be explained by the observations of TCP and TC characteristics in Texas. Simple models based only on global variables still have predictive and cross validation skill.

6. EXTREMES IN TROPICAL CYCLONE PRECIPITATION AND DISCHARGE IN WATERSHEDS NEAR HOUSTON

6.1 Land Use/Cover Change for the Selected Watersheds

The third objective is to examine how extreme TCP effects discharge in watersheds near Houston. The San Jacinto River is the study area for objective 3. It is located in southeastern Texas (Figure 3.2) and includes watersheds covering the metro and suburban area of Houston. They are either dominated by intensely developed land or have been undergoing rapid urbanization. The eight selected river gauges have complete data record (Table 3.3) and covers different types of watershed characteristics (size, shape, and land use condition). Thiessen polygons were then used to calculate the weighted surface precipitation for each selected watershed. Historical Land Use/Cover data from four periods (1980, 1992, 2001 and 2006) were used to evaluate the influence of urbanization on discharge in selected watersheds. Different statistical tests were then used to examine the variability and trends in the time series of maximum annual precipitation, TCP, daily discharge and TCP-related discharge.

Land use/land cover data from 4 years between 1980 and 2009 have been used in this study (Figure 6.1 & 6.2). Figure 6.1 demonstrates the dramatic changes in land surface near Houston. The urban area has been expanding in every direction (especially to the north Houston), while vegetated areas have been decreasing at the same time. Figure 6.2 shows variations in the proportion of land cover associated with the five most common land use types (wetlands, water, forest, grass and agriculture, developed land). Figure 6.2a to 6.2d shows changes in land cover over time for watersheds located near

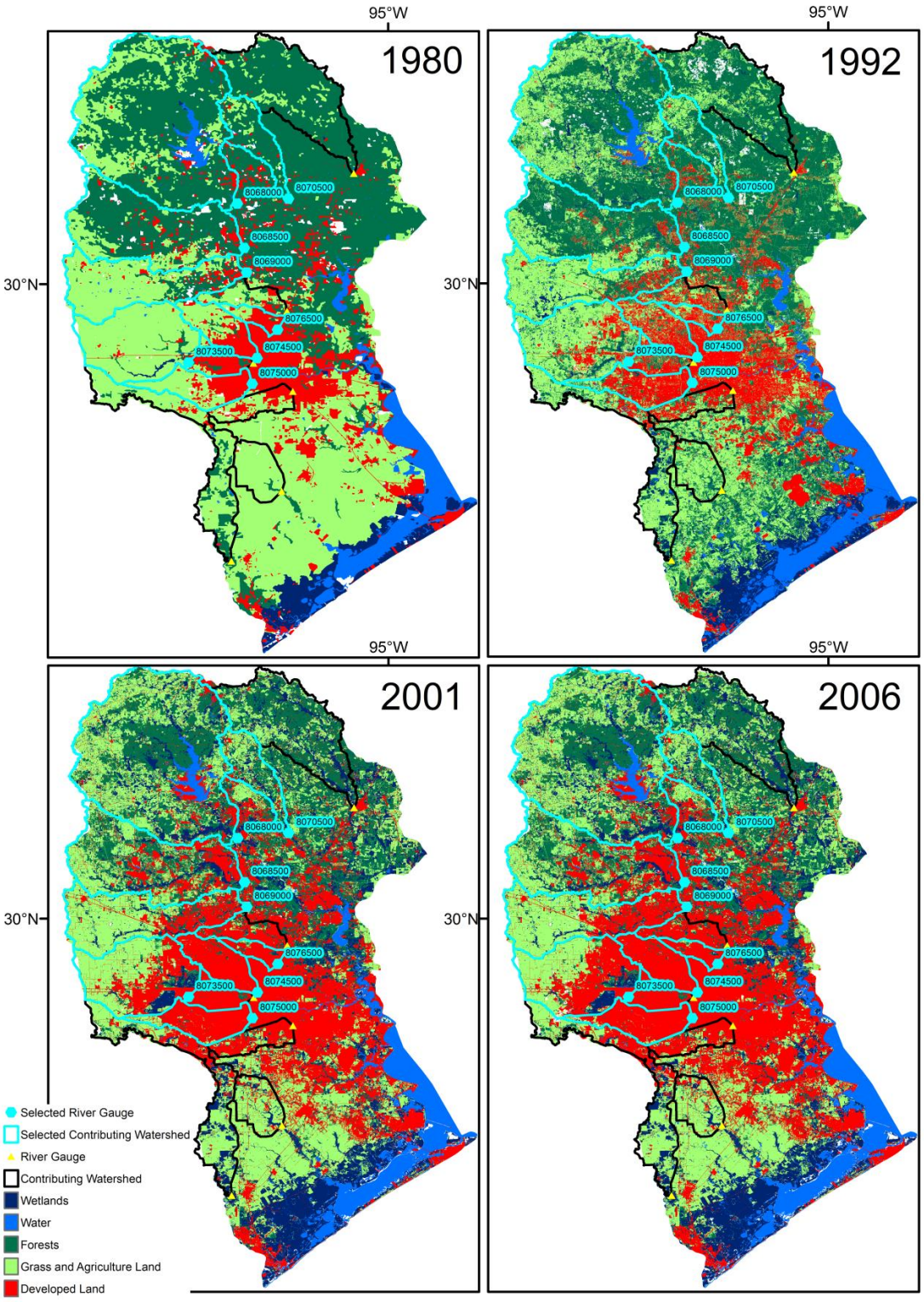

Figure 6.1. Land Use and Land Cover for Houston area between 1980 and 2006.

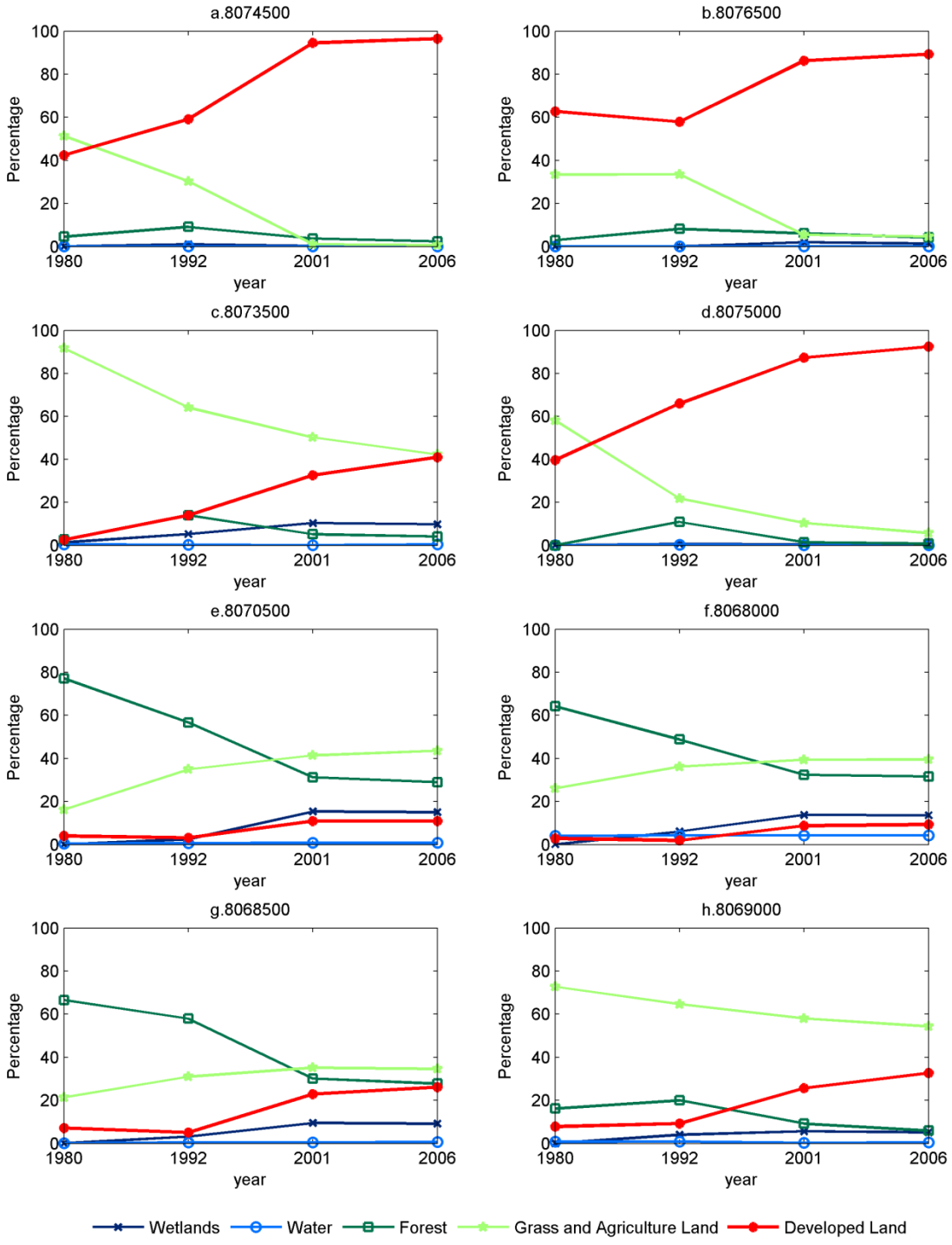

Figure 6.2. Changes in land cover (in percentage) for different watersheds between 1980 and 2006 (8074500: Whiteoak Bayou, 8076500: Halls Bayou, 8073500: Buffalo Bayou, 8075000: Brays Bayou, 8070500: Caney Ck, 8068000: W Fk San Jacinto Rv, 8068500: Spring Ck, 8069000: Cypress Ck).

downtown Houston. Figure 6.2e to 6.2h shows changes in land cover for suburban watersheds located in the northern Houston. Most of the downtown watersheds show dramatic increases in the developed land (+40%) and decreases in grassland and agriculture (-40%) from 1980 to 2006. There are also significant increases in developed land in the suburban watersheds (~20%) and most of them have seen reductions in forested area by approximately -40%.

6.2 Annual Maximum Discharge, TCP and Related Discharge

In Figure 6.3 many maximum TCP discharge ratios (red lines) are similar to the annual maximum discharges ratio (black lines). This shows the importance of TCP in producing the extreme discharge in those watersheds. There is a great deal of interannual variability exists in the discharge ratios and precipitation, but generally large TCP discharge ratios correspond to large amounts of TCP (blue bars). This indicates that TCP is an important cause of extreme discharge.

Watersheds with a great proportion of developed land (Figure 6.1a, b, and d) have larger annual maximum discharge ratios (both in terms of the mean and maximum) than watersheds that are less developed (Figure 6.1e, f, g, and h). Buffalo Bayou (8073500) is one exception. It has low discharge ratios even though it is highly developed. This can be explained by a flood control project completed before the 1950s and modified in the 1950s and 1960s. Addricks and Barker reservoirs are two large floodwater detention basins that are located upstream of Buffalo Bayou (where gauge 8073500 is located). Baker Dam was completed in 1945 and Addicks Dam in 1948

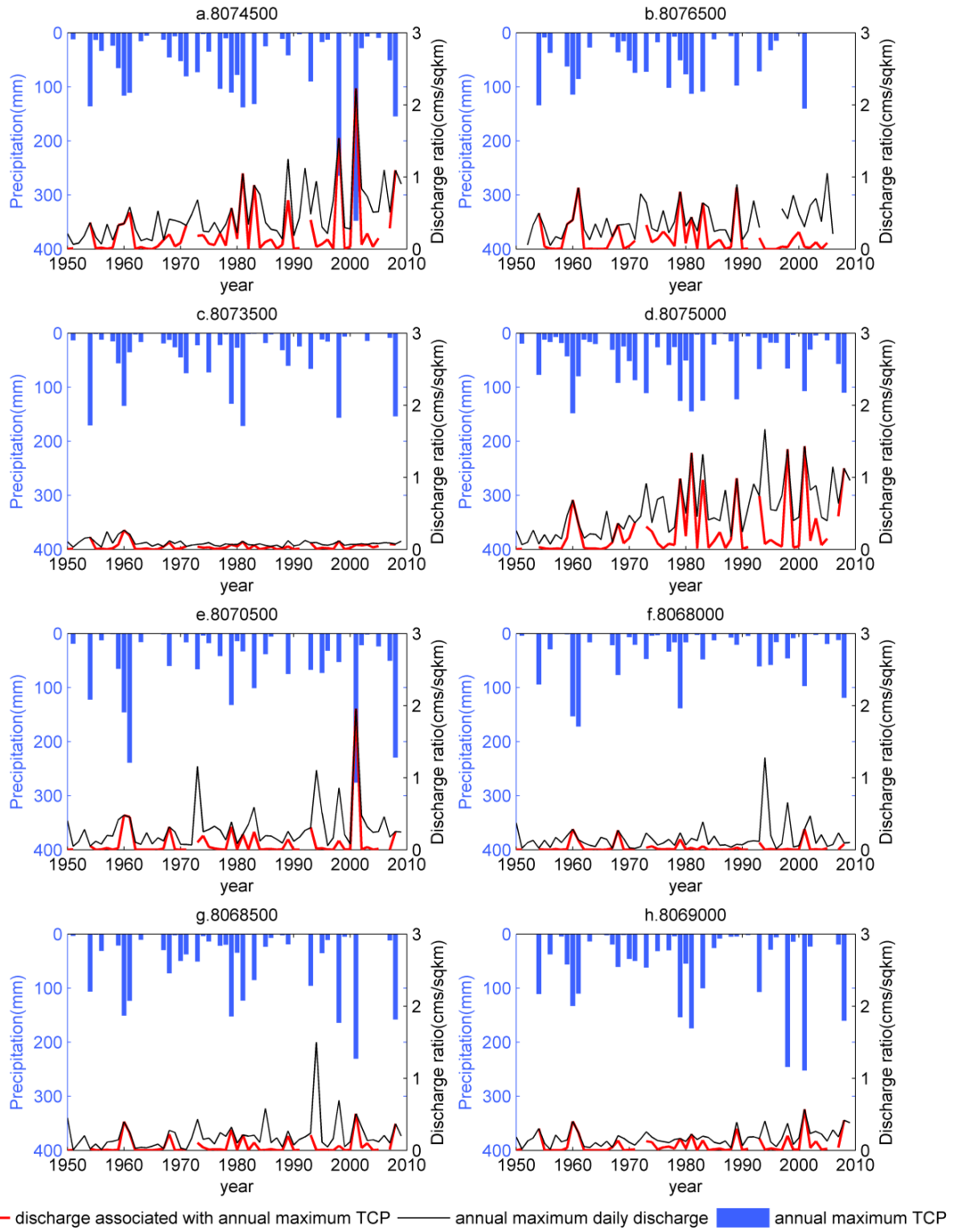

Figure 6.3. Annual maximum TCP (mm), annual maximum daily discharge ratio (cm km^{-2}) and maximum daily discharge ratio associated with the annual maximum TCP for each watershed (8074500: Whiteoak Bayou, 8076500: Halls Bayou, 8073500: Buffalo Bayou, 8075000: Brays Bayou, 8070500: Caney Ck, 8068000: W Fk San Jacinto Rv, 8068500: Spring Ck, 8069000: Cypress Ck).

[*Storey*, 1998]. Since both of these flood control structures were built before 1950, the extreme discharge ratios (Figure 6.3e) for Buffalo Bayou (gauge 8073500) do not vary much from year to year.

The change points, linear trends and stationarity have been tested for time series in Figure 6.3 and their variances. Most watersheds have significant increasing trends or change points in the annual maximum discharge ratios (Mann-Kendall Test, 95% Significance, Figure 6.4a). Watersheds for Caney Ck and Cypress Ck (gauge 8070500 and 8069000) have statistically significant change points in the variance of annual maximum discharge ratios (Figure 6.4b). This means that the amplitude of interannual variation in the annual maximum discharge ratios in these two watersheds have increased since 1993.

There is no statistically significant trend or change point in the mean and variance of maximum TCP and TCP-related discharge due to the large interannual variability in TC activity. During the Tropical Storm Allison in 2001, gauge 8074500 received >350 mm of TCP. This is the largest daily TCP event to occur in the eight watersheds (Figure 6.3).

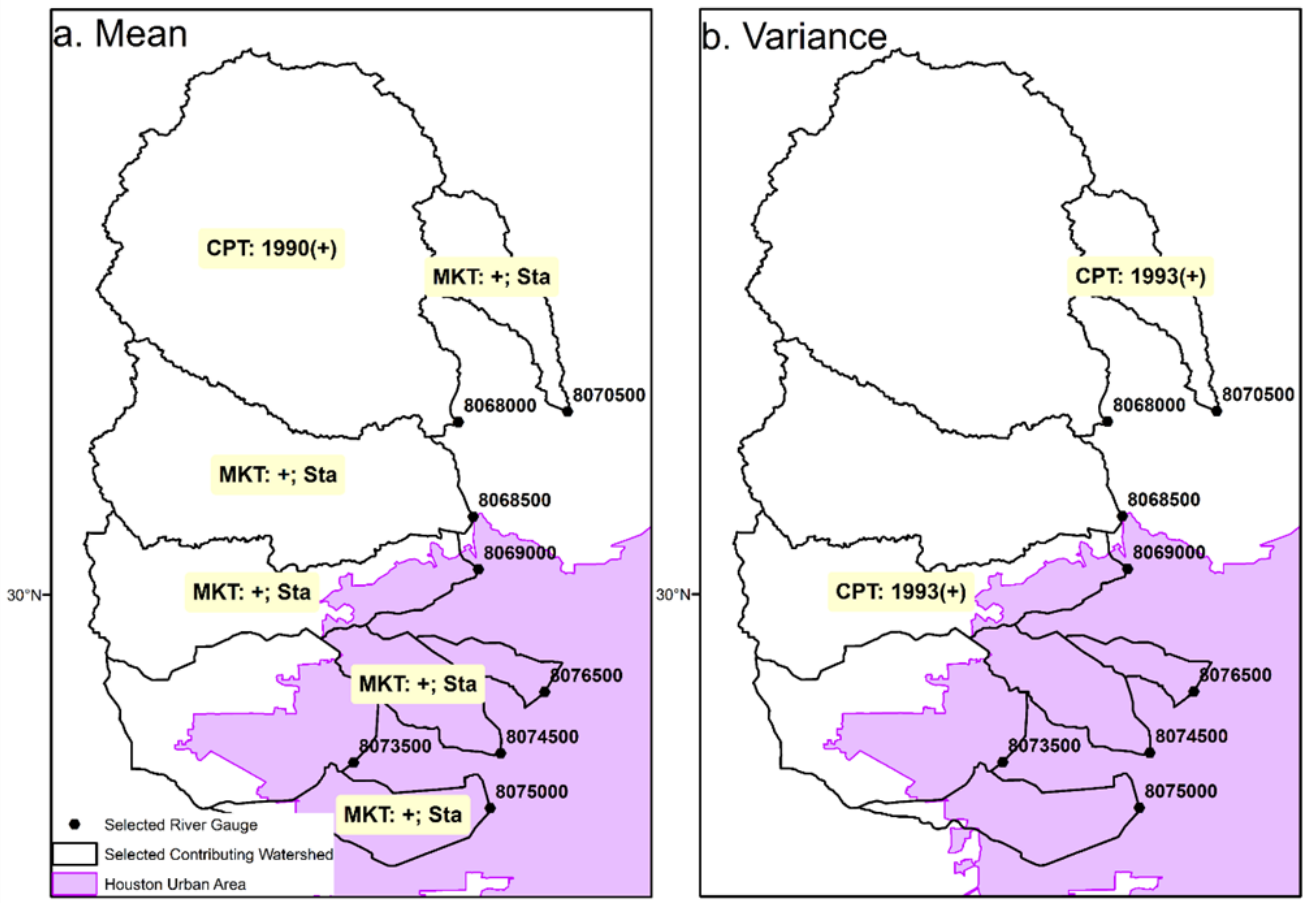

Figure 6.4. Significant linear trends and change points in time series of mean and variance of the annual maximum discharge ratio for selected watersheds. MKT represents the Mann-Kendall linear trend test, a + (-) indicates the trend is increasing (decreasing); Sta (No Sta) means trend is stationary (not) tested by the Kwiatkowski–Phillips–Schmidt–Shin approach; CPT is for the change point passed by the Pettitt test, the year of change is also presented with a + (-) meaning increased (decreased) mean/variance after the change point.

Two very large TCP events are observed in Whiteoak Bayou watershed (gauge 8074500) in 1998 and 2001 (Figure 6.3a). The watershed contains a large portion of downtown Houston and has the largest percentage of developed land (Figure 6.1 and 6.2). Many extreme TCP cases (>200 mm) also happened in suburban watersheds located in the north of Houston (gauge 8070500, 8068500, 8069000, Figure 6.1). Those events can be possibly related to the precipitation enhancing effect from the transported aerosols [*Orville et al.*, 2001; *Li et al.*, 2008]. Some studies argued that the sea breeze can transport the aerosols to the downwind direction (North) of the pollutant sources in Houston and produce enhanced precipitation in north Houston [*Darby*, 2005; *Fast et al.*, 2006]. Since most of the TCs made landfall in Texas travelled towards north or northwest directions [*Zhu and Quiring*, 2013], they may bring some anthropogenic aerosols to northern Houston and enhance TCP.

Maximum TCP discharge shows larger differences between the more urbanized and less urbanized watersheds (red line, Figure 6.3). Watersheds that are more urbanized generally have a larger maximum TCP discharge ratios, except for Buffalo Bayou watershed (gauge 8073500). Whiteoak Bayou (Gauge 8074500) reached the largest discharge ratio (2.22 mm km^{-2}) in 2001 from Tropical Storm Allison. This is due to the large amount of precipitation and the fact that this watershed has the highest percentage of developed land. Watersheds for Whiteoak Bayou (gauge 8074500) and Brays Bayou (gauge 8075000) frequently experienced extreme discharges after 1980, especially TCP-related discharges. In both watersheds the percentage of developed land changed from ~40% in 1980 to >90% in 2006 (Figure 6.2a & 6.2d). They also had the grass and

agriculture land reduced from >50% in the 1980s to near zero in 2006. Urban development results in more impervious surface in the watershed, it reduces infiltration of rainfall into the soil and the time of concentration for runoff, and it increases discharge [*Hollis*, 1975; *Hundecha and Bardossy*, 2004]. Therefore, the frequency and magnitude of extreme discharge expected to increase due to these changes [*Jennings and Jarnagin*, 2002; *Ogden et al.*, 2011]. The larger discharge ratios in Whiteoak Bayou (gauge 8074500), Halls Bayou (gauge 8076500) and Brays Bayou (gauge 8075000) are likely associated with increases in impervious surfaces due to urbanization. The less urbanized watersheds (8070500, 8068000, 8068500, 8069000) also have seen increases in developed land. Several high values exist in the time series of maximum discharge ratios. The events in Caney Ck (gauge 8070500), W Fk San Jacinto Rv (gauge 8068000) and Spring Ck (gauge 8068500) may also be associated with the reduction in forested area in these watersheds after 1980 (Figure 6.1 & 6.2)

6.3 Annual Daily Precipitation and TCP Days Exceeding the 90th Percentile

The annual 90th percentile daily precipitation is indicated by the red line in Figure 6.5 and the TCP days exceeding the 90th percentile is indicated with the blue line. Linear trend and stationarity tests have been done for both time series and the change point test has been processed only for the 90th percentile daily precipitation. Many change points have been detected in both annual daily precipitation and its variance in a number of watersheds (Figure 6.6a & 6.6b). All more urbanized watersheds have increasing change point or linear trend in their time series for the 90th percentile daily precipitation (8074500, 8076500, 8073500 and 8075000, Figure 6.6a). All of the change

points occur after 1970 in the more urbanized watersheds (Figure 6.6a). The mean values after the change points are ~3-5 mm larger than before. These results match with the rapid urbanization that has occurred in these watersheds (Figure 6.1 & 6.2). The less urbanized watersheds also demonstrate increases in the 90th percentile daily precipitation. Watersheds for W Fk San Jacinto Rv (gauge 8068000) and Caney Ck (gauge 8070500) have a statistically significant positive linear trend. They are both are located north of Houston. Watersheds for Spring Ck and Cypress Ck (gauge 8068500 and 8069000) have change points in 1956, with the post-1956 precipitation being significantly greater. The majority of the variance of the 90th percentile daily precipitation has a change point or linear trend that is associated with increasing precipitation variability in the latter part of the record (Figure 6.6b). This indicates that most watersheds have experienced increases in the interannual variability of the 90th percentile daily precipitation.

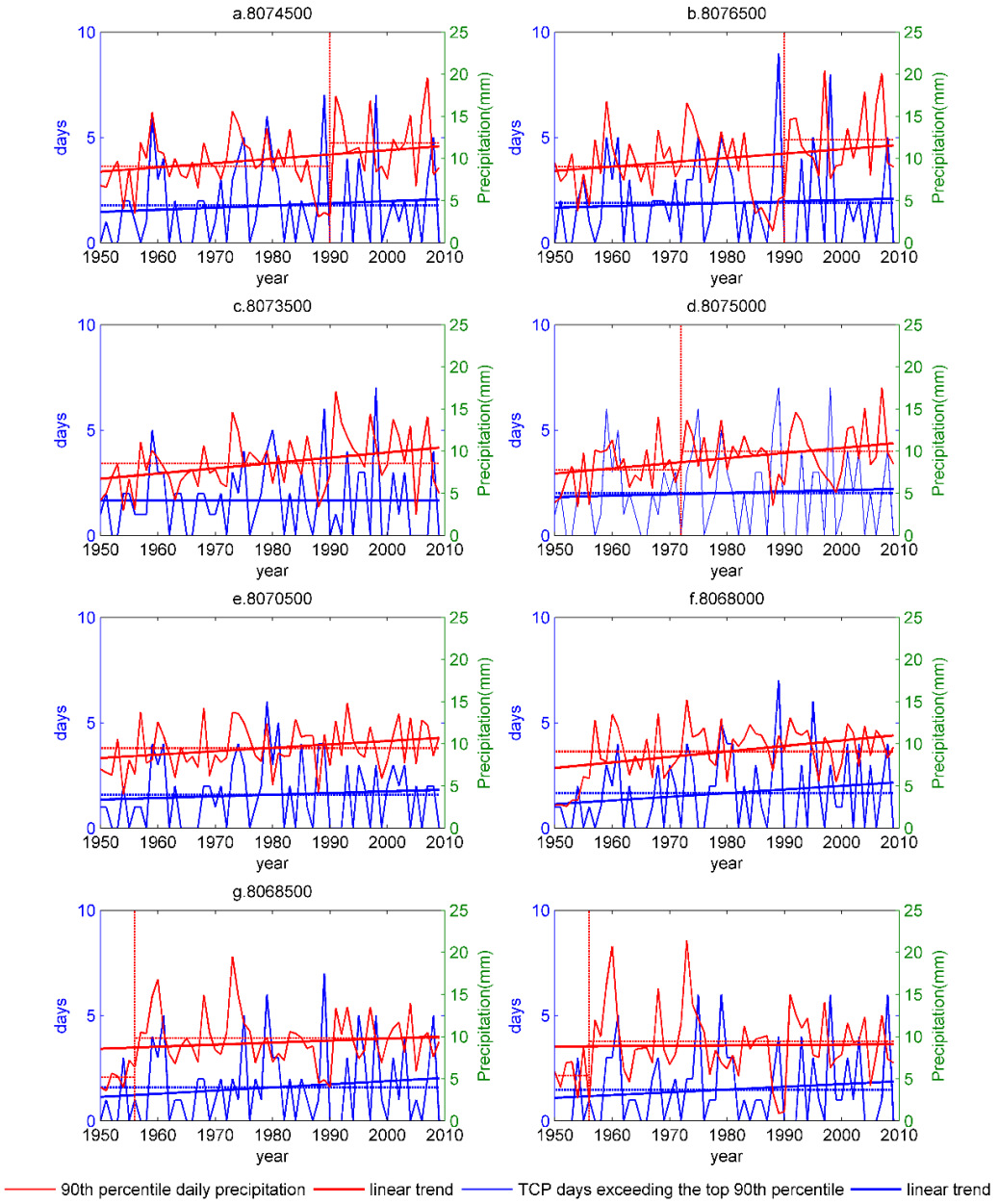

Figure 6.5. Time series of the 90th percentile daily precipitation and TCP days with precipitation larger than the 90th percentile daily precipitation. Change points (Pettitt) are detected for the time series of the 90th percentile daily precipitation. Mean values before and after the change point are displayed if the change point is statistically significant at the 5% level (dash lines), otherwise the whole sample mean is displayed (dash lines). Linear trends are also shown for time series (solid straight lines) (8074500: Whiteoak Bayou, 8076500: Halls Bayou, 8073500: Buffalo Bayou, 8075000: Brays Bayou, 8070500: Caney Ck, 8068000: W Fk San Jacinto Rv, 8068500: Spring Ck, 8069000: Cypress Ck).

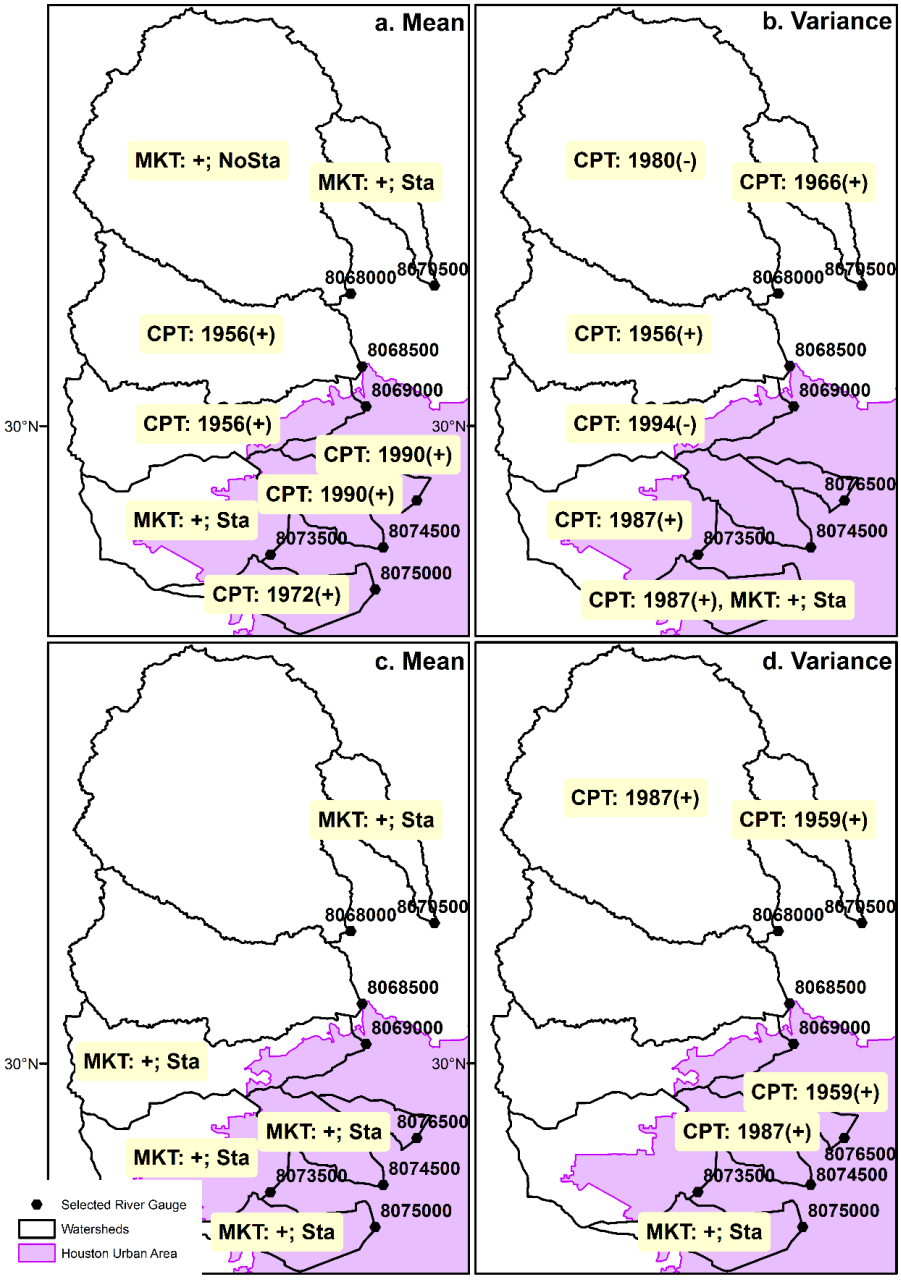

Figure 6.6. Significant linear trends and change points in the time series of mean and variance of the 90th percentile precipitation (6.6a & 6.6b) and 90th percentile discharge (6.6c & 6.6d) for all watersheds. MKT represents the Mann-Kendall linear trend test, a "+" ("-") indicates the trend is increasing (decreasing); "Sta" ("No Sta") means the trend is stationary (not stationary) as determined by the Kwiatkowski–Phillips–Schmidt–Shin approach; CPT indicates change points that were identified by the Pettitt test. The year of the change is also indicated as well as whether the changes was due to an increase ("+") (decrease "-").

No statistically significant trend exists in the TCP days above the 90th percentile daily precipitation (blue line in Figure 6.5). There is also not a significant difference in the mean between the more developed and less developed watersheds. However, the more urbanized watersheds tend to have higher values in extreme years (>15 days), and most of the extreme years have occurred after 1980. Watersheds for Buffalo Bayou (gauge 8073500) and W Fk San Jacinto Rv (gauge 8068000) have significant increasing trends in the variance of TCP days above the 90th percentile. This indicates that there is increased interannual variability in the frequency of TCP events. There is a great deal of interannual variability in the time series of TCP days exceeding the 90th percentile. This variability is controlled by the number of rain-generating TCs that make landfall in the study area, how fast they move across the study area, how much precipitation they brought, and how large an area they effected. Whether there is increase in the global landfall TC frequencies is still under debate [*Henderson-Sellers et al.*, 1998; *Landsea et al.*, 2006]. This regional analysis reveals no significant trends in the number of TCP days above the 90th percentile, but the mean value of the 90th percentile precipitation has increased in most watersheds. This indicates that there has been an increase in the intensity of heavy TCP events (exceeding the 90th percentile threshold), but generally no change in the frequency. The increased variance means more interannual variability in the magnitude and frequency of these heavy TCP events.

6.4 Annual Discharge Ratios and TCP-related Discharge Ratios Exceeding the 90th Percentile

The 90th percentile daily discharge ratio has a very different pattern than the 90th percentile daily precipitation (Figure 6.6c & 6.6d & 6.7). There are statistically significant increasing trends in most of the highly urbanized watersheds (8073500, 8074500, and 8075000), and in half of the less urbanized watersheds (8069000 and 8075000). That means that the extreme discharge ratios are steadily increasing in most watersheds. Figure 6.7 demonstrates the steep slope of the 90th percentile discharges in watersheds with more developed land (gauge 8074500, 8073500 and 8075000). Nearly all of the more urbanized watersheds in Figure 6.2 have experienced statistically significant increases in developed land (>40%) between 1980 and 2006. The absence of significant increasing trend in Halls Bayou watershed (gauge 8076500) may be due to the already very high proportion of developed land at the beginning of the 1980s (~60%, Figure 6.2). There are also 3 years of missing discharge data in this watershed after 2006.

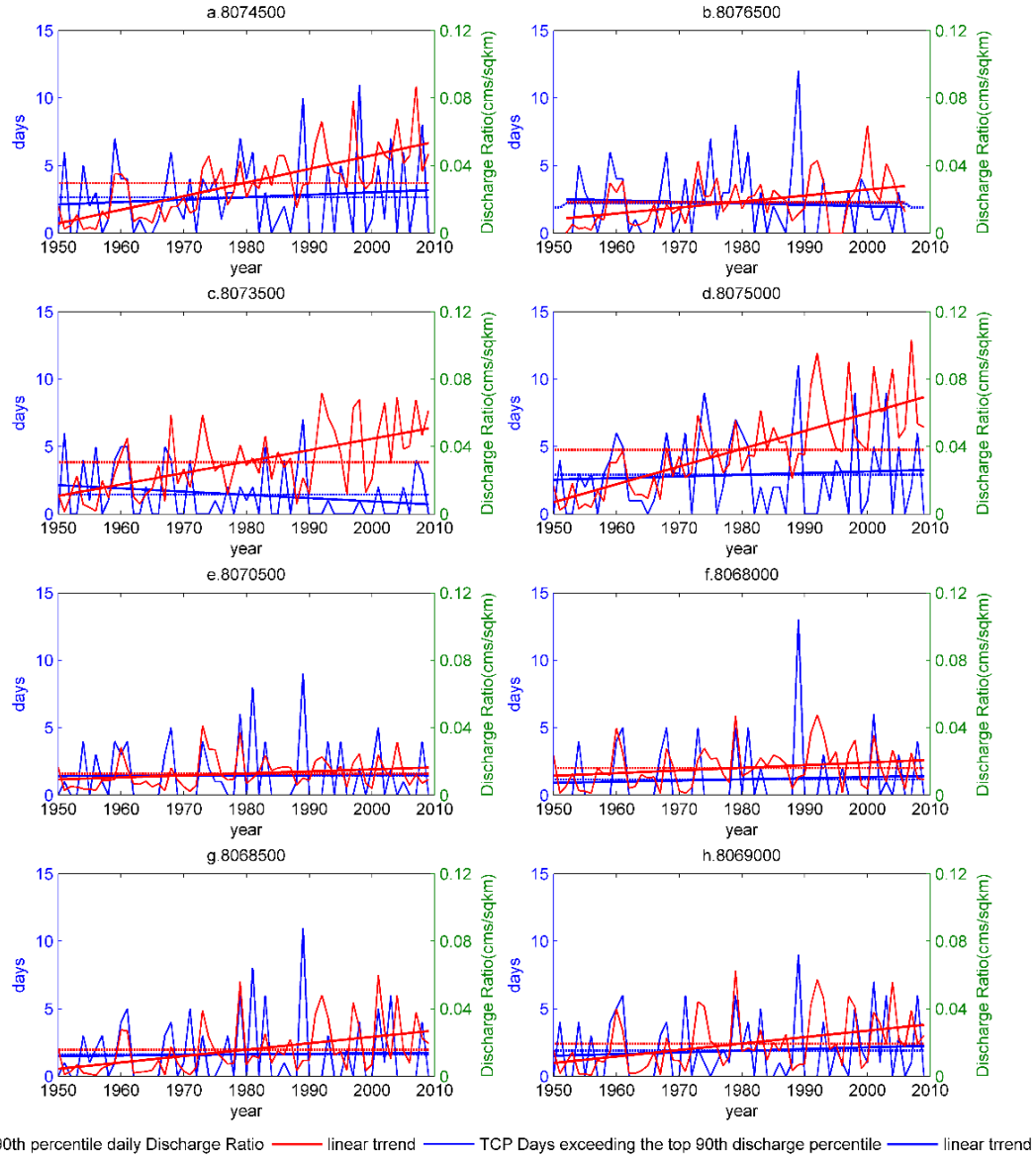

Figure 6.7. Time series of the 90th percentile of daily discharge and days with TCP-related discharge (-1 to +2 days to the TCP day) larger than the 90th percentile of daily discharge. Change points (Pettitt) are detected for the time series of the 90th percentile of daily discharge. The sample mean is shown (dash lines). Linear trends are also shown for time series (solid straight lines) (8074500: Whiteoak Bayou, 8076500: Halls Bayou, 8073500: Buffalo Bayou, 8075000: Brays Bayou, 8070500: Caney Ck, 8068000: W Fk San Jacinto Rv, 8068500: Spring Ck, 8069000: Cypress Ck).

Among the less urbanized watersheds, Caney Ck (gauge 8070500) and Cypress Ck (gauge 8069000) show significantly increasing trends in the 90th percentile discharge. Watershed for Caney Ck (gauge 8070500) has the largest reduction in forested area (> 50%) between 1980 and 2006 (Figure 6.2). Watershed for Cypress Ck (gauge 8069000) had a ~20% increase in developed land and ~10% reduction in both forest and grassland. Forests have shown to play an important role in reducing runoff, even extreme rainfall, and reducing the magnitude of discharge [*Jones and Grant*, 1996; *Prosser and Williams*, 1998; *Sun et al.*, 2002]. Developed land generates more runoff due to the increased impervious surface. Increases in the 90th percentile discharge in less urbanized watersheds may be due to decreases in forested area and increases in impervious surfaces.

Several increasing change points and one statistically significant increasing trend have been detected in the variance of the 90th percentile discharge ratio (Figure 6.6d). Increases in the variance indicate that there has been an increase in the interannual variability in extreme discharge. Several watersheds are showing increases (either change point or linear trend) in both the mean and the variance (gauge 8074500, 8075000 and 8070500). This may make flood control and prevention more difficult because it means that extreme discharge is increasing and interannual variability is also increasing. Based on these results, it is apparent that changes in land use/cover have a major influence on the extreme discharge in watersheds near Houston.

No significant trend can be detected in the TCP-related daily discharge ratios that exceed the 90th percentile (blue line in Figure 6.7). Therefore, the mean number of

extreme TCP discharge events is basically unchanged in all of the selected watersheds during the last 60 years. However, the mean number of extreme events in the more urbanized watersheds is ~1-2 days more than that in the less urbanized watersheds. For example, both Whiteoak Bayou (gauge 8074500) and Brays Bayou (gauge 8075000) have seen more active years (> 10 days) in the time series, especially after 1980 (Figure 6.7a & 6.7d). Both of these watersheds are highly developed and have experienced substantial urbanization between 1980 and 2006.

There is substantial interannual variability in the time series of TCP discharge ratios exceeding the 90th percentile. Whiteoak Bayou (gauge 8074500) is the only one showing statistically significant increasing trends in the variance. However, most of the years with >10 days have occurred since 1980. The increases in the 90th percentile along with the substantial interannual variability suggest that the risk of flooding due to extreme TCP-generated discharge has increased.

In this section, precipitation and discharge data have been reorganized into composites corresponding to the four periods of the available land use data (Figure 6.1). This approach will help to quantify how urbanization has influenced TCP and discharge. Decadal means have been calculated for the precipitation and discharge ratios using the year from which land use data is available as the mid-point. For example, land use data from 1980 is compared to precipitation and discharge data from 1976 to 1985. The 1980 land use data are assumed to be representative of the entire 10 year period.

Figure 6.8 shows variations in the annual maximum daily precipitation/TCP, and annual maximum daily discharge ratio/TCP discharge ratio. The annual maximum

precipitation had more pronounced changes in the more urbanized watersheds. Three out of four (8074500, 8076500, and 8073500) watersheds with more developed land have increases in annual maximum precipitation (Figure 6.8, blue lines). Two out of four (8068500 and 8069000) of the less urbanized watersheds also show increases in annual maximum precipitation. They are the two showing largest increased in developed land among the four less urbanized watersheds (Figure 6.2).

There are more variations in the annual maximum TCP (red lines in Figure 6.8) during the four periods. Several watersheds show no change or slight decreases in maximum TCP. This is due to the high interannual variability in the TCP. Watersheds for Whiteoak Bayou (gauge 8074500) and Caney Ck (gauge 8070500) are the two demonstrating some increasing patterns in the maximum TCP.

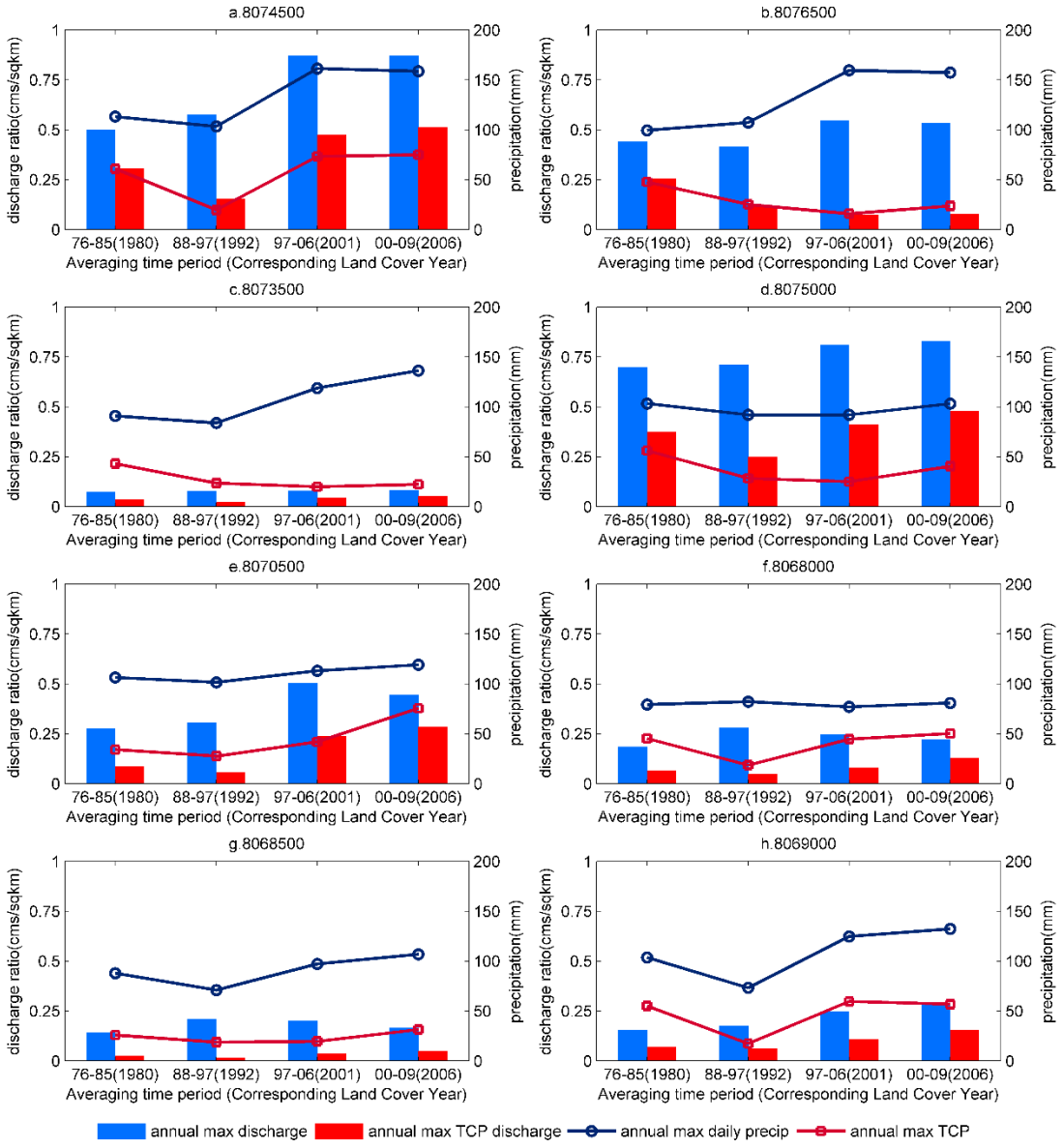

Figure 6.8. Variations of the annual maximum daily precipitation, maximum TCP, maximum discharge, and maximum TCP discharge for different watersheds between 1980 and 2006 (8074500: Whiteoak Bayou, 8076500: Halls Bayou, 8073500: Buffalo Bayou, 8075000: Brays Bayou, 8070500: Caney Ck, 8068000: W Fk San Jacinto Rv, 8068500: Spring Ck, 8069000: Cypress Ck).

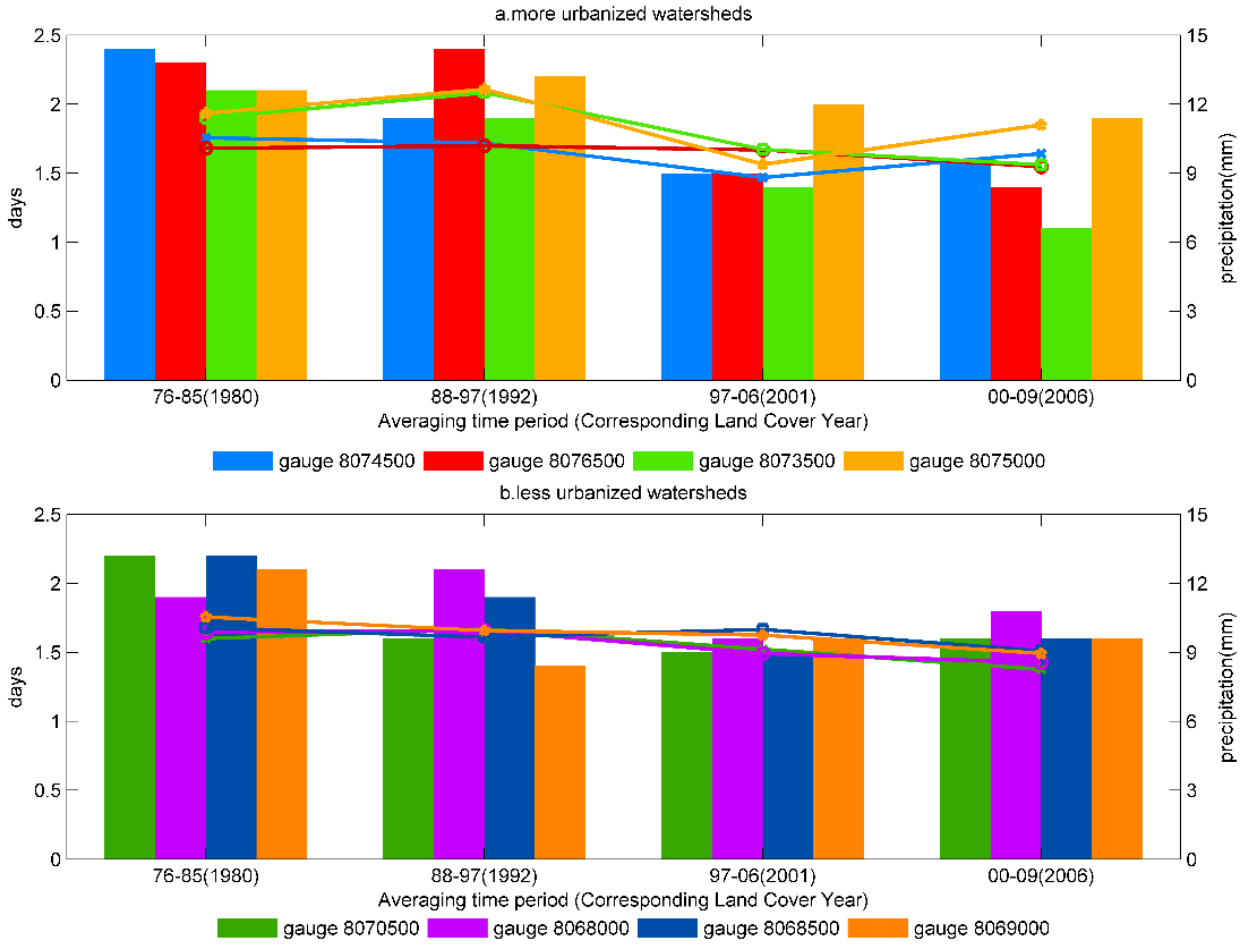

Figure 6.9. Variations of the annual 90 percentile precipitation (lines) and TCP days passing the annual 90 percentile precipitation (bars) for different watersheds between 1980 and 2006 (8074500: Whiteoak Bayou, 8076500: Halls Bayou, 8073500: Buffalo Bayou, 8075000: Brays Bayou, 8070500: Caney Ck, 8068000: W Fk San Jacinto Rv, 8068500: Spring Ck, 8069000: Cypress Ck.

Patterns of the maximum discharge ratios have larger contrasts between the more urbanized and less urbanized watersheds (bars in Figure 6.8). Except for the engineering controlled watershed (Buffalo Bayou, gauge 8073500), all other three more developed watersheds (8074500, 8076500, and 8075000) have significantly larger composite discharge ratios than the less urbanized watersheds. The majority of watersheds have increased discharge ratios (both annual maximum and TCP related maximum) from the 1980 era to the 2006 era, even though some watersheds show no change or even decrease in the annual maximum precipitation or maximum TCP. This demonstrates that urbanization has a strong and widespread effect on intensifying discharges in the rivers around Houston.

Finally, the same 10-year averages have been calculated for the 90th percentile precipitation/discharge ratios and TCP days/discharge ratios exceeding the 90th percentile (Figure 6.9 & 6.10). Figure 6.9 shows no significant changes in the 90th percentile daily precipitation for almost all watersheds from the 1980 composite to the 2006 composite (lines). The TCP days exceeding the 90th percentile have not changed or have slightly decreased for several watersheds, with larger averages in the more urbanized watersheds (bars in Figure 6.9a).

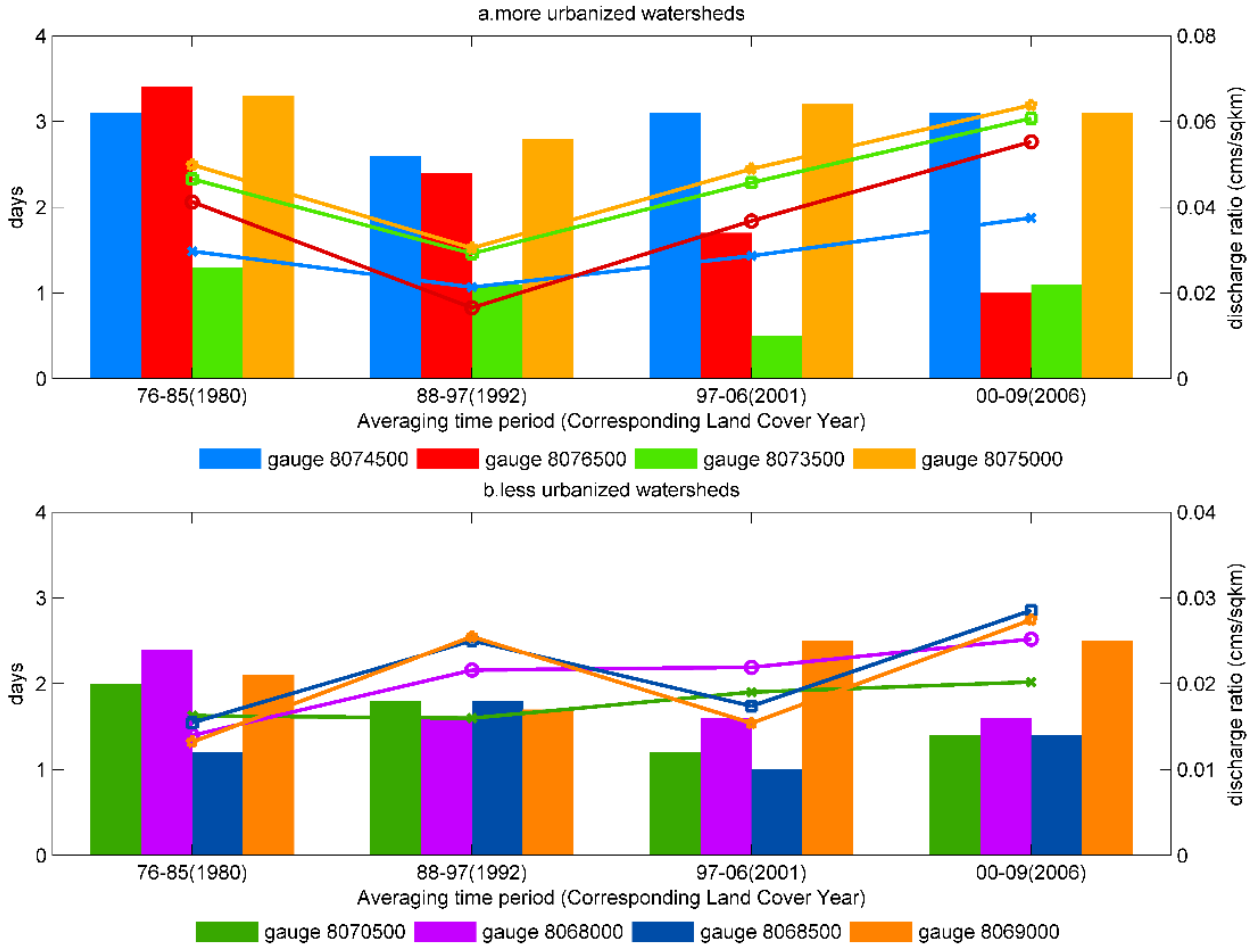

Figure 6.10. Variations of the annual 90 percentile discharge ratio (lines) and TCP related discharges passing the annual 90 percentile discharge ratio (bars) for different watersheds between 1980 and 2006 (8074500: Whiteoak Bayou, 8076500: Halls Bayou, 8073500: Buffalo Bayou, 8075000: Brays Bayou, 8070500: Caney Ck, 8068000: W Fk San Jacinto Rv, 8068500: Spring Ck, 8069000: Cypress Ck).

The 90th percentile discharge ratios again show very noticeable increases for all 8 watersheds (lines in Figure 6.10). Mean values of the discharge ratio for the more urbanized watershed (Figure 6.10a) are almost twice of the less urbanized watersheds. This is impressive because Figure 6.9 shows that there is not much difference in the 90th percentile precipitation between the more and less urbanized watersheds. The composites generally agree with the results obtained from the 60-year time series analysis. Most of the changes in TCP-related discharge are mainly due to the land use change.

6.6 Conclusion and Discussion

Objective 3 investigated variations in TCP and extreme discharge in watersheds undergoing rapid land use/cover change near Houston. More urbanized watersheds have larger annual maximum discharge ratios. Many watersheds undergoing rapid urbanization have significant increasing trends or change points in their annual maximum discharge ratios. This is partially due to more runoff rapidly generated from the impervious surface and less infiltration from the reduced vegetation. Engineering projects (such as dams and water holes) also play an important role in reducing the peak flows in one controlled watersheds. Many of the annual maximum discharge events are caused by TCP. This is especially pronounced after 1980. No trend exists in the maximum TCP and most watersheds receive similar mean TCP. In certain years, some watersheds have much larger extreme TCP values than other watersheds. These extreme TCP events tended to occur more often after 1980.

Some watersheds have statistically significant increasing trends in the 90th percentile of annual precipitation and some have increased change points. No change is observed in the annual TCP days exceeding the 90th percentile. All watersheds have ~ 5 days every year with TCP greater than the annual 90th percentile precipitation. This demonstrates the importance of TC systems in generating extreme precipitation in Texas. Years with more severe TCPs are more likely to happen in watersheds with more developed land cover after 1980 (gauge 8076500, 8073500 and 8075000). There are watersheds showing increased variances in both the 90th percentile precipitation and the frequency of TCP days exceeding that threshold. This indicates that the risk of heavy TCP has increased and that variability in TCP has also increased.

The annual 90th percentile discharge ratio demonstrates a larger spatial contrast determined by the land use. The more urbanized watersheds basically have larger mean discharge ratios. The most highly urbanized watersheds have the most pronounced increasing trends. Many of time series have both experienced increases in both the mean and variance. Two less urbanized watersheds also demonstrate statistical significant increasing trends, but their magnitudes are not as big as those for the more urbanized watersheds.

The more urbanized watersheds also have more TCP discharge exceeding the 90th percentile (~3 cases annually on average) than the less urbanized watersheds (< 2 cases). Because of the high interannual variability in TC activity, no statistically significant trend exists in the TCP discharge exceeding the 90th percentile. Only Whiteoak Bayou watershed (gauge 8074500) has an increasing trend in its variance. The

more urbanized watersheds tend to have more years with >10 TCP discharges exceeding the 90th percentile after 1980.

The composite analysis shows similar results to the 60-year time series. Many watersheds have increased annual maximum precipitation and TCP from the 1980 era to the 2006 era. The increasing patterns are more uniform for the annual and TCP-related maximum discharge ratios. Urbanized watersheds have larger extreme discharge ratios on average. No change is evident in the 90th percentile precipitation. The TCP days exceeding the 90th percentile basically have no change or slight decreases. Despite this, the 90th percentile discharge ratios have substantial increased in all watersheds. The more urbanized watersheds also have around twice the 90th percentile discharge ratios as compared with the less urbanized watersheds. Most watersheds show no changed or slightly decreased number of TCP discharge events that exceed the 90th percentile.

This is the first study exploring the contributions from both the TCP and urbanization to the extreme precipitation and discharge in watersheds located in the rapidly developing city of Houston. There are increases in the annual maximum and the 90th percentile precipitation. The increases in the maximum and the 90th percentile discharge ratios are more obvious than the precipitation. The discharge intensifying effects from more impervious surfaces are very strong and widespread, with more pronounced effects in the more urbanized watersheds. No trend can be detected in the TCP days and discharges exceeding the 90th percentile thresholds. But the TC contributed many cases of the annual maximum discharge and very large discharges. Years with many extreme TCP and discharges tend to happen more in the more

urbanized watersheds after 1980. Some watersheds also show increased variances in the annual TCP discharge ratios exceeding the thresholds. Although no long-term trend exists in the TCP and TCP-related extreme discharge, there may be an increased risk of floods from the TCP because of the statistically significant increases in annual maximum discharge and 90^{th} percentile discharge that have been observed. There is increased uncertainty in this flood risk because the increased variability in the most extreme precipitation like TCP, possibly influenced by urban heat island, aerosols, and climate change.

7. SUMMARY AND CONCLUSIONS

7.1 Summary

Tropical cyclones (TC) can cause lots of damage to the environment and people in Texas. Heavy precipitation is a very important component of TCs and is one of the major causes of inland flooding in Texas. This dissertation used 60 years of precipitation and streamflow data to improve understanding of three related topics on TCP in Texas: 1) How has TCP varied temporally and spatially in Texas? 2) Which global, regional and local factors control the interannual variations in TCP in Texas? 3) How does TCP contribute to annual extreme precipitation and discharge events in Houston watersheds undergoing rapid urbanization? TCP has been extracted from rain gauges using a newly developed objective method (MRBT). Spatial patterns and temoporal trends have been analyzed for the daily, monthly and annual TCP metrics. Regional and large-scale climatic and oceanic forcing variables have been extracted from the NCEP/NCAR reanalysis. Seasonal forecasting models have been constructed for the annual TCP, TCP percentage and TCP event of Texas. Interpretations of physical mechanisms have been made for all parameters in the constructed models by using the current knowledge and available observations. Finally, TCP was compared with annual extreme precipitation and discharge in watersheds near Houston. Land use/cover change was analyzed to determine how it has influenced TCP-related extreme discharge in these watersheds.

7.2 Conclusions

This study uses both quantitative evaluations and statistical models to investigate a long-term climatology of TCP and its impacts in Texas. The spatial pattern of the TCP reveals that most extreme daily TCP (>300 mm) occurs near the center of circulation and in the front half and right side of the TC. The largest TCP events in Texas are associated with slow moving or stalled TC systems. August and September recieve the most extensive and heaviest TCP in Texas. Coastal areas generally have more frequent and intense daily TCP (>50 or >100 mm). Rare TCs can produce extreme daily TCP at some inland locations (Hurricane Gilbert, >400 mm) in western Texas. Texas has 123.5 mm and 17.8 km^3 of TCP annually, which accounts for ~20% of all TCP that occurs in the U.S. No statistically significant long-term trend (>50 years) can be observed in the annual and daily TCP metrics. There are statistically significant increasing and decreasing trends at some gauges over shorter time periods (10-30 years). Texas TCP is dominated by interannual, biennual, 5-8 year, and >10 year oscillations.

ENSO is the most important variable in the statistical models. La Niña reduces vertical shear in the Caribbean and tropical Atlantic and increases the probability of cyclogenesis [Gray, 1984a; b]. The addition of thermo-dynamic predictors (MPV and vorticity) have significantly increased predictive skill and cross-validation accuracy of the comprehensive models for the annual TCP and TCP percentage. Pre-season MPV in the Gulf of Mexico and vorticity in the MDR are connected to the maximum wind speed, translation speed and size of TCs that make lanfall in Texas. Other predictors in our models all have physical connections to seasonal TCP in Texas. For example, low sea

level pressure in the Gulf of Mexico is favorable to the formation and development of TCs in the Gulf of Mexico and it produces more TCP in Texas. Warmer than normal SSTs in the Caribbean enhance TC genesis and also support TCs that formed in the Atlantic and then move through the region. The negative NAO may produce more westward "straight moving" TCs and less winter precipitation, and therefore increase TCP in Texas.

Urbanization may enhancing annual maximum precipitation and maximum TCP. There are increases in the annual maximum and the 90th percentile precipitation thresholds. Increases in the maximum discharge and the 90th percentile discharge ratios are more obvious than the precipitation. Increases in discharge appear to be driven by the increased impervious surfaces and they are most pronounced in the more urbanized watersheds. No trend can be detected in TCP days and TCP discharge exceeding the 90th percentile. However, TCs are frequently responsible for the annual maximum discharge. There is a tendency for their to be more extreme TCP events since 1980. Some watersheds also show increased variance in the annual TCP discharge ratios. Although no long-term trend can be observed in the TCP and TCP-related extreme discharge, there may be an increased risk of floods from TCP because of the statistically significant increases in annual maximum discharge and 90th percentile discharge that have been observed. There is increased uncertainty about flood risk because of the increased variability in extreme precipitation (including TCP).

The three major findings of this disservation are:

- A new MRBT method provides more complete and accurate estimations of daily TCP rain regions by considering both the TC size and TC translation speed from observations.
- Multiple linear regression models can provide good skill in forecasting annual TCP, TCP percentage, and TCP events in Texas. The comprehensive models can explain between 32% and 43% of the variance of the seasonal TCP metrics, and the simple models can explain 18% to 27% of the variance. Nearly all the parameters in the final models have statistical significant p values (<0.05) and reasonable physical interpretations. The modeled and cross-validation statistics show that most of the models are stable and robust.
- The case study of Houston reveals that urbanization may intensify the impacts of TCP-related flooding.

7.3 Future Research

I will keep improving my objective method (MRBT) by targeting uncertainties in the missing values of TC sizes and the observation bias of gauged precipitation introduced by high wind speeds. I will compare the results from the improved objective method with remotely-sensed precipitation products such as the TRMM Multisatellite Precipitation Analysis (TMPA) and radar data. I also plan to construct long-term TCP climatology for other regions.

I would like to investigate how urbanization influences extreme discharge (especially the TC-related discharge) in the whole U.S. This will involve analyzing

historical patterns and trends in the TCP extracted by the improved MRBT method and the river gauge data. This can also help to identify hot spots for physically-based modeling studies. I also plan to couple the high resolution Weather Research & Forecasting Model (WRF) and the fully distributed hydrological model to investigate the TCP's hydrological response in selected watersheds.

I want investigate the impacts of TCP on infrastructure and society. For example, I plan to incorporate the extreme TCP and floods into the prediction models for hurricane power outages. I plan to new versions of power outage prediction models, compare their performance, and evaluate the role of TCP in them.

REFERENCES

Arndt, D. S., J. B. Basara, R. A. McPherson, B. G. Illston, G. D. McManus, and D. B. Demko (2009), Observations of the Overland Reintensification of Tropical Storm Erin (2007), *B Am Meteorol Soc*, *90*(8), 1079-1093, doi:10.1175/2009bams2644.1.

Atallah, E., L. F. Bosart, and A. R. Aiyyer (2007), Precipitation Distribution Associated with Landfalling Tropical Cyclones over the Eastern United States, *Mon Weather Rev*, *135*(6), 2185-2206, doi:10.1175/Mwr3382.1.

Barlow (2011), Influence of Hurricane-related Activity on North American Extreme Precipitation, *Geophys. Res. Lett.*, *38*, L04705, doi:10.1029/2010GL046258.

Belanger, J. I., J. A. Curry, and P. J. Webster (2010), Predictability of North Atlantic Tropical Cyclone Activity on Intraseasonal Time Scales, *Mon Weather Rev*, *138*(12), 4362-4374, doi:10.1175/2010mwr3460.1.

Bender, M. A., T. R. Knutson, R. E. Tuleya, J. J. Sirutis, G. A. Vecchi, S. T. Garner, and I. M. Held (2010), Modeled Impact of Anthropogenic Warming on the Frequency of Intense Atlantic Hurricanes, *Science*, *327*(5964), 454-458, doi:10.1126/science.1180568.

Bosart, L. F., J. M. Cordeira, T. J. Galarneau, B. J. Moore, and H. M. Archambault (2011), An Analysis of Multiple Predecessor Rain Events ahead of Tropical Cyclones Ike and Lowell: 10–15 September 2008, *Mon Weather Rev*, *140*(4), 1081-1107, doi:10.1175/mwr-d-11-00163.1.

Bosart, L. F., C. S. Velden, W. E. Bracken, J. Molinari, and P. G. Black (2000), Environmental Influences on the Rapid Intensification of Hurricane Opal (1995) Over the Gulf of Mexico, *Mon Weather Rev*, *128*(2), 322-352, doi:10.1175/1520-0493(2000)128<0322:EIOTRI>2.0.CO;2.

Brody, S. D., S. E. Davis, W. E. Highfield, and S. P. Bernhardt (2008), A Spatial-temporal Analysis of Section 404 Wetland Permitting in Texas and Florida: Thirteen years of impact along the coast, *Wetlands*, *28*(1), 107-116, doi:10.1672/07-90.1.

Burian, S. J., and J. M. Shepherd (2005), Effect of Urbanization on the Diurnal Rainfall Pattern in Houston, *Hydrological Processes*, *19*(5), 1089-1103, doi:10.1002/hyp.5647.

Burnett, J. (2008), *Flash floods in Texas*, 1st ed., xv, 330 p. pp., Texas A&M University Press, College Station.

Camargo, S. J., and A. H. Sobel (2010), Revisiting the Influence of the Quasi-Biennial Oscillation on Tropical Cyclone Activity, *J Climate*, *23*(21), 5810-5825, doi:10.1175/2010jcli3575.1.

Camargo, S. J., M. C. Wheeler, and A. H. Sobel (2009), Diagnosis of the MJO Modulation of Tropical Cyclogenesis Using an Empirical Index, *J Atmos Sci*, *66*(10), 3061-3074, doi:10.1175/2009jas3101.1.

Cerveny, R. S., and L. E. Newman (2000), Climatological Relationships between Tropical Cyclones and Rainfall, *Mon Weather Rev*, *128*(9), 3329-3336, doi:10.1175/1520-0493(2000)128<3329:CRBTCA>2.0.CO;2.

Chang, E. K. M., and Y. J. Guo (2007), Is the Number of North Atlantic Tropical Cyclones Significantly Underestimated Prior to the Availability of Satellite Observations?, *Geophys Res Lett*, *34*(14), L14801, doi:Artn L14801.

Cleveland, W. S. (1979), Robust Locally Weighted Regression and Smoothing Scatterplots, *Journal of the American Statistical Association*, *74*(368), 829-836, doi:10.2307/2286407.

Collier, C. G. (2006), The Impact of Urban Areas on Weather, *Quarterly Journal of the Royal Meteorological Society*, *132*(614), 1-25, doi:10.1256/qj.05.199.

Corbosiero, K. L., and J. Molinari (2002), The Effects of Vertical Wind Shear on the Distribution of Convection in Tropical Cyclones, *Mon Weather Rev*, *130*(8), 2110-2123, doi:10.1175/1520-0493(2002)130<2110:TEOVWS>2.0.CO;2

Cry, G. W. (1967), *Effects of Tropical Cyclone Tainfall on the Distribution of Precipitation over the Eastern and Southern United States*, iv, 67 p. pp., U.S. Dept. of Commerce, Environmental Science Services Administration, Washington.

Darby, L. S. (2005), Cluster Analysis of Surface Winds in Houston, Texas, and the Impact of Wind Patterns on Ozone, *Journal of Applied Meteorology*, *44*(12), 1788-1806, doi:10.1175/JAM2320.1.

Davies, T. V. (1948), LX. Rotatory Flow on the Surface of the Earth.— Part I. Cyclostrophic Motion, *Philosophical Magazine Series 7*, *39*(293), 482-491, doi:10.1080/14786444808521699.

Davis, C. A., and K. A. Emanuel (1991), Potential Vorticity Diagonostics of Cyclogenisis, *Mon Weather Rev*, *119*(8), 1929-1953, doi:10.1175/1520-0493(1991)119<1929:pvdoc>2.0.co;2.

DeMaria, M. (1996), The Effect of Vertical Shear on Tropical Cyclone Intensity Change, *J Atmos Sci*, *53*(14), 2076-2087, doi:10.1175/1520-0469(1996)053<2076:TEOVSO>2.0.CO;2.

Deser, C., and J. M. Wallace (1987), El Niño Events and Their Relation to the Southern Oscillation: 1925-1986, *J Geophys Res-Oceans*, *92*(C13), 14189-14196, doi:10.1029/JC092iC13p14189.

Easterling, D. R., G. A. Meehl, C. Parmesan, S. A. Changnon, T. R. Karl, and L. O. Mearns (2000), Climate Extremes: Observations, Modeling, and Impacts, *Science*, *289*(5487), 2068-2074, doi:10.1126/science.289.5487.2068

Elsner, J. B. (2003), Tracking Hurricanes, *B Am Meteorol Soc*, *84*(3), 353-356, doi:10.1175/bams-84-3-353.

Elsner, J. B., and T. H. Jagger (2004), A Hierarchical Bayesian Approach to Seasonal Hurricane Modeling, *J Climate*, *17*(14), 2813-2827, doi:10.1175/1520-0442(2004)017<2813:ahbats>2.0.co;2.

Elsner, J. B., and T. H. Jagger (2006), Prediction Models for Annual U.S. Hurricane Counts, *J Climate*, *19*(12), 2935-2952, doi:10.1175/jcli3729.1.

Elsner, J. B., A. B. Kara, and M. A. Owens (1999), Fluctuations in North Atlantic hurricane frequency, *J Climate*, *12*(2), 427-437, doi:10.1175/1520-0442(1999)012<0427:finahf>2.0.co;2.

Elsner, J. B., and B. Kocher (2000), Global tropical cyclone activity: Link to the North Atlantic oscillation, *Geophys Res Lett*, *27*(1), 129-132, doi:10.1029/1999GL010893.

Elsner, J. B., and C. P. Schmertmann (1993), Improving Extended-Range Seasonal Predictions of Intense Atlantic Hurricane Activity, *Weather Forecast*, *8*(3), 345-351, doi:10.1175/1520-0434(1993)008<0345:ierspo>2.0.co;2.

Emanuel, K. (1991), The Theory of Hurricanes, *Annu Rev Fluid Mech*, *23*, 179-196, doi:10.1146/annurev.fluid.23.1.179.

Emanuel, K. (1995), Sensitivity of Tropical Cyclones to Surface Exchange Coefficients and a Revised Steady-State Model incorporating Eye Dynamics, *J Atmos Sci*, *52*(22), 3969-3976, doi:10.1175/1520-0469(1995)052<3969:sotcts>2.0.co;2.

Emanuel, K. (2003), Tropical Cyclones, *Annu Rev Earth Pl Sc*, *31*, 75-104, doi:10.1146/annurev.earth.31.100901.141259.

Emanuel, K. (2005), Increasing Destructiveness of Tropical Cyclones Over the Past 30 Years, *Nature*, *436*(7051), 686-688, doi:10.1038/Nature03906.

Emanuel, K. (2007), Environmental Factors Affecting Tropical Cyclone Power Dissipation, *J Climate*, *20*(22), 5497-5509, doi:10.1175/2007jcli1571.1.

Emanuel, K. (2011), Global Warming Effects on US Hurricane Damage, *Weather Clim. Soc.*, *3*(4), 261-268, doi:10.1175/Wcas-D-11-00007.1.

Emanuel, K., R. Sundararajan, and J. Williams (2008), Hurricanes and Global Warming: Results from Downscaling IPCC AR4 Simulations, *B Am Meteorol Soc*, *89*(3), 347-+, doi:10.1175/Bams-89-3-347.

Evans, C., R. S. Schumacher, and T. J. Galarneau (2011), Sensitivity in the Overland Reintensification of Tropical Cyclone Erin (2007) to Near-Surface Soil Moisture Characteristics, *Mon Weather Rev*, *139*(12), 3848-3870, doi:10.1175/2011mwr3593.1.

Fast, J. D., W. I. Gustafson, R. C. Easter, R. A. Zaveri, J. C. Barnard, E. G. Chapman, G. A. Grell, and S. E. Peckham (2006), Evolution of Ozone, Particulates, and Aerosol Direct Radiative Forcing in the Vicinity of Houston using a Fully Coupled Meteorology-chemistry-aerosol Model, *Journal of Geophysical Research: Atmospheres*, *111*(D21), D21305, doi:10.1029/2005JD006721.

Flatau, M., W. H. Schubert, and D. E. Stevens (1994), The Role of Baroclinic Processes in Tropical Cyclone Motion - the Influence of Vertical Tilt, *J Atmos Sci*, *51*(18), 2589-2601, doi:10.1175/1520-0469(1994)051<2589:TROBPI>2.0.CO;2.

Frauenfeld, O. W., R. E. Davis, and M. E. Mann (2005), A Distinctly Interdecadal Signal of Pacific Ocean–Atmosphere Interaction, *J Climate*, *18*(11), 1709-1718, doi:10.1175/jcli3367.1.

Ghil, M., et al. (2002), Advanced Spectral Methods for Climatic Time Series, *Rev. Geophys.*, *40*(1), 1003, doi:10.1029/2000rg000092.

Goldenberg, S. B., C. W. Landsea, A. M. Mestas-Nunez, and W. M. Gray (2001), The Recent Increase in Atlantic Hurricane Activity: Causes and Implications, *Science*, *293*(5529), 474-479, doi:10.1126/science.1060040

Goldenberg, S. B., and L. J. Shapiro (1996), Physical Mechanisms for the Association of El Nifio and West African Rainfall with Atlantic Major Hurricane Activity, *J Climate*, *9*(6), 1169-1187, doi:10.1175/1520-0442(1996)009<1169:PMFTAO>2.0.CO;2.

Gray, W. M. (1968), Global View of the Origin of Tropical Disturbances and Storms, *Mon Weather Rev*, *96*(10), 669-700, doi:10.1175/1520-0493(1968)096<0669:gvotoo>2.0.co;2.

Gray, W. M. (1984a), Atlantic Seasonal Hurricane Frequency .1. El-Nino and 30-Mb Quasi-Biennial Oscillation Influences, *Mon Weather Rev*, *112*(9), 1649-1668, doi:10.1175/1520-0493(1984)112<1649:ASHFPI>2.0.CO;2.

Gray, W. M. (1984b), Atlantic Seasonal Hurricane Frequency .2. Forecasting Its Variability, *Mon Weather Rev*, *112*(9), 1669-1683, doi:10.1175/1520-0493(1984)112<1669:ASHFPI>2.0.CO;2.

Gray, W. M., C. W. Landsea, P. W. Mielke, and K. J. Berry (1992), Predicting Atlantic Seasonal Hurricane Activity 6–11 Months in Advance, *Weather Forecast*, *7*(3), 440-455, doi:10.1175/1520-0434(1992)007<0440:PASHAM>2.0.CO;2.

Gray, W. M., C. W. Landsea, P. W. Mielke, and K. J. Berry (1993), Prediction of Seasonal Atlantic Basin Tropical Cyclone Activity from 1 August, *Weather Forecast*, *8*(1), 73-86, doi:10.1175/1520-0434(1993)008<0073:pabstc>2.0.co;2.

Gray, W. M., C. W. Landsea, P. W. Mielke, and K. J. Berry (1994), Predicting Atlantic Basin Seasonal Tropical Cyclone Activity by 1 June, *Weather Forecast*, *9*(1), 103-115, doi:10.1175/1520-0434(1994)009<0103:PABSTC>2.0.CO;2.

Groisman, P. Y., R. W. Knight, D. R. Easterling, T. R. Karl, G. C. Hegerl, and V. A. N. Razuvaev (2005), Trends in Intense Precipitation in the Climate Record, *J Climate*, *18*(9), 1326-1350, doi:10.1175/JCLI3339.1.

Groisman, P. Y., R. W. Knight, T. R. Karl, D. R. Easterling, B. Sun, and J. H. Lawrimore (2004), Contemporary Changes of the Hydrological Cycle over the Contiguous United States: Trends Derived from In Situ Observations, *Journal of Hydrometeorology*, *5*(1), 64-85, doi:10.1175/1525-7541(2004)005<0064:CCOTHC>2.0.CO;2.

Hamed, K. H. (2008), Trend Detection in Hydrologic Data: The Mann-Kendall Trend Test Under the Scaling Hypothesis, *J Hydrol*, *349*(3-4), 350-363, doi:10.1016/j.jhydrol.2007.11.009.

Hamed, K. H., and A. Ramachandra Rao (1998), A modified Mann-Kendall Trend Test for Autocorrelated Data, *J Hydrol*, *204*(1–4), 182-196, doi:10.1016/S0022-1694(97)00125-X.

Hart, R. E., and J. L. Evans (2001), A Climatology of the Extratropical Transition of Atlantic Tropical Cyclones, *J Climate*, *14*(4), 546-564, doi:10.1175/1520-0442(2001)014<0546:ACOTET>2.0.CO;2.

Henderson-Sellers, A., et al. (1998), Tropical Cyclones and Global Climate Change: A Post-IPCC Assessment, *B Am Meteorol Soc*, *79*(1), 19-38, doi:10.1175/1520-0477(1998)079<0019:TCAGCC>2.0.CO;2.

Hirsch, R. M., J. R. Slack, and R. A. Smith (1982), Techniques of Trend Analysis for Monthly Water Quality Data, *Water Resour Res*, *18*(1), 107-121, doi:10.1029/WR018i001p00107.

Holland, G. J. (1983), Tropical Cyclone Motion - Environmental Interaction Plus a Beta-Effect, *J Atmos Sci*, *40*(2), 328-342, doi:10.1175/1520-0469(1983)040<0328:TCMEIP>2.0.CO;2.

Holland, G. J. (1997), The Maximum Potential Intensity of Tropical Cyclones, *J Atmos Sci*, *54*(21), 2519-2541.

Holland, G. J., and P. J. Webster (2007), Heightened Tropical Cyclone Activity in the North Atlantic: Natural Variability or Climate Trend?, *Philos T R Soc A*, *365*(1860), 2695-2716, doi:10.1098/rsta.2007.2083.

Hollis, G. E. (1975), The Effect of Urbanization on Floods of Different Recurrence Interval, *Water Resour Res*, *11*(3), 431-435, doi:10.1029/WR011i003p00431.

Hoskins, B. J., M. E. McIntyre, and A. W. Robertson (1985), On the Use and Significance of Isentropic Potential Vorticity Maps, *Quarterly Journal of the Royal Meteorological Society*, *111*(470), 877-946, doi:10.1256/smsqj.47001.

Hundecha, Y., and A. Bardossy (2004), Modeling of the Effect of Land use Changes on the Runoff Generation of a River Basin through Parameter Regionalization of a Watershed Model, *J Hydrol*, *292*(1-4), 281-295, doi:DOI 10.1016/j.jhydrol.2004.01.002.

Hurrell, J. W. (1995), Decadal Trends in the North Atlantic Oscillation: Regional Temperatures and Precipitation, *Science*, *269*(5224), 676-679, doi:10.1126/science.269.5224.676.

Inoue, M., I. C. Handoh, and G. R. Bigg (2002), Bimodal Distribution of Tropical Cyclogenesis in the Caribbean: Characteristics and Environmental Factors, *J Climate*, *15*(20), 2897-2905, doi:10.1175/1520-0442(2002)015<2897:bdotci>2.0.co;2.

Islam, T., W. Merrell, W. Seitz, and R. Harriss (2009), Origin, Distribution, and Timing of Texas Hurricanes: 1851–2006, *Natural Hazards Review*, *November 2009*, 136-144, doi:10.1061/(ASCE)1527-6988(2009)10:4(136).

Jagger, T. H., and J. B. Elsner (2006), Climatology Models for Extreme Hurricane Winds near the United States, *J Climate*, *19*(13), 3220-3236, doi:10.1175/jcli3913.1.

Jennings, D. B., and S. T. Jarnagin (2002), Changes in Anthropogenic Impervious Surfaces, Precipitation and Daily Streamflow Discharge: A Historical Perspective in a Mid-atlantic Subwatershed, *Landscape Ecology*, *17*(5), 471-489, doi:10.1023/a:1021211114125.

Jiang, H. Y., J. B. Halverson, and E. J. Zipser (2008), Influence of Environmental Moisture on TRMM-derived Tropical Cyclone Precipitation over Land and Ocean, *Geophys Res Lett*, *35*(17), doi:10.1029/2008gl034658.

Jones, J. A., and G. E. Grant (1996), Peak Flow Responses to Clear-cutting and Roads in Small and Large Basins, Western Cascades, Oregon, *Water Resour Res*, *32*(4), 959-974, doi:10.1029/95wr03493.

Jones, S. C., et al. (2003), The Extratropical Transition of Rropical Cyclones: Forecast Challenges, Current Understanding, and Future Directions, *Weather Forecast*, *18*(6), 1052-1092, doi:10.1175/1520-0434(2003)018<1052:tetotc>2.0.co;2.

Kalnay, E., and M. Cai (2003), Impact of Urbanization and Land-use Change on Climate, *Nature*, *423*(6939), 528-531, doi:10.1038/nature01675.

Karl, T. R., and K. E. Trenberth (2003), Modern Global Climate Change, *Science*, *302*(5651), 1719-1723, doi:10.1126/science.1090228.

Katz, R., and B. Brown (1992), Extreme Events in a Changing Climate: Variability is more Important than Averages, *Climatic Change*, *21*(3), 289-302, doi:10.1007/BF00139728.

Keim, B. D., and R. A. Muller (2007), Spatiotemporal Patterns and Return Periods of Tropical Storm and Hurricane Strikes from Texas to Maine, *J Climate*, *20*(14), 3498-3509, doi:10.1175/jcli4187.1.

Kendall, M. G. (1975), *Rank Correlation Measures*, Charles Griffin, London.

Kim, H. M., P. J. Webster, and J. A. Curry (2009), Impact of Shifting Patterns of Pacific Ocean Warming on North Atlantic Tropical Cyclones, *Science*, *325*(5936), 77-80, doi:10.1126/science.1174062.

Kimball, S. K., and M. S. Mulekar (2004), A 15-year Climatology of North Atlantic Tropical Cyclones. Part I: Size parameters, *J Climate*, *17*(18), 3555-3575, doi:10.1175/1520-0442(2004)017<3555:AYCONA>2.0.CO;2.

Klotzbach, P. J. (2011), El Nino-Southern Oscillation's Impact on Atlantic Basin Hurricanes and U.S. Landfalls, *J Climate*, *24*(4), 1252-1263, doi:Doi 10.1175/2010jcli3799.1.

Klotzbach, P. J., and W. M. Gray (2003), Forecasting September Atlantic Basin Tropical Cyclone Activity, *Weather Forecast*, *18*(6), 1109-1128, doi:10.1175/1520-0434(2003)018<1109:FSABTC>2.0.CO;2.

Knaff, J. A. (1997), Implications of Summertime Sea Level Pressure Anomalies in the Tropical Atlantic Region, *J Climate*, *10*(4), 789-804, doi:10.1175/1520-0442(1997)010<0789:iosslp>2.0.co;2.

Knaff, J. A., S. A. Seseske, M. DeMaria, and J. L. Demuth (2004), On the Influences of Vertical Wind Shear on Symmetric Tropical Cyclone Structure Derived from AMSU, *Mon Weather Rev*, *132*(10), 2503-2510, doi:Doi 10.1175/1520-0493(2004)132<2503:Otiovw>2.0.Co;2.

Knight, D. B., and R. E. Davis (2007), Climatology of Tropical Cyclone Rainfall in the Southeastern United States, *Phys Geogr*, *28*(2), 126-147, doi:10.2747/0272-3646.28.2.126.

Knight, D. B., and R. E. Davis (2009), Contribution of Tropical Cyclones to Extreme Rainfall Events in the Southeastern United States, *J Geophys Res-Atmos*, *114*, D23102, doi:10.1029/2009jd012511.

Knutson, T. R., J. L. McBride, J. Chan, K. Emanuel, G. Holland, C. Landsea, I. Held, J. P. Kossin, A. K. Srivastava, and M. Sugi (2010), Tropical Cyclones and Climate Change, *Nat Geosci*, *3*(3), 157-163, doi:10.1038/Ngeo779.

Knutson, T. R., and R. E. Tuleya (2004), Impact of CO2-induced Warming on Simulated Hurricane Intensity and Precipitation: Sensitivity to the Choice of Climate Model and Convective Parameterization, *J Climate*, *17*(18), 3477-3495, doi:10.1175/1520-0442(2004)017<3477:IOCWOS>2.0.CO;2.

Konrad, C. E. (2001), The Most Extreme Precipitation Events over the Eastern United States from 1950 to 1996: Considerations of Scale, *J Hydrometeorol*, *2*(3), 309-325, doi:10.1175/1525-7541(2001)002<0309:tmepeo>2.0.co;2.

Konrad, C. E., M. F. Meaux, and D. A. Meaux (2002), Relationships between Tropical Cyclone Attributes and Precipitation Totals: Considerations of Scale, *Int J Climatol*, *22*(2), 237-247, doi:10.1002/Joc.721.

Konrad, C. E., and L. B. Perry (2010), Relationships between Tropical Cyclones and Heavy Rainfall in the Carolina Region of the USA, *Int J Climatol*, *30*(4), 522-534, doi:Doi 10.1002/Joc.1894.

Kossin, J. P., S. J. Camargo, and M. Sitkowski (2010), Climate Modulation of North Atlantic Hurricane Tracks, *J Climate*, *23*(11), 3057-3076, doi:10.1175/2010jcli3497.1.

Kunkel, K. E., D. R. Easterling, D. A. R. Kristovich, B. Gleason, L. Stoecker, and R. Smith (2010), Recent Increases in U.S. Heavy Precipitation Associated with Tropical Cyclones, *Geophysical Research Letters*, *37*, doi:10.1029/2010gl045164.

Kunkel, K. E., D. R. Easterling, D. A. R. Kristvich, B. Gleason, L. Stoecker, and R. Smith (2012), Meteorological Causes of the Secular Variations in Observed Extreme Precipitation Events for the Conterminous United States, *Journal of Hydrometeorology*, *13*(3), 1131-1141, doi:10.1175/jhm-d-11-0108.1.

Kunkel, K. E., T. R. Karl, and D. R. Easterling (2007), A Monte Carlo Assessment of Uncertainties in Heavy Precipitation Frequency Variations, *Journal of Hydrometeorology*, *8*(5), 1152-1160, doi:10.1175/jhm632.1.

Kwiatkowski, D., P. C. B. Phillips, P. Schmidt, and Y. C. Shin (1992), Testing the Null Hypothesis of Stationarity Against the Alternative of a Unit Root: How Sure Are We That Economic Time Series Have a Unit Root?, *Journal of Econometrics*, *54*(1-3), 159-178, doi:10.1016/0304-4076(92)90104-y.

Lamb, P. J., and R. A. Peppler (1987), North Atlantic Oscillation: Concept and an Application, *B Am Meteorol Soc*, *68*(10), 1218-1225, doi:10.1175/1520-0477(1987)068<1218:naocaa>2.0.co;2.

Landsea, C. W., G. D. Bell, W. M. Gray, and S. B. Goldenberg (1998), The Extremely Active 1995 Atlantic Hurricane Season: Environmental Conditions and Verification of Seasonal Forecasts, *Mon Weather Rev*, *126*(5), 1174-1193, doi:10.1175/1520-0493(1998)126<1174:teaahs>2.0.co;2.

Landsea, C. W., B. A. Harper, K. Hoarau, and J. A. Knaff (2006), Can We Detect Trends in Extreme Tropical Cyclones?, *Science*, *313*(5786), 452-454, doi:10.1126/science.1128448.

Landsea, C. W., R. A. Pielke, A. Mestas-Nunez, and J. A. Knaff (1999), Atlantic Basin Hurricanes: Indices of Climatic Changes, *Climatic Change*, *42*(1), 89-129, doi:10.1023/A:1005416332322.

Larson, J., Y. P. Zhou, and R. W. Higgins (2005), Characteristics of Landfalling Tropical Cyclones in the United States and Mexico: Climatology and Interannual Variability, *J Climate*, *18*(8), 1247-1262, doi:10.1175/JCLI3317.1.

Larson, S., S. K. Lee, C. Z. Wang, E. S. Chung, and D. Enfield (2012), Impacts of Non-canonical El Nino Patterns on Atlantic Hurricane Activity, *Geophys Res Lett*, *39*, L14706, doi:10.1029/2012gl052595.

Lau, K. M., Y. P. Zhou, and H. T. Wu (2008), Have Tropical Cyclones been feeding more Extreme Rainfall?, *J Geophys Res-Atmos*, *113*(D23), D23113, doi:10.1029/2008jd009963.

Lee, S. K., C. Z. Wang, and D. B. Enfield (2010), On the Impact of Central Pacific Warming Events on Atlantic Tropical Storm Activity, *Geophys Res Lett*, *37*, L17702, doi:10.1029/2010gl044459.

Li, G. H., Y. Wang, and R. Y. Zhang (2008), Implementation of a Two-moment Bulk Microphysics Scheme to the WRF Model to Investigate Aerosol-cloud Interaction, *Journal of Geophysical Research-Atmospheres*, *113*(D15), doi:10.1029/2007jd009361.

Lonfat, M., F. D. Marks, and S. Y. S. Chen (2004), Precipitation Distribution in Tropical Cyclones Using the Tropical Rainfall Measuring Mission (TRMM) Microwave Imager: A global perspective, *Mon Weather Rev*, *132*(7), 1645-1660, doi:10.1175/1520-0493(2004)132<1645:PDITCU>2.0.CO;2.

Mann, H. B. (1945), Non-parametric Tests against Trend, *Econometrica*, *13*, 245-259.

Mann, M., and J. Lees (1996), Robust Estimation of Background Noise and Signal Detection in Climatic Time Series, *Climatic Change*, *33*(3), 409-445, doi:10.1007/bf00142586.

Mann, M. E., J. D. Woodruff, J. P. Donnelly, and Z. H. Zhang (2009), Atlantic Hurricanes and Climate over the Past 1,500 years, *Nature*, *460*(7257), 880-U115, doi:10.1038/nature08219.

Mattar, C., J. A. Sobrino, Y. Julien, and L. Morales (2011), Trends in Column Integrated Water Vapour over Europe from 1973 to 2003, *Int J Climatol*, *31*(12), 1749-1757, doi:10.1002/Joc.2186.

Matyas, C. (2008), Shape Measures of Rain Shields as Indicators of Changing Environmental Conditions in a Landfalling Tropical Storm, *Meteorol Appl*, *15*(2), 259-271, doi:10.1002/met.70.

Matyas, C. J. (2010), Associations between the Size of Hurricane Rain Fields at Landfall and Their Surrounding Environments, *Meteorol Atmos Phys*, *106*(3-4), 135-148, doi:10.1007/s00703-009-0056-1.

Maxwell, J. T., P. T. Soule, J. T. Ortegren, and P. A. Knapp (2012), Drought-Busting Tropical Cyclones in the Southeastern Atlantic United States: 1950-2008, *Ann. Assoc. Am. Geogr.*, *102*(2), 259-275, doi:10.1080/00045608.2011.596377.

May, P. T., and G. J. Holland (1998), The Role of Potential Vorticity Generation in Tropical Cyclone Rainbands., *Symposium on Tropical Cyclone Intensity Change*, 95-98.

McCabe, G. J., and D. M. Wolock (2002a), A Step Increase in Streamflow in the Conterminous United States, *Geophysical Research Letters*, *29*(24), 38-31-38-34, doi:10.1029/2002GL015999.

Medlin, J. M., S. K. Kimball, and K. G. Blackwell (2007), Radar and Rain Gauge Analysis of the Extreme Rainfall during Hurricane Danny's (1997) Landfall, *Mon Weather Rev*, *135*(5), 1869-1888, doi:10.1175/Mwr3368.1.

Meehl, G. A., et al. (2000), An Introduction to Trends in Extreme Weather and Climate Events: Observations, Socioeconomic Impacts, Terrestrial Ecological Impacts, and Model Projections*, *Bulletin of the American Meteorological Society*, *81*(3), 413-416, doi:10.1175/1520-0477(2000)081<0413:AITTIE>2.3.CO;2.

Merrill, R. T. (1984), A Comparison of Large and Small Tropical Cyclones, *Mon Weather Rev*, *112*(7), 1408-1418, doi:10.1175/1520-0493(1984)112<1408:ACOLAS>2.0.CO;2

Miller, A. J. (2002), *Subset Selection in Regression*, 2nd ed., xvii, 238 p. pp., Chapman & Hall/CRC, Boca Raton.

Min, S. K., X. B. Zhang, F. W. Zwiers, and G. C. Hegerl (2011), Human Contribution to More-intense Precipitation Extremes, *Nature*, *470*(7334), 378-381, doi:10.1038/Nature09763.

Molinari, J., P. Moore, and V. Idone (1999), Convective Structure of Hurricanes as Revealed by Lightning Locations, *Mon Weather Rev*, *127*(4), 520-534, doi:10.1175/1520-0493(1999)127<0520:CSOHAR>2.0.CO;2.

Morin, E. (2011), To Know What We Cannot Know: Global Mapping of Minimal Detectable Absolute Trends in Annual Precipitation, *Water Resour Res*, *47*, doi:10.1029/2010wr009798.

Nielsen-Gammon, J. W., F. Q. Zhang, A. M. Odins, and B. Myoung (2005), Extreme Rainfall in Texas: Patterns and Predictability, *Phys Geogr*, *26*(5), 340-364, doi:10.2747/0272-3646.26.5.340.

Nogueira, R. C., and B. D. Keim (2010), Annual Volume and Area Variations in Tropical Cyclone Rainfall over the Eastern United States, *J Climate*, *23*(16), 4363-4374, doi:10.1175/2010jcli3443.1.

Ogden, F. L., N. R. Pradhan, C. W. Downer, and J. A. Zahner (2011), Relative Importance of Impervious Area, Drainage Density, Width Function, and Subsurface Storm drainage on flood runoff from an urbanized catchment, *Water Resour Res*, *47*, doi:10.1029/2011wr010550.

Olivera, F., and B. B. DeFee (2007), Urbanization and Its Effect On Runoff in the Whiteoak Bayou Watershed, Texas, *J Am Water Resour As*, *43*(1), 170-182, doi:DOI 10.1111/j.1752-1688.2007.00014.x.

Orville, R. E., G. Huffines, J. Nielsen-Gammon, R. Y. Zhang, B. Ely, S. Steiger, S. Phillips, S. Allen, and W. Read (2001), Enhancement of Cloud-to-Ground Lightning over Houston, Texas, *Geophysical Research Letters*, *28*(13), 2597-2600, doi:10.1029/2001gl012990.

Pettitt, A. N. (1979), A Non-Parametric Approach to the Change-Point Problem, *Journal of the Royal Statistical Society. Series C (Applied Statistics)*, *28*(2), 126-135, doi:10.2307/2346729.

Pielke, R., J. Gratz, C. Landsea, D. Collins, M. Saunders, and R. Musulin (2008), Normalized Hurricane Damage in the United States: 1900–2005, *Natural Hazards Review*, *9*(1), 29-42, doi:10.1061/(ASCE)1527-6988(2008)9:1(29).

Pielke, R. A., M. W. Downton, and J. B. Miller (2002), *Flood Damage in the United States, 1996–2000: a Reanalysis of National Weather Service Estimates*, University Corporation for Atmospheric Research, Boulder, CO, USA.

Pielke, R. A., and C. N. Landsea (1999), La Nina, El Nino, and Atlantic hurricane damages in the United States, *B Am Meteorol Soc*, *80*(10), 2027-2033, doi:10.1175/1520-0477(1999)080<2027:LNAENO>2.0.CO;2.

Pielke, R. A., and C. W. Landsea (1998), Normalized Hurricane Damages in the United States: 1925-95, *Weather Forecast*, *13*(3), 621-631, doi:10.1175/1520-0434(1998)013<0621:nhditu>2.0.co;2.

Price, C. V., Nakagaki, N., Hitt, K.J., and Clawges, R.C., (2006), Enhanced Historical Land-Use and Land-Cover Data Sets of the U.S. Geological Survey, edited.

Prosser, I. P., and L. Williams (1998), The Effect of Wildfire on Runoff and Erosion in Native Eucalyptus Forest, *Hydrological Processes*, *12*(2), 251-265, doi:10.1002/(sici)1099-1085(199802)12:2<251::aid-hyp574>3.0.co;2-4.

Quiring, S., A. Schumacher, C. Labosier, and L. Zhu (2011), Variations in Mean Annual Tropical Cyclone Size in the Atlantic, *J Geophys Res-Atmos*, *116*, doi:10.1029/2010jd015011.

Rappaport, E. N. (2000), Loss of life in the United States associated with recent Atlantic tropical cyclones, *B Am Meteorol Soc*, *81*(9), 2065-2073, doi:10.1175/1520-0477(2000)081<2065:LOLITU>2.3.CO;2.

Ray, C. L. (1935), Relation of Tropical Cyclone Frequency to Summer Pressures and Ocean Surface-Water TemperatureS, *Mon Weather Rev*, *63*(1), 10-12, doi:10.1175/1520-0493(1935)63<10:rotcft>2.0.co;2.

Reeves, J., J. Chen, X. L. Wang, R. Lund, and Q. Q. Lu (2007), A Review and Comparison of Changepoint Detection Techniques for Climate Data, *Journal of Applied Meteorology and Climatology*, *46*(6), 900-915, doi:10.1175/JAM2493.1.

Rego, J. L., and C. Y. Li (2009), On the Importance of the Forward Speed of Hurricanes in Storm Surge Forecasting: A Numerical Study, *Geophys Res Lett*, *36*, doi:10.1029/2008gl036953.

Ren, F. M., Y. M. Wang, X. L. Wang, and W. J. Li (2007), Estimating Tropical Cyclone Precipitation from Station Observations, *Adv Atmos Sci*, *24*(4), 700-711, doi:10.1007/s00376-007-0700-y.

Ren, F. M., G. X. Wu, W. J. Dong, X. L. Wang, Y. M. Wang, W. X. Ai, and W. J. Li (2006), Changes in Tropical Cyclone Precipitation over China, *Geophys Res Lett*, *33*(20), doi:10.1029/2006gl027951.

Rodgers, E. B., J. J. Baik, and H. F. Pierce (1994a), The Environmental Influence on Tropical Cyclone Precipitation, *J Appl Meteorol*, *33*(5), 573-593, doi:10.1175/1520-0450(1994)033<0573:TEIOTC>2.0.CO;2.

Rodgers, E. B., and H. F. Pierce (1995), Environmental Influence on Typhoon-Bobbie Precipitation Distribution, *J Appl Meteorol*, *34*(11), 2513-2532, doi:10.1175/1520-0450(1995)034<2513:EIOTBP>2.0.CO;2.

Rogers, R., S. Y. Chen, J. Tenerelli, and H. Willoughby (2003), A Numerical Study of the Impact of Vertical Shear on the Distribution of Rainfall in Hurricane Bonnie (1998), *Mon Weather Rev*, *131*(8), 1577-1599, doi:10.1175//2546.1.

Rose, S., and N. E. Peters (2001), Effects of Urbanization on Streamflow in the Atlanta Area (Georgia, USA): A Comparative Hydrological Approach, *Hydrological Processes*, *15*(8), 1441-1457, doi:10.1002/hyp.218.

Rossby, C. G. (1949), On a Mechanism for the Release of Potential Energy in the Atmosphere, *Journal of Meteorology*, *6*(3), 164-180, doi:10.1175/1520-0469(1949)006<0164:OAMFTR>2.0.CO;2.

Shapiro, L. J. (1982), Hurricane Climatic Fluctuations. Part II: Relation to Large-Scale Circulation, *Mon Weather Rev*, *110*(8), 1014-1023, doi:10.1175/1520-0493(1982)110<1014:hcfpir>2.0.co;2.

Shapiro, L. J. (1992), Hurricane Vortex Motion and Evolution in a 3-Layer Model, *J Atmos Sci*, *49*(2), 140-153, doi:10.1175/1520-0469(1992)049<0140:HVMAEI>2.0.CO;2.

Shepherd, J. M., M. Carter, M. Manyin, D. Messen, and S. Burian (2010), The Impact of Urbanization on Current and Future Coastal Precipitation: A Case Study for Houston, *Environ Plann B*, *37*(2), 284-304, doi:10.1068/B34102t.

Shepherd, J. M., A. Grundstein, and T. L. Mote (2007), Quantifying the Contribution of Tropical Cyclones to Extreme Rainfall along the Coastal Southeastern United States, *Geophys Res Lett*, *34*(23), doi:10.1029/2007gl031694.

Sippel, J. A., and F. Q. Zhang (2010), Factors Affecting the Predictability of Hurricane Humberto (2007), *J Atmos Sci*, *67*(6), 1759-1778, doi:10.1175/2010jas3172.1.

Smith, J. A., M. L. Baeck, J. E. Morrison, P. Sturdevant-Rees, D. F. Turner-Gillespie, and P. D. Bates (2002), The Regional Hydrology of Extreme Floods in an Urbanizing Drainage Basin, *Journal of Hydrometeorology*, *3*(3), 267-282, doi:10.1175/1525-7541(2002)003<0267:trhoef>2.0.co;2.

Smith, J. A., M. L. Baeck, G. Villarini, and W. F. Krajewski (2010), The Hydrology and Hydrometeorology of Flooding in the Delaware River Basin, *Journal of Hydrometeorology*, *11*(4), 841-859, doi:10.1175/2010JHM1236.1.

Smith, R. K., W. Ulrich, and G. Sneddon (2000), On the Dynamics of Hurricane-like Vortices in Vertical-shear Flows, *Quarterly Journal of the Royal Meteorological Society*, *126*(569), 2653-2670, doi:10.1002/qj.49712656903.

Smith, S. R., J. Brolley, J. J. O'Brien, and C. A. Tartaglione (2007), ENSO's Impact on Regional U.S. Hurricane Activity, *J Climate*, *20*(7), 1404-1414, doi:10.1175/jcli4063.1.

Storey, A. L. (1998), Riding the Waves of Change: 60 Years of Service *Rep.*, Harris County Flood Control District.

Sun, G., S. G. McNulty, D. M. Amatya, R. W. Skaggs, L. W. Swift, J. P. Shepard, and H. Riekerk (2002), A Comparison of the Watershed Hydrology of Coastal Forested Wetlands and the Mountainous Uplands in the Southern US, *J Hydrol*, *263*(1-4), 92-104, doi:10.1016/s0022-1694(02)00064-1.

Thiessen, A. H. (1911), Precipitation Averages for Large Areas, *Monthly Weather Review*, *39*(7), 1082-1089, doi:10.1175/1520-0493(1911)39<1082b:PAFLA>2.0.CO;2.

Thomson, D. J. (1982), Spectrum Estimation and Harmonic Analysis, *Proceedings of the IEEE*, *70*(9), 1055-1096, doi:10.1109/proc.1982.12433.

Tomozeiu, R., A. Busuioc, V. Marletto, F. Zinoni, and C. Cacciamani (2000), Detection of Changes in the Summer Precipitation Time Series of the Region Emilia-Romagna, Italy, *Theoretical and Applied Climatology*, *67*(3-4), 193-200, doi:10.1007/s007040070008.

Trenberth, K. E., and T. J. Hoar (1996), The 1990-1995 El Nino Southern Oscillation Event: Longest on Record, *Geophys Res Lett*, *23*(1), 57-60, doi:10.1029/95gl03602.

Trenberth, K. E., and D. J. Shea (1987), On the Evolution of the Southern Oscillation, *Mon Weather Rev*, *115*(12), 3078-3096, doi:10.1175/1520-0493(1987)115<3078:oteots>2.0.co;2.

Vecchi, G. A., and T. R. Knutson (2008), On Estimates of Historical North Atlantic Tropical Cyclone Activity, *J Climate*, *21*(14), 3580-3600, doi:10.1175/2008jcli2178.1.

Vecchi, G. A., and B. J. Soden (2007), Increased Tropical Atlantic Wind Shear in Model Projections of Global Warming, *Geophys Res Lett*, *34*(8), doi:L08702 10.1029/2006gl028905.

Vecchi, G. A., K. L. Swanson, and B. J. Soden (2008), CLIMATE CHANGE Whither Hurricane Activity?, *Science*, *322*(5902), 687-689, doi:10.1126/science.1164396.

Villarini, G., F. Serinaldi, J. A. Smith, and W. F. Krajewski (2009), On the Stationarity of Annual Flood Peaks in the Continental United States during the 20th Century, *Water Resour Res*, *45*(8), W08417, doi:10.1029/2008WR007645.

Villarini, G., and J. A. Smith (2010), Flood Peak Distributions for the Eastern United States, *Water Resour Res*, *46*, W06504 doi:10.1029/2009wr008395.

Villarini, G., J. A. Smith, M. L. Baeck, T. Marchok, and G. A. Vecchi (2011a), Characterization of Rainfall Distribution and Flooding Associated with U.S. Landfalling Tropical Cyclones: Analyses of Hurricanes Frances, Ivan, and Jeanne (2004), *J Geophys Res-Atmos*, *116*(D23), D23116, doi:10.1029/2011jd016175.

Villarini, G., and G. A. Vecchi (2012), Twenty-first-century Projections of North Atlantic Tropical Storms from CMIP5 Models, *Nature Clim. Change*, *2*(8), 604-607, doi:10.1038/nclimate1530.

Villarini, G., G. A. Vecchi, and J. A. Smith (2010), Modeling the Dependence of Tropical Storm Counts in the North Atlantic Basin on Climate Indices, *Mon Weather Rev*, *138*(7), 2681-2705, doi:10.1175/2010mwr3315.1.

Villarini, G., G. A. Vecchi, and J. A. Smith (2011b), U.S. Landfalling and North Atlantic Hurricanes: Statistical Modeling of Their Frequencies and Ratios, *Mon Weather Rev*, *140*(1), 44-65, doi:10.1175/mwr-d-11-00063.1.

Waylen, P. (1991), Modeling the Effects of Tropical Cyclones on Flooding in the Santa Fe River Basin, Florida, *GeoJournal*, *23*(4), 361-373, doi:10.1007/BF00193609.

Wu, C. C., and K. A. Emanuel (1995), Potential Vorticity Diagnostics of Hurricane Movement .2. Tropical-Storm-Ana (1991) and Hurricane-Andrew (1992), *Mon Weather Rev*, *123*(1), 93-109, doi:10.1175/1520-0493(1995)123<0093:PVDOHM>2.0.CO;2.

Wu, L. G., S. A. Braun, J. Halverson, and G. Heymsfield (2006), A Numerical Study of Hurricane Erin (2001). Part I: Model Verification and Storm Evolution, *J Atmos Sci*, *63*(1), 65-86, doi:10.1175/jas3597.1.

Zane, D. F., T. M. Bayleyegn, J. Hellsten, R. Beal, C. Beasley, T. Haywood, D. Wiltz-Beckham, and A. F. Wolkin (2011), Tracking Deaths Related to Hurricane Ike, Texas, 2008, *Disaster Medicine and Public Health Preparedness*, *5*(1), 23-28.

Zhang, X. P., L. Zhang, J. Zhao, P. Rustomji, and P. Hairsine (2008), Responses of Streamflow to Changes in Climate and Land use/cover in the Loess Plateau, China, *Water Resour Res*, *44*, doi:10.1029/2007wr006711.

Zhu, L. Y., and S. Quiring (2013), Variations in Tropical Cyclone Precipitation in Texas (1950 to 2009), *J. Geophys. Res.*, doi:10.1029/2012JD018554.